NILU
TEKNISK NOTAT 16/77
REFERANSE: 03275
DATO: NOVEMBER 1977

RURAL AEROSOL MEASUREMENTS WITH A HIGH-VOLUME SIERRA IMPACTOR

VAL VITOLS

NORWEGIAN INSTITUTE FOR AIR RESEARCH
P.O.BOX 130, N-2001 LILLESTRØM
NORWAY

LIST OF CONTENTS

ABSTRACT

Mass concentrations and size distributions of various water-soluble ions and trace elements in aerosols were measured with a high-volume Sierra cascade impactor at a rural site in south-eastern Norway in January and February, 1976.

Conclusions based on the results of the measurements and on the experience gained with the Sierra impactor were as follows:

(a) variations in mass concentrations of the various chemical components in the aerosols were not pronounced during the generally stagnant sampling periods;

(b) sulphate, ammonium, lead and polycyclic aromatic hydrocarbons were found almost entirely in the "accumulation mode" of the fine particle fraction;

(c) calcium was confined to the coarse particle fraction, while copper and zinc occupied an intermediate position;

(d) due to its relatively high sampling rate and adequate intake efficiency, the high-volume sampler was well suited for measurements of rural aerosols;

(e) too long sampling periods, moisture, stage substrate materials, and the non-ideal collection characteristics of the impactor can affect the representativeness of measured particle size distributions.

RURAL AEROSOL MEASUREMENTS WITH A HIGH-VOLUME SIERRA IMPACTOR

1 INTRODUCTION

Studies of airborne particles during the last decade have resulted in much improved understanding of the physical and chemical properties, the sources, transport, residence time and sinks, and the effects on receptors of atmospheric aerosols. In particular, the "fine particle fraction" (i.e., particles smaller than about 2 μm in diameter) has been clearly implicated in causing most of the visibility reduction, containing most of the chemical components having biological effects, and constituting practically all of the aerosol mass resulting from chemical reactions in the atmosphere. A knowledge of airborne particle size distributions, as well as the chemical nature of the size fractions is, therefore, essential for the assessment of their potential effects, and in planning abatement strategies.

Measurement results of urban, rural, and background aerosols in Norway, particularly on sulphate-bearing particle concentrations, are now available, but there is a scarcity of information on their size distribution characteristics. To date, studies by NILU at Birkenes (as part of an SNSF-project) have provided data on background size-mass distributions of sulphate-, chloride-, calcium-, and lead-containing particles (DOVLAND, 1975), and on sea salt at a coastal site on Karmøy (VITOLS, 1977). These studies also provided the opportunity to assess the performance and suitability of several commercially available size-fractionating samplers. For the present study, a high-volume cascade impactor was selected to measure the size-mass distributions of various chemical constituents in airborne

particles at a rural site east of metropolitan Oslo during nine sampling runs in January/February 1976.

Cascade impactors classify particles according to their aerodynamic size, which is a very useful parameter in assessing the potential effects of particles (e.g., inhalation health hazards), as well as in predicting the performance of various types of particulate samplers and control devices.

In the less polluted rural and remote areas, the levels of certain chemical constituents, which have low inputs from natural sources, are much more sensitive indicators of anthropogenic air pollution than the concentrations of total suspended particulates (JANSSENS & DAMS, 1975).

2 OBJECTIVES OF STUDY

The objectives of this particular measurement programme* were to:

a) sample ambient air particulate matter at a rural site in Romerike district in Norway with the Sierra high-volume cascade impactor;

b) obtain information on mass concentrations and size distributions of particulate matter containing various trace elements and water-soluble ions; and

c) assess the suitability for measurements of the Sierra high-volume cascade impactor, its non-ideal performance characteristics, and the problems encountered with the sampler.

---

*for a description of the other phases of the measurement programme, cf. Dovland, H., and Eliassen, A.: "Estimates of dry deposition on snow" (SNSF-project, Ås, Norway, IR 34/77).

3 EXPERIMENTAL

3.1 Sampling site

Sampling of airborne suspended particulate matter was conducted at the rural site Yssen about 1.5 km east of the small settlement of Frogner, approximately 30 km northeast of Oslo, Norway (Fig. 1). The area is characterized by undulating terrain, consisting of cultivated farm lands, interspersed with forested areas, dwellings and farm buildings. The distances of the sampling site to the nearest population centres of Leirsund, Skedsmokorset, Kjeller and Lillestrøm range from about 4 km to 10 km.

The shelter of the Sierra high-volume cascade impactor was located on a gently-sloping, partially ploughed field, about 200 m north of the nearest paved road and about 65 m north of the closest farm buildings. Across the paved road to the south are the buildings of an auto body refinishing establishment, usually surrounded by parked cars and trucks. For most of the particulate matter sampling period, the fields were fully covered with snow, but during three brief periods of thaw a few crests of ploughed soil could be seen above the snow surface.

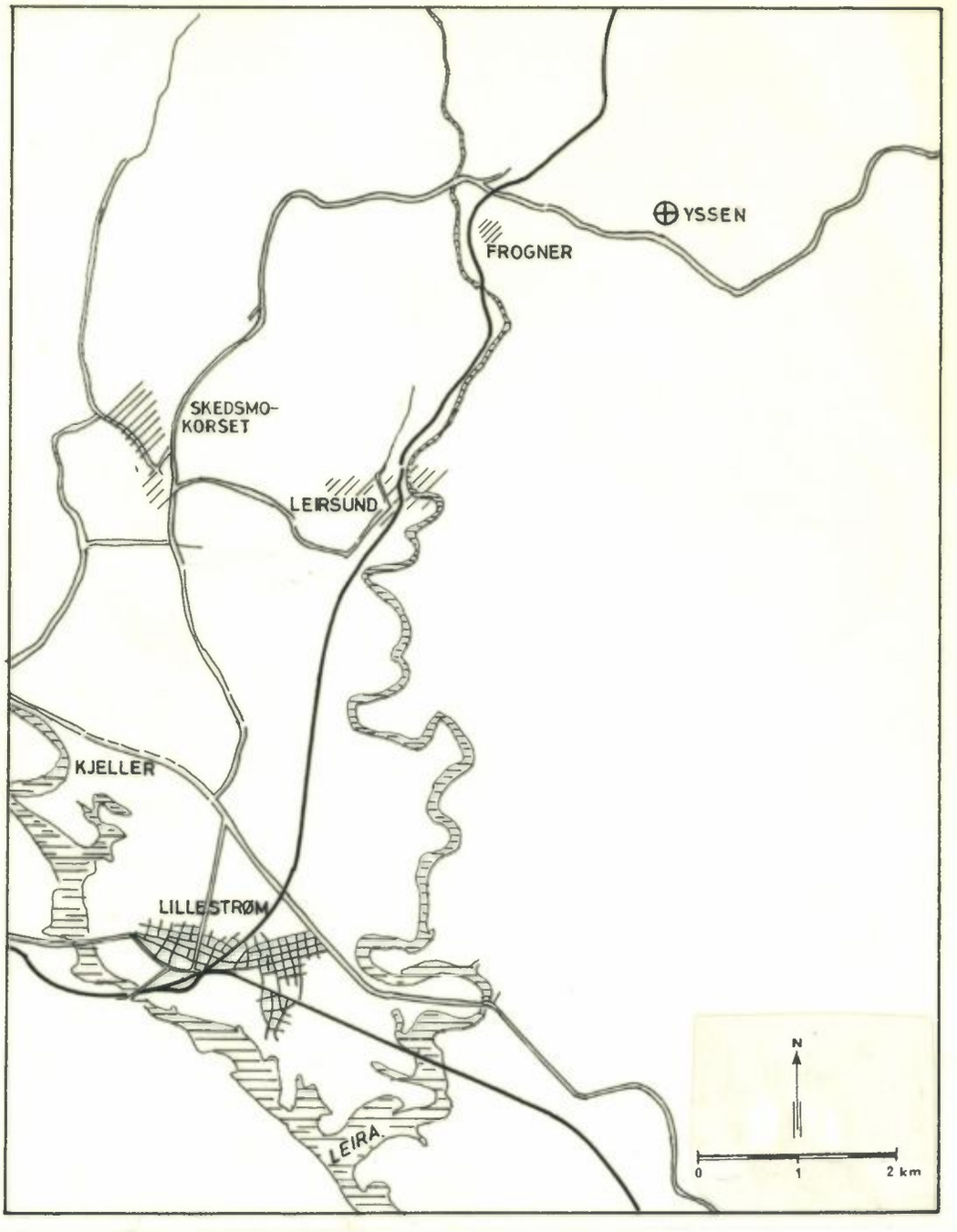

Figure 1: Map of the Yssen measurement area. The sampling site is marked by a cross.

3.2 The sampler

The air sampler used for the collection and size-classification of particulate matter was a General Metal Works Model GMWL 2000 high-volume sampler (Hi-Vol)*, equipped with a Sierra Model 235 high-volume cascade impactor, and a Sierra Model 310A constant flow controller. The sampler and the accessories were housed in the "standard" Hi-Vol shelter (Fig. 2). Electric power to the sampler was supplied via an about 40 m long extension cord from the instrument shelter, used in the other phases of the measurement programme.

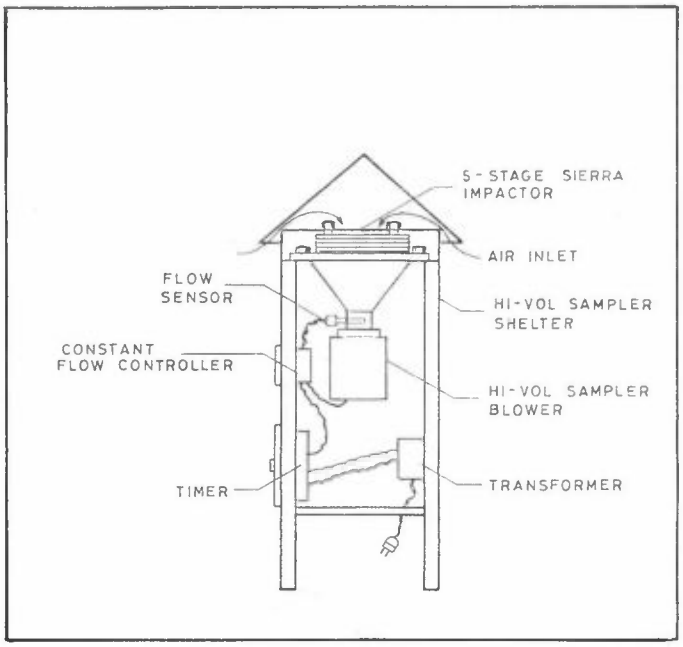

Figure 2: High-volume sampler and Sierra high-volume cascade impactor in "standard" square shelter.

*cf. for example, Lee et al. (1972); Lawrence Berkeley Laboratory (1975).

The Model 235 is a 5-stage, multi-slot cascade impactor, used with glass-fibre after-filter and the Hi-Vol sampler pump (WILLEKE, 1975). The Model 310A uses a constant-temperature anemometer to measure mass flow of the sampled air. It enables automatic correction for changes in filter loading, pressure drop across the filter, line voltage, and air temperature and pressure (KURZ & OLIN, 1975).

3.3 Air sampler calibration

3.3.1 Sampler flowrates

The constant flow controller of the Hi-Vol sampler was adjusted to the recommended operating flowrate, at the STP conditions of 25°C and 760 mm Hg, for the Sierra cascade impactor in the field prior to sampling by means of a Sierra Model 331 calibration orifice kit. After the first sampling run, the operating flowrate was again rechecked and readjusted, but the actual flowrates (1.09 m^3/min and 1.07 m^3/min) nevertheless differed slightly from the recommended (design) flowrate of 1.13 m^3/min (cf. also Sec. 6.1). Rough checks of the operating flowrates were also made at the beginning of each sampling run by means of the Hi-Vol sampler "visifloat" flowmeter, but the exact flowrates were assumed to be those determined with the calibration orifice kit.

3.3.2 Cascade impactor ECD's*

Cascade impactors separate airborne particles in size ranges according to their aerodynamic behaviour, and their stage cut-off diameters, ECD's, are given in terms of equivalent aerodynami diameters**.

---

* *ECD, the "effective cut-off diameter", is that diameter of unit density spherical particles of which 50% will collect on the given impactor stage and 50% will penetrate the stage.*

** *"equivalent aerodynamic diameter" of an irregularly-shaped particle is the diameter of a unit density spherical particle which has the same aerodynamic properties (e.g. terminal velocity) as the particle in question, without regard to its actual size, shape, and density.*

The ECD's for the high-volume Sierra cascade impactor with slotted glass-fibre collection substrates have been determined by WILLEKE (1975), and are the same as given in the manufacturer's instruction manual for the impactor.

During the early part of the measurement programme, Whatman 40 slotted cellulose filters were used as collection substrates. After problems with excessive moisture were encountered, Gelman Spectrograde Type A glass-fibre slotted substrates were substituted for the remaining sampling periods. Although the particulate matter retention characteristics of the Whatman 40 substrates may be different from those of glass-fibre substrates (cf. Sec. 6.4), the cascade impactor stage ECD's were assumed to be the same with both substrate materials.

Stage ECD's for the cascade impactor at the two operating flowrates were calculated from the relationship (LEE & GORANSON, 1972):

$$ECD_s = ECD_c \sqrt{Q_c/Q_s} \qquad (1)$$

where ECD_c and ECD_s are the calibration and sampling ECD's for a given stage, respectively, and Q_c and Q_s the corresponding calibration and sampling flowrates. Table A1 in the Appendix gives calibration and sampling ECD's for the two flowrates at which the impactor was operated.

3.4 Sampler preparation

Before assembling the cascade impactor at NILU, all external and internal surfaces of the impactor were rinsed with distilled water and swabbed with moist, lint-free tissue paper. The impactor was then prepared for sample collection by placing with forceps the slotted Whatman 40, or glass-fibre substrates on the collection stages and inserting the glass-fibre after-filter in its filter holder.

Stage substrates and after-filters to be used for blank determinations were exposed to the "loading room" environment during this time, but were not actually inserted in the impactor or in the filter holder. The assembled impactor was then wrapped in clean plastic sheet for transport to the sampling site.

3.5 Sampling of airborne particulate matter

At the start of each sampling run, the pre-loaded cascade impactor was attached to the Hi-Vol sampler in the shelter and the rain shield put in place. The timer of the Hi-Vol sampler was not used, but the sampler was started and shut off manually.

Airborne particulate matter was sampled with the high-volume Sierra cascade impactor during nine sampling periods from 17 January to 25 February, 1976.

No fixed-duration sampling schedule was maintained during the measurement programme. All sampling runs, however, were of considerably longer duration than the customary 24-hour period for Hi-Vol samplers. After two initial runs, of about 5 days duration each, had revealed excessive overloading of all impaction stages, the length of sampling was decreased. The actual lengths of sampling runs ranged from a low of 2870 minutes to a high of 10050 minutes, giving corresponding minimum and maximum air sample volumes of 3068 m^3 and 10745 m^3, respectively.

3.6 Sample handling

After each sampling period, the cascade impactor was removed from the shelter, wrapped in the clean plastic sheet, and returned to NILU. The impactor stage substrates and the after-filter were then removed with forceps from the impactor and placed in clean, labelled and sealable polyethylene bags before chemical analysis.

After the 9-13 February run, all the slotted jet-plates of the impactor (except for the over-sized support plate for Stage 5 substrate and the after-filter holder) were immersed in distilled water in sealable polyethylene bags and cleaned ultrasonically (cf. Sec. 6.3).

Hoar frost during one sampling period (13-17 February), caused heavy rime deposits on Stage 1 jet-plate around the impaction jet slots. The rime was carefully scraped-off and transferred to a clean polyethylene bag for analysis. No other attempts were made, however, to routinely recover possible deposits of particles on Stage 1 jet-plate of the impactor.

3.7 Sample analysis and calculations

The airborne particulate matter samples were analyzed at NILU for nine water-soluble ions and trace elements. One exception was the sample from the 5-9 February run, which was forwarded to the Central Institute for Industrial Research (SI) for special analyses of various species of polycyclic aromatic hydrocarbons (PAH) by methods developed at the Institute (BJØRSETH & LUNDE, 1975; 1977). The analytical methods used at NILU were:

- spectrophotometric for sulphate (SO_4), ammonium (NH_4), and chloride (Cl);
- atomic absorption for lead (Pb), copper (Cu), zinc (Zn), calcium (Ca), and magnesium (Mg); and
- flame emission for sodium (Na).

To obtain solution aliquots for the analyses, the impactor stage substrates and after-filters, as well as the selected substrate and filter blanks, were leached in distilled water (for SO_4, NH_4, Ca, Cl, Na, and Mg) or 1N HNO_3 acid (for Pb, Cu, Zn, and Ca).

The same analyses were also performed on measured aliquots of the wash waters of the ultrasonically cleaned impactor jet-plates.

Some cursory light-microscope examinations of the stage collections from the 9-13 February period were made*, and scrapings of deposits around and inside jet slots were analyzed by the electron microprobe analyzer technique at the Institutt for Atomenergi (IFA)*.

The results of the impaction stage substrate and after-filter analyses were then adjusted to account for trace metal and water-soluble ion content in the substrate and filter blanks, as well as in the distilled water and acid used for the leaching and washing. The amounts of the various components found in the rime deposits (13-17 February period) were considered part of Stage 1 collection.

Sample air volumes were calculated from sampling period durations and sampling flowrates. Details on sampling period lengths and flowrates, and the calculated sample volumes for all sampling periods are given in Table A2 of the Appendix.

---

*Anda, O., NILU, personal communication, March 1976.

4 EXPERIMENTAL RESULTS

4.1 Mass concentrations

Table 1 summarizes the measured mass concentrations of the various trace elements and water-soluble ions in airborne particles during the 17 January - 25 February, 1976 sampling periods.

"Total" concentration, as used here, refers to the various constituents found in particles of all sizes, as sampled by the high-volume Sierra cascade impactor. "Adjusted" concentration includes measured or estimated interstage losses, i.e., particles not collected on the appropriate impaction stages, but deposited on and recovered from the impactor jet-plates by ultrasonic cleaning (cf. Sec. 6.3). Since interstage losses were determined for only one of the samples, the adjusted concentrations for all other sampling periods were calculated by assuming that the relative magnitudes of losses for the various chemical components on all impaction stages remained constant, but were proportional to the respective total concentrations*.

Table 1 also includes concentrations of SO_4, Pb, Cl, Na, and Mg during periods for which results from NILU's automatic air sampler were available. Since this sampler takes 24-hour samples, the concentrations shown are time-weighted averages for the appropriate periods. These correspond to the "total" concentrations from the high-volume Sierra cascade impactor.

---

*$\text{Adjusted concentration} = \text{Total concentration of sample} + \frac{(\text{Total interstage loss, 9-13 February sample})(\text{Total concentration of sample})}{(\text{Total concentration, 9-13 February sample})}$

Table 1: Concentrations of water-soluble ions and trace elements in airborne particulate matter at Yssen, as measured by the high-volume Sierra cascade impactor during the 17 Jan. - 25 Feb. 1976 sampling periods.

Period of sampling[b]	Concentration[a], ng/m³										
	SO_4			NH_4[f]	Pb			Cu		Zn	
	Tot.[c]	Adj.[d]	K.K.[e]	Tot.	Tot.	Adj.	K.K.[e]	Tot.	Adj.	Tot.	Adj.
17 Jan. - 23 Jan.	2240	2570		1170	107	118		83	105	59	80
23 Jan. - 30 Jan.	4500	5160		1500	169	186		122	155	76	103
30 Jan. - 3 Feb.	6310	7240		2930	182	200		101	128	65	88
3 Feb. - 5 Feb.	5760	6610		2770	183	202		107	136	95	128
9 Feb. - 13 Feb.	8550	9810		1800	90	99		88	112	67	91
13 Feb. - 17 Feb.	11180	12830	11550	2460	114	126	119	105	133	117	158
17 Feb. - 21 Feb.	10730	12320	13100	3530	104	115	70	174	221	86	116
21 Feb. - 25 Feb.	6750	7750	8540	1440	64	70	56	83	105	64	86

Period of sampling[b]	Concentration[a], ng/m³											
	Ca			Cl			Na			Mg		
	Tot.[g]	Adj.[g]	Tot.[h]	Tot.	Adj.	K.K[i]	Tot.	Adj.	K.K.[i]	Tot.	Adj.	K.K.[i]
17 Jan. - 23 Jan.	104	129	194	790	830	460	390	410	150	29	36	8
23 Jan. - 30 Jan.	167	208	235	600	630		480	510		44	51	
30 Jan. - 3 Feb.	49	61	102	660	690		480	510		7	9	
3 Feb. - 5 Feb.	63	78	207	130[k]	140[k]		210	220		(ℓ)	(ℓ)	
9 Feb. - 13 Feb.	659	820	612	3650[j]	3830[j]		2850[j]	3020[j]		193	237	
13 Feb. - 17 Feb.	209	260	87	7920[k]	8300[k]	690	7370[k]	7810[k]	220	216	265	18
17 Feb. - 21 Feb.	197	197	138	1290	1350		1340	1420		31[m]	38[m]	
21 Feb. - 25 Feb.	151	151	108	480	500		770	820		28	34	

(a) at 25°C and 760 mm Hg

(b) details on the time and duration of sampling, sampling rates, and sample volumes are given in Table A2 of the Appendix

(c) sum of the concentrations found on Stages 1 through 5 of the cascade impactor and after-filter

(d) total concentrations adjusted for interstage losses (cf. 4.1)

(e) time-weighted average of concentrations measured by the "Kommunekasse" automatic sampler at 0.2 m and 2 m above ground

(f) adjusted concentrations not calculated due to uncertain interstage losses

(g) impactor substrates and after-filter leached in distilled water

(h) impactor substrates and after-filter leached in 1N HNO_3

(i) time-weighted average of concentration sampled by the "Kommunekasse" automatic sampler at 2 m above ground, and analyzed by x-ray fluorescence technique at the Institutt for atomenergi (IFA)

(j) possible contamination of impactor Stage 1 and 2 collections

(k) possible contamination of entire sample

(ℓ) concentration equal or less than blank concentration on Stages 1 and 5, and after-filter

(m) concentration equal or less than blank concentration on after-filter

The analysis by SI* of the 5-9 February sample identified 24 distinct PAH compounds in the airborne particles. The total concentration of all PAH in the sample was found to be about 20 ng/m^3. The concentration of benzo(a)pyrene (BaP), usually serving as an indicator of the level of PAH pollution, was about 1660 pg/m^3.

4.2 Size distributions

Table 2 gives equivalent aerodynamic mass median diameters (MMD's) of the various trace elements and water-soluble ions measured by the high-volume Sierra cascade impactor during each sampling period.

Figures 3 through 9 show the distributions of mass concentration averages and ranges of the various chemical components collected on the different stages** and after-filter of the impactor for the 17 January to 5 February and the 9 February to 25 February sampling periods (cf. Table A3 in the Appendix for detailed data). Figure 10 gives concentration distributions of benzo(a)pyrene and total PAH for the 5-9 February sampling run, based on the analytical results supplied by SI*.

Figures 11 through 17 show cumulative size-mass distributions on log-normal probability plots for the same chemical components during the 17 January - 5 February and 9-25 February periods. Figure 18 shows similar information on the PAH's for the 5-9 February run.

---

* *analysis report from A. Bjørseth and B. Olufsen: "PAH i tørravsetningen som funksjon av partikkelstørrelsen," Sentralinstituttet for industriell forskning, Blindern, Oslo, 8 oktober 1976.*

** *not adjusted for interstage losses.*

Table 2: Estimates of mass median diameters(MMD's) of airborne particles at Yssen containing the various water-soluble ions and trace elements shown, as measured by the high-volume Sierra cascade impactor during the 17 Jan. - 25 Feb. 1976 sampling periods.*

Period of sampling		Mass median diameter*, µm						
		SO_4	NH_4	Pb	Cu	Zn	Ca	
							water-leached	acid-leached
17 Jan. - 23 Jan.		0.55	0.64	0.26	0.90	0.72	1.0	1.5
23 Jan. - 30 Jan.		0.57	0.56	0.13	0.90	0.60	3.6	3.1
30 Jan. - 3 Feb.		0.60	0.64	0.30	1.0	0.55	0.7	2.5
3 Feb. - 5 Feb.		0.62	0.64	0.45	1.2	0.72	3.2	3.4
9 Feb. - 13 Feb.		0.90	0.73	0.80	1.3	0.92	5.8	7.0
13 Feb. - 17 Feb.		0.66	0.68	0.78	1.3	0.88	1.4	1.8
17 Feb. - 21 Feb.		0.98	0.80	0.78	1.6	1.0	5.5	5.2
21 Feb. - 25 Feb.		0.60	0.58	0.70	1.4	0.82	1.5	3.0
Average	17 Jan.- 9 Feb. periods	0.6	0.6	0.2	1.0	0.6	1.5	2.4
	9 Feb. - 25 Feb. periods	0.8	0.7	0.8	1.4	0.9	$5.5^{+}/1.5^{++}$	$6.5^{+}/2.5^{++}$

* equivalent aerodynamic diameter

\+ average of 9-13 Feb. and 17-21 Feb. periods

++ average of 13-17 Feb. and 21-25 Feb. periods

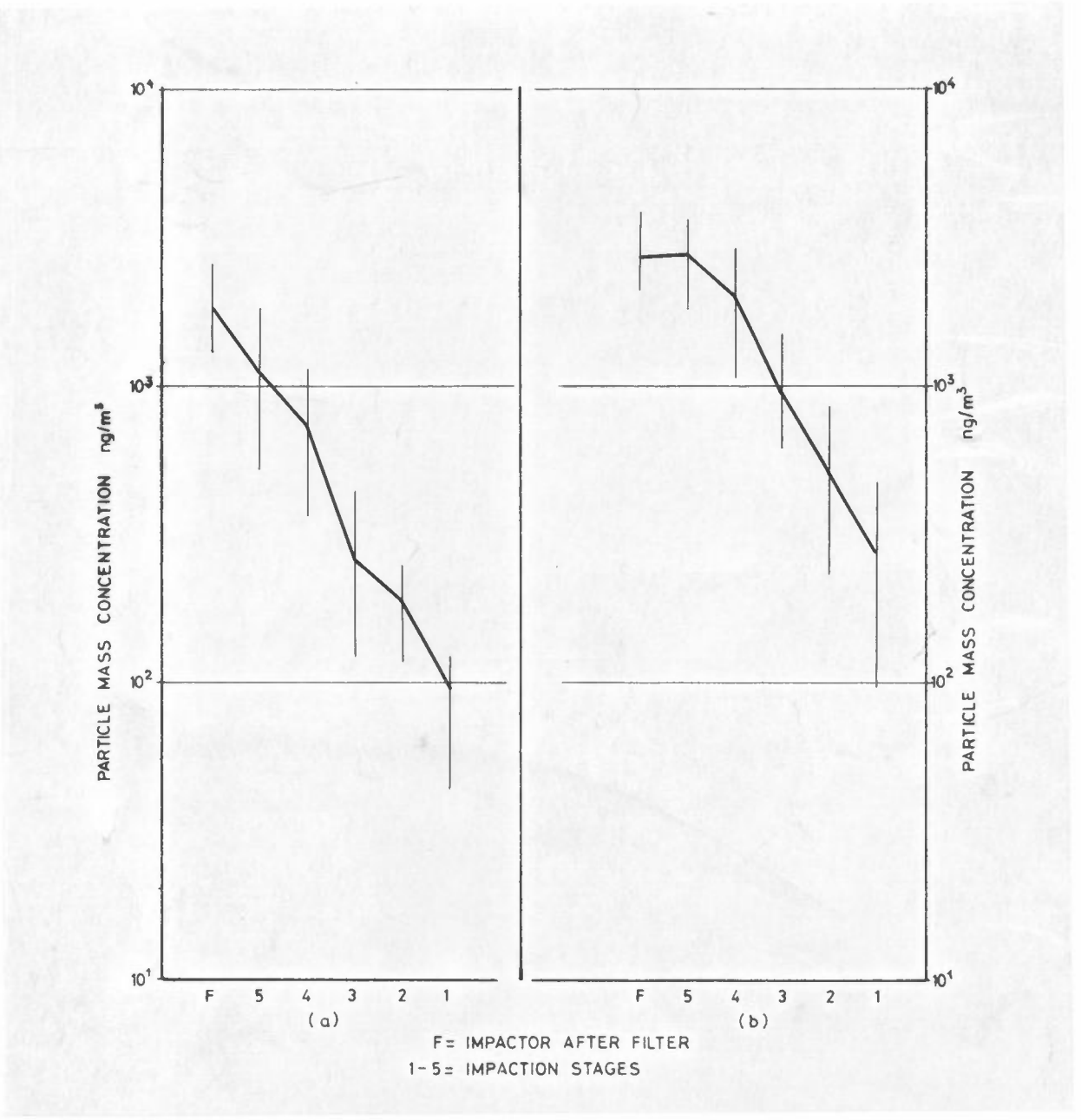

Figure 3: Average and range of size-mass concentration distributions of SO_4-containing particles at Yssen, as measured by the high-volume Sierra cascade impactor during:*

a) 17 January - 5 February 1976, and
b) 9 February- 25 February 1976

sampling periods.

Particle diameter intervals, in µm:

Stage 1:	*> 7.40*	*Stage 4:*	*0.98-1.54*
Stage 2:	*3.09-7.40*	*Stage 5:*	*0.50-0.98*
Stage 3:	*1.54-3.09*	*After-filter:*	*<0.50*

**Not adjusted for interstage losses.*

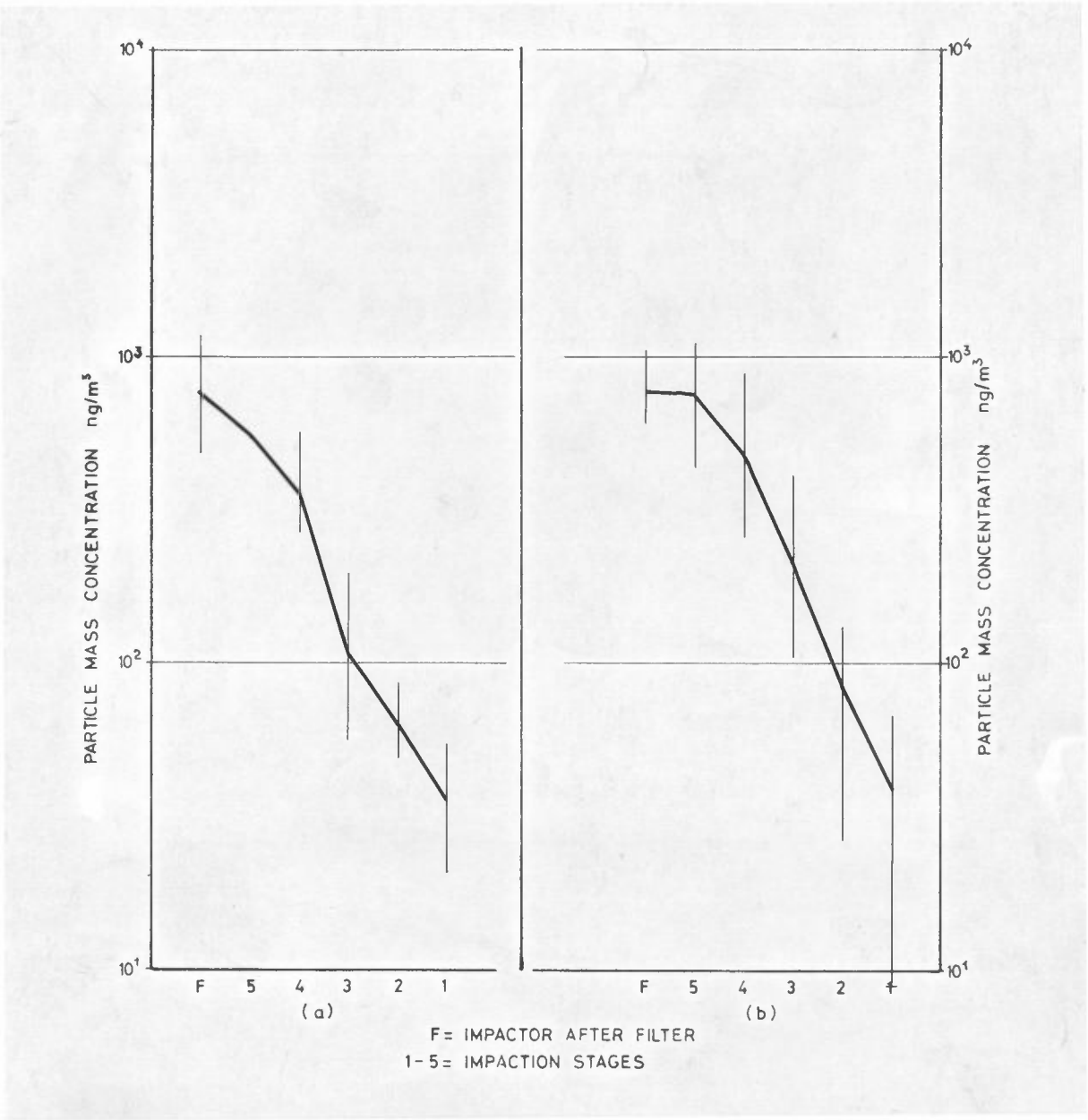

Figure 4: Average and range of size-mass concentration distributions of NH_4-containing particles at Yssen, as measured by the high-volume Sierra cascade impactor during:*

a) 17 January - 5 February 1976, and
b) 9 February- 25 February 1976

sampling periods.

Particle diameter intervals as per Figure 3.

**Not adjusted for interstage losses.*

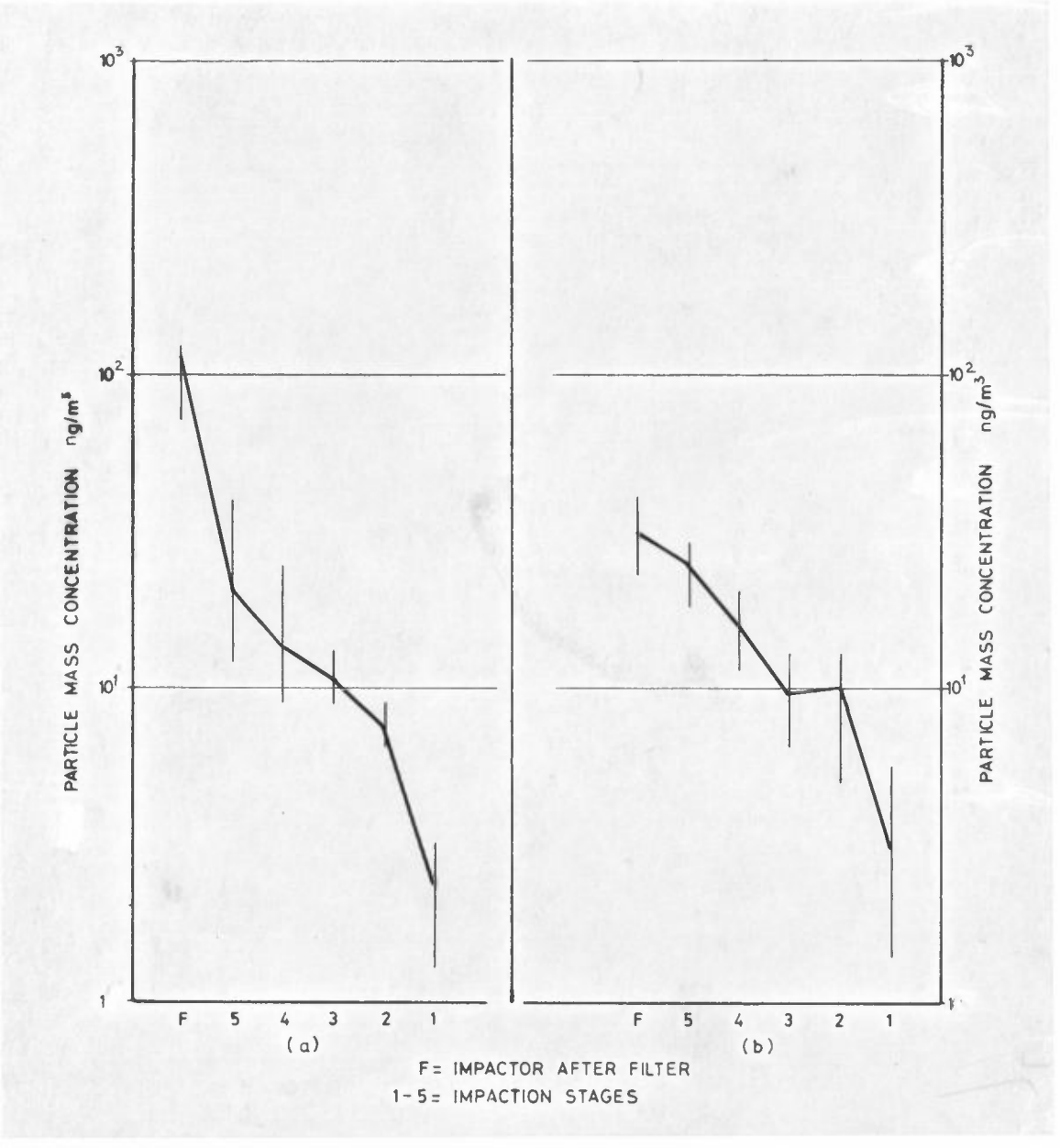

Figure 5: *Average and range of size-mass concentration* distributions of Pb-containing particles at Yssen, as measured by the high-volume Sierra cascade impactor during:*

a) 17 January - 5 February 1976, and
b) 9 February- 25 February 1976

sampling periods.

Particle diameter intervals as per Figure 3.

**Not adjusted for interstage losses.*

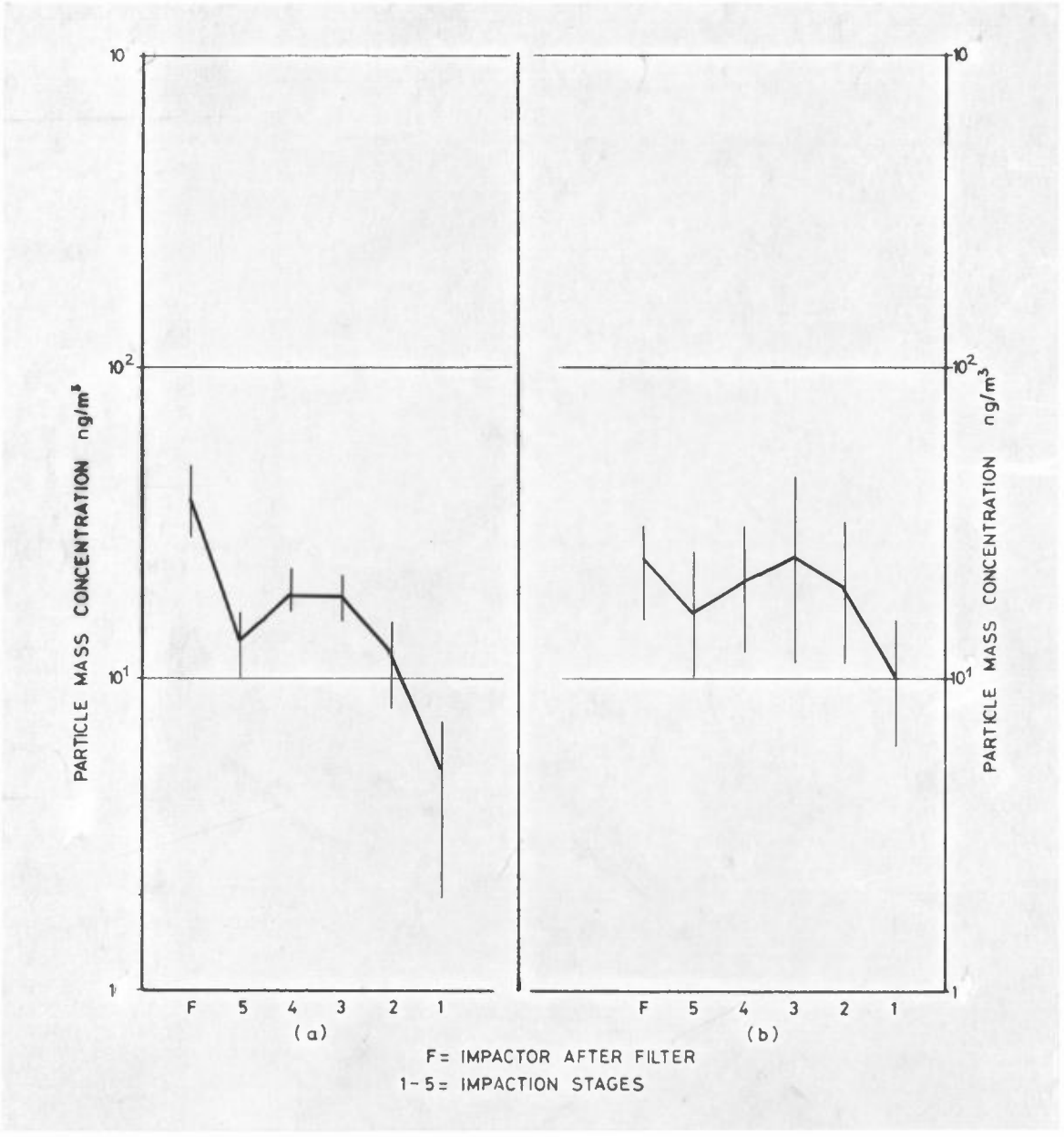

Figure 6: Average and range of size-mass concentration distributions of Cu-containing particles at Yssen, as measured by the high-volume Sierra cascade impactor during:*

a) 17 January - 5 February 1976, and
b) 9 February- 25 February 1976

sampling periods.

Particle diameter intervals as per Figure 3.

**Not adjusted for interstage losses.*

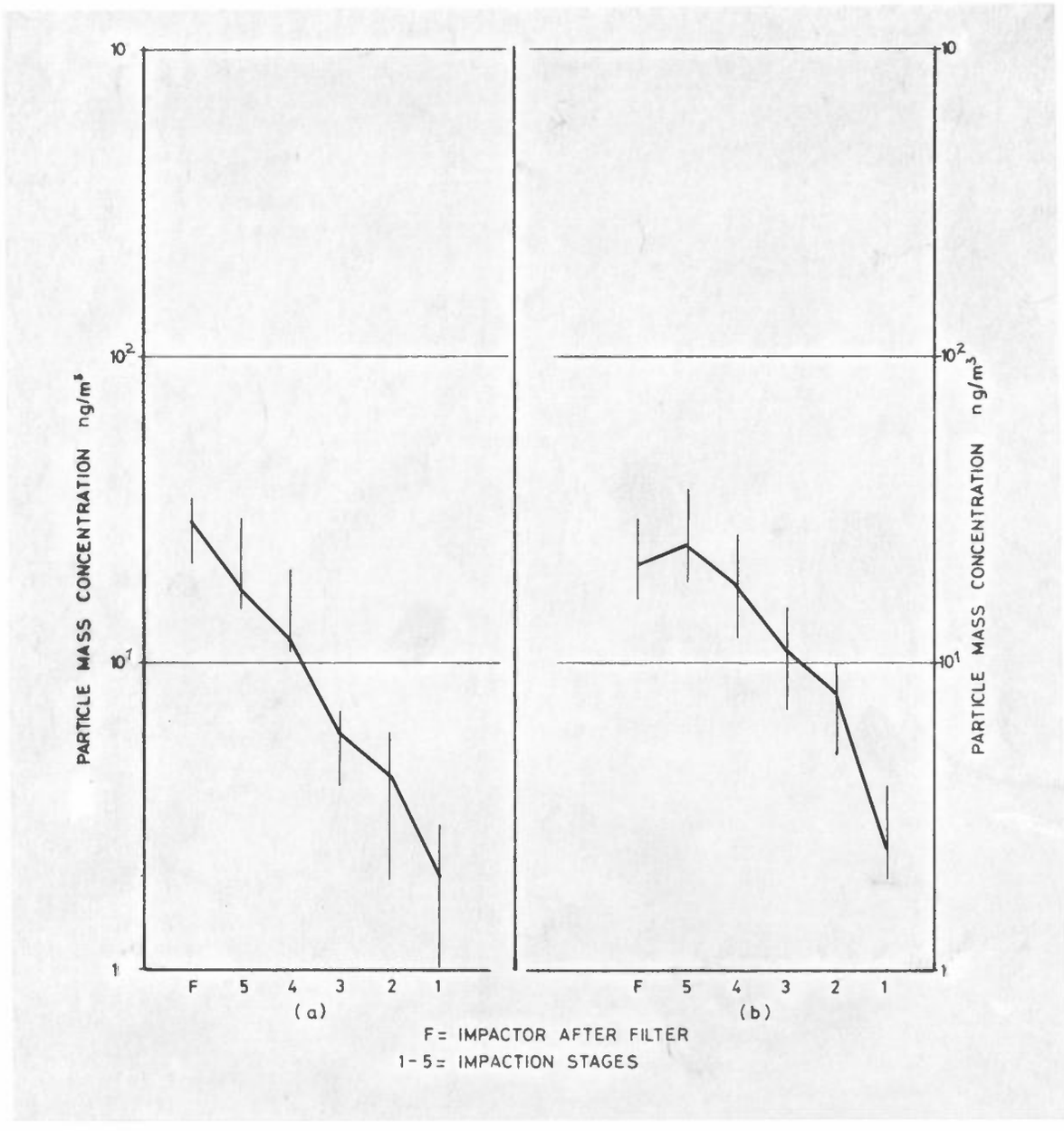

Figure 7: Average and range of size-mass concentration distributions of Zn-containing particles at Yssen, as measured by the high-volume Sierra cascade impactor during:*

a) 17 January - 5 February 1976, and
b) 9 February- 25 February 1976

sampling periods.

Particle diameter intervals as per Figure 3.

**Not adjusted for interstage losses.*

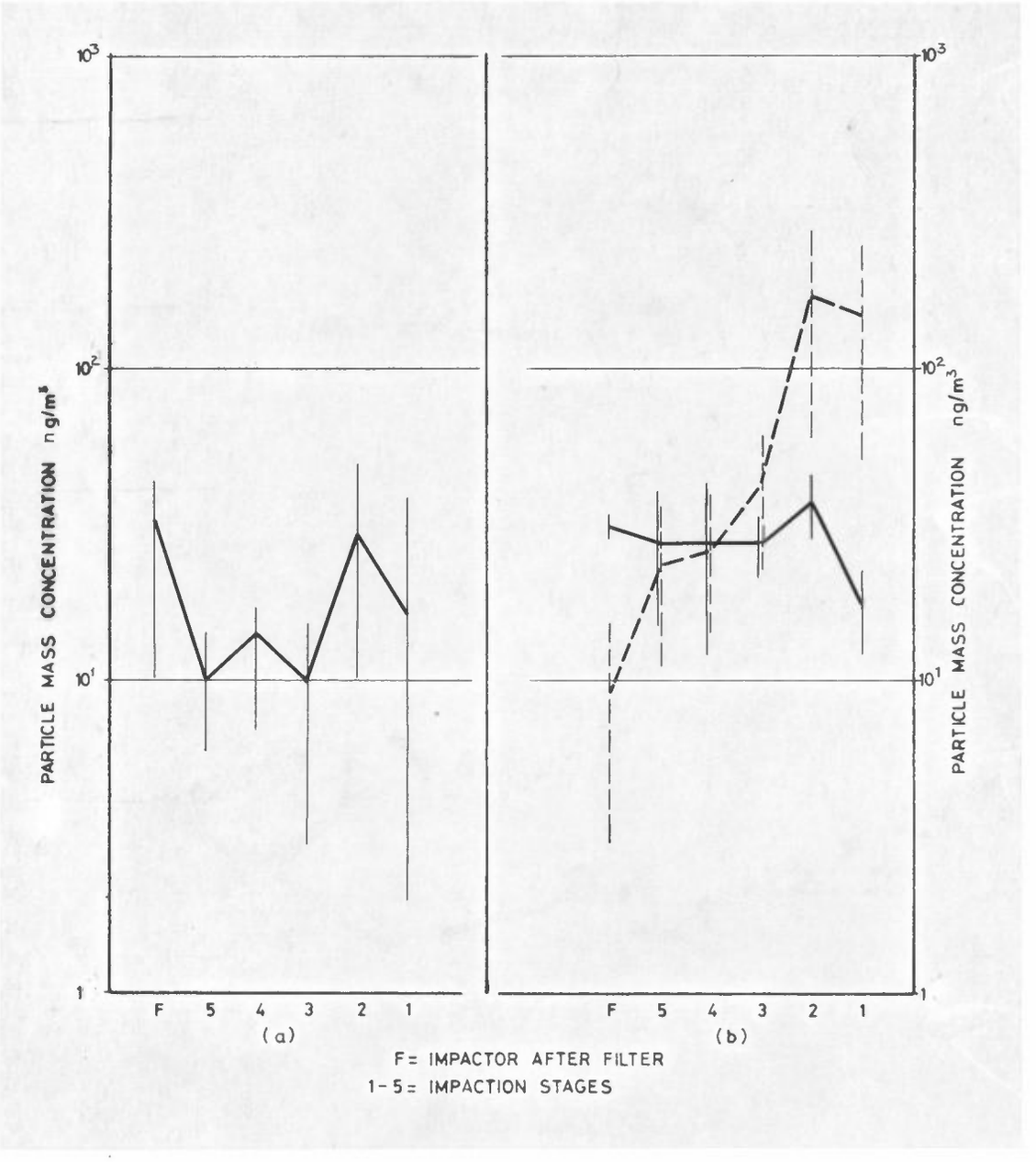

Figure 8: Average and range of size-mass concentration distributions of water-leached Ca-containing particles at Yssen, as measured by the high-volume Sierra cascade impactor during:*

a) 17 January - 5 February 1976, and
b) 9-13 February/17-21 February 1976 (– – –), and
13-17 February/21-25 February 1976 (———)

sampling periods.

Particle diameter intervals as per Figure 3.

**Not adjusted for interstage losses.*

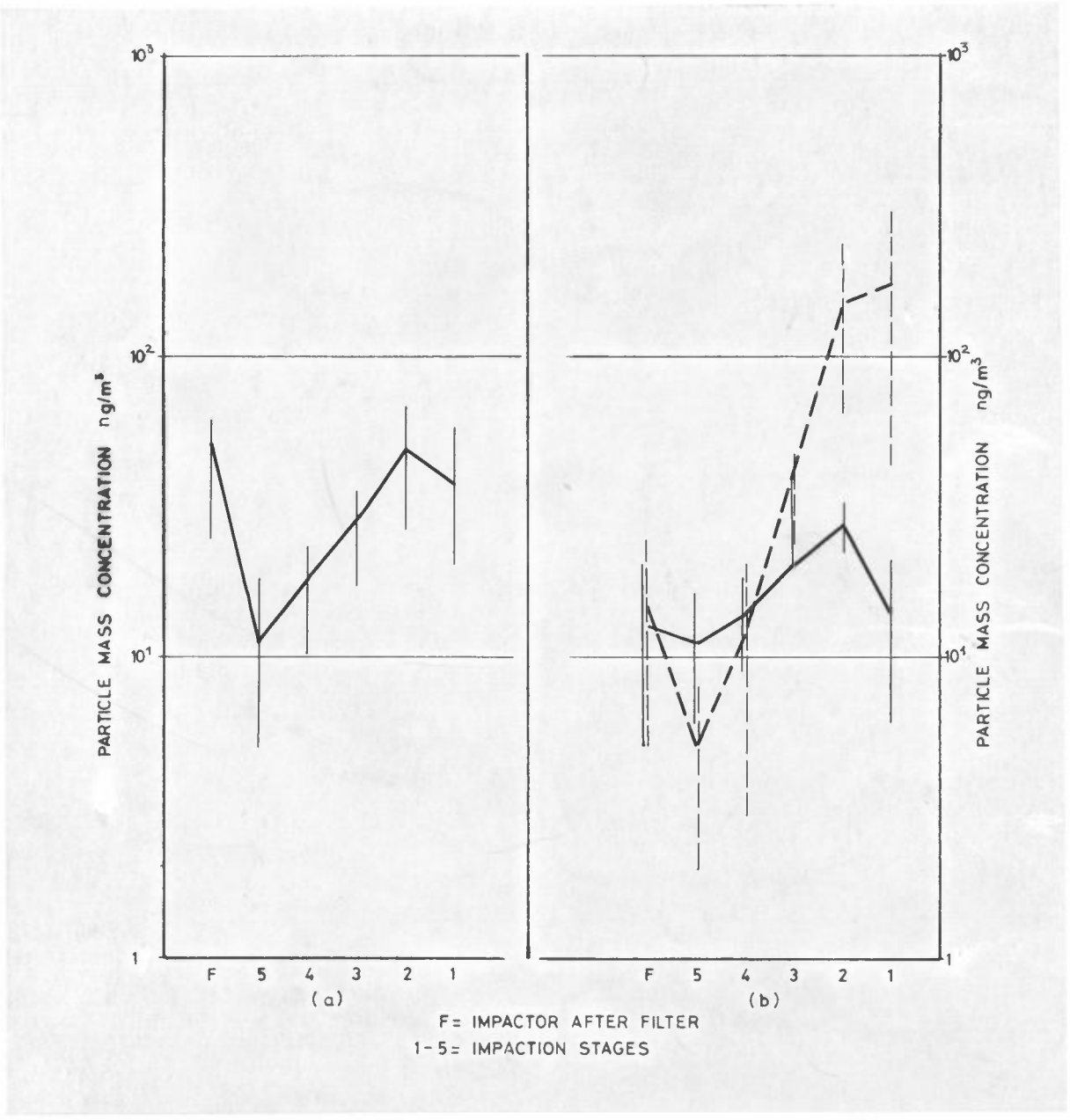

Figure 9: Average and range of size-mass concentration distributions of acid-leached Ca-containing particles at Yssen, as measured by the high-volume Sierra cascade impactor during:*

a) 17 January - 5 February 1976, and
b) 9-13 February/17-21 February 1976 (– – –), and
13-17 February/21-25 February 1976 (———)

sampling periods.

Particle diameter intervals as per Figure 3.

**Not adjusted for interstage losses.*

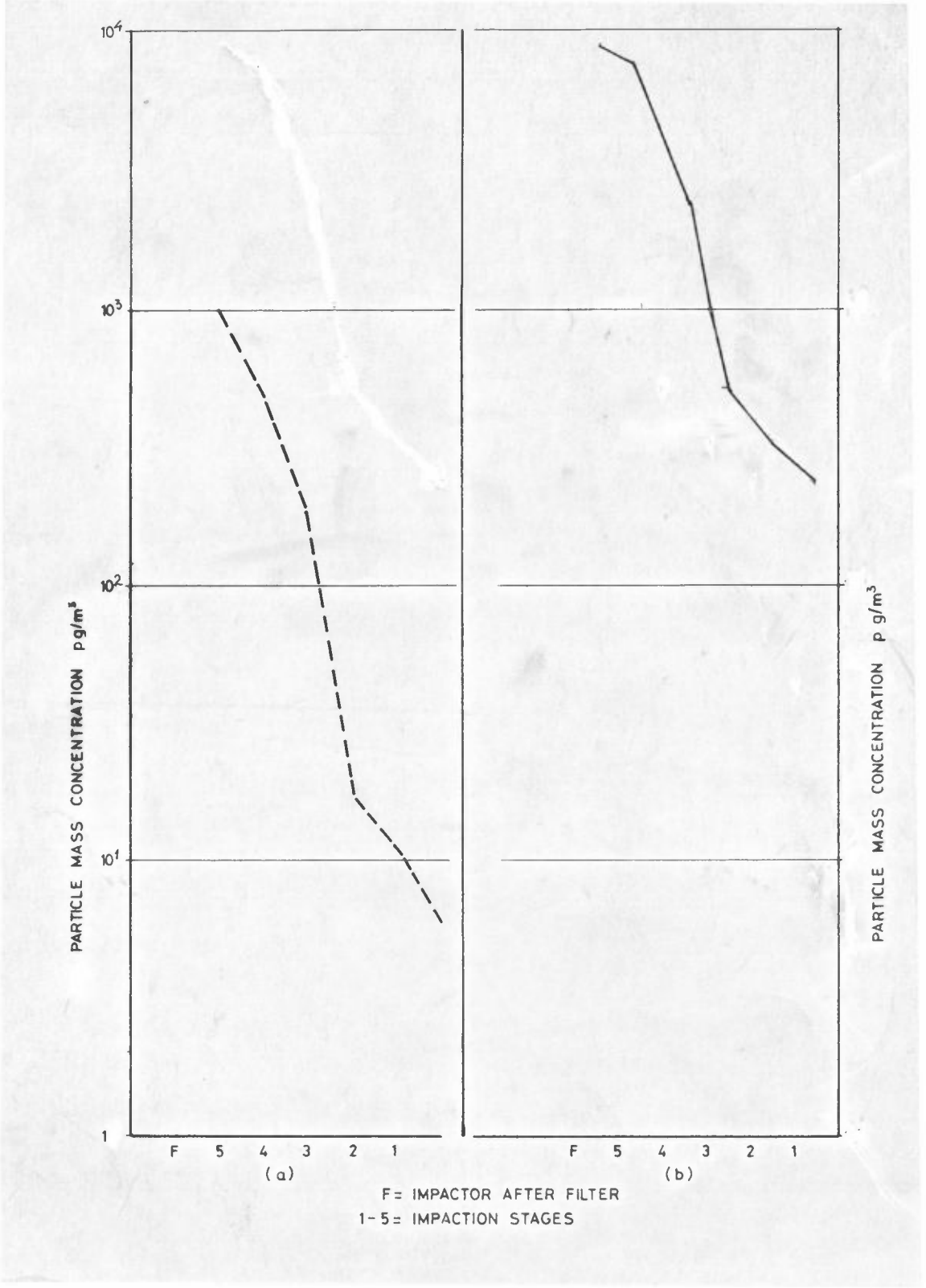

Figure 10: Mass concentration distributions of (a) benzo (a) pyrene (BaP) and (b) total polycyclic aromatic hydrocarbons (PAH) in particles from high-volume Sierra cascade impactor sampling at Yssen during the 5 February - 9 February 1976 period.

Particle diameter intervals as per Figure 3.

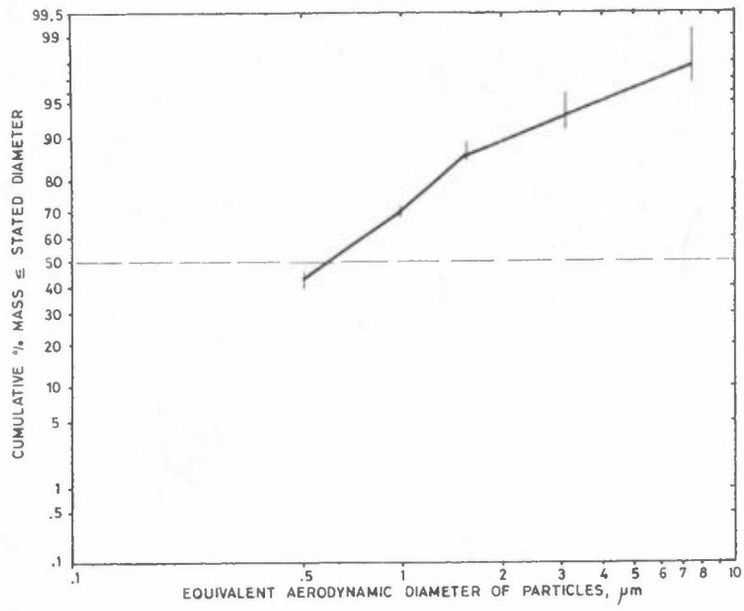

a)

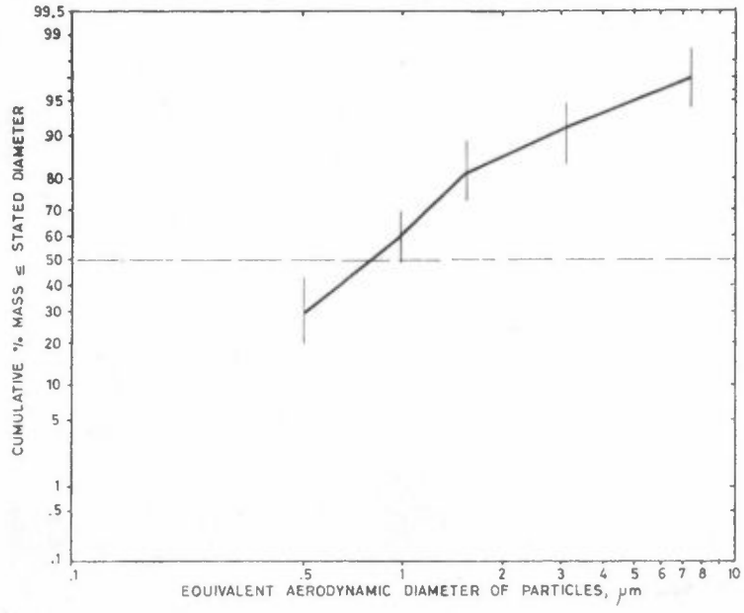

b)

Figure 11: Average and range of cumulative size-mass distributions of SO_4-containing particles at Yssen, as measured by the high-volume Sierra cascade impactor during:

a) 17 January - 5 February 1976, and
b) 9 February- 25 February 1976

sampling periods.

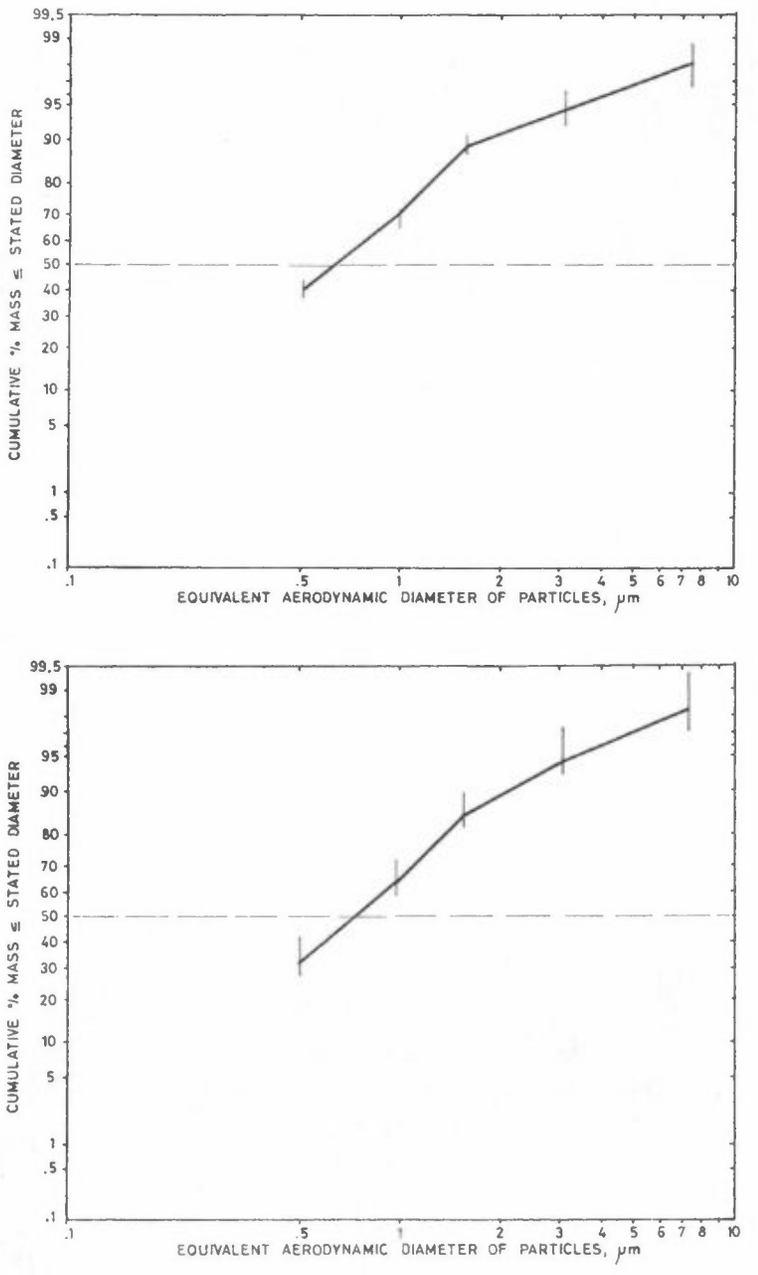

Figure 12: Average and range of cumulative size-mass distributions of NH_4-containing particles at Yssen, as measured by the high-volume Sierra cascade impactor during:

a) 17 January - 5 February 1976, and
b) 9 February- 25 February 1976

sampling periods.

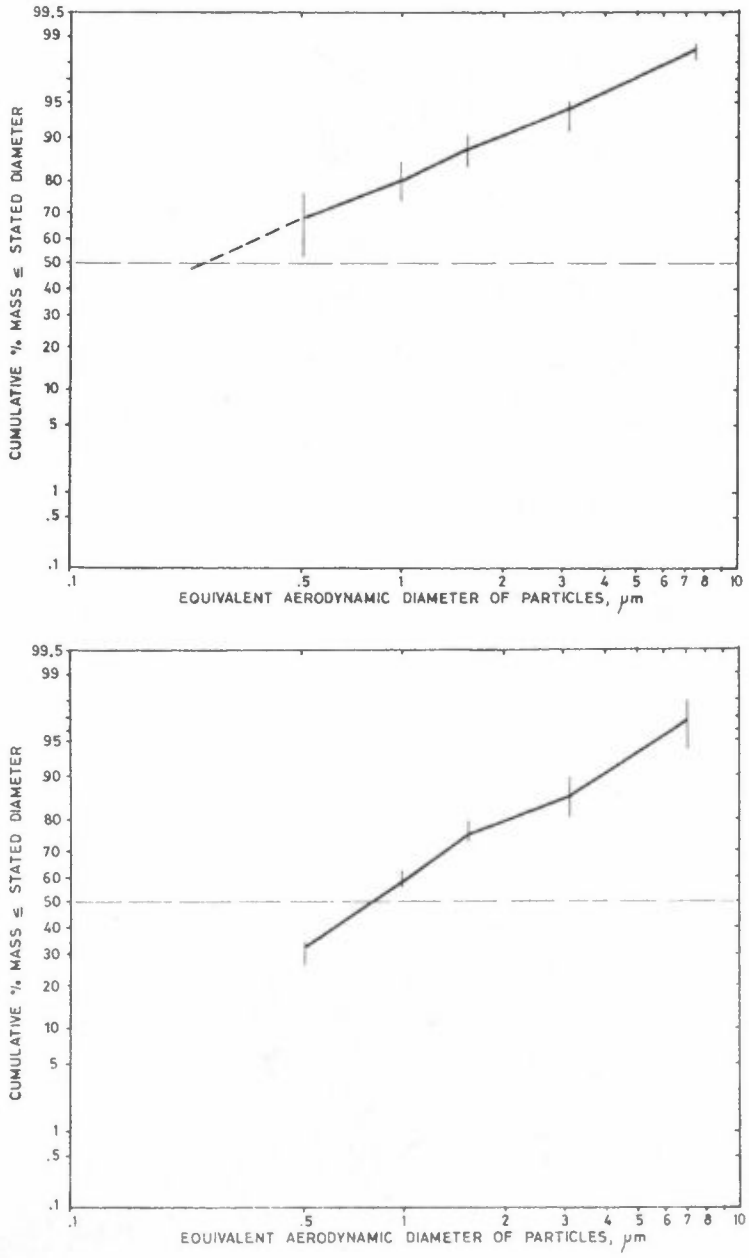

Figure 13: Average and range of cumulative size-mass distributions of Pb-containing particles at Yssen, as measured by the high-volume Sierra cascade impactor during:

a) 17 January - 5 February 1976, and
b) 9 February- 25 February 1976

sampling periods.

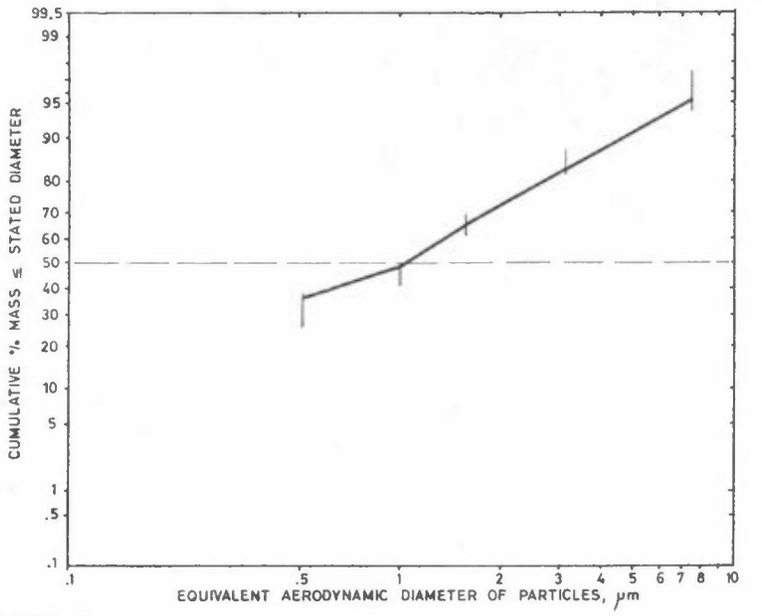

a)

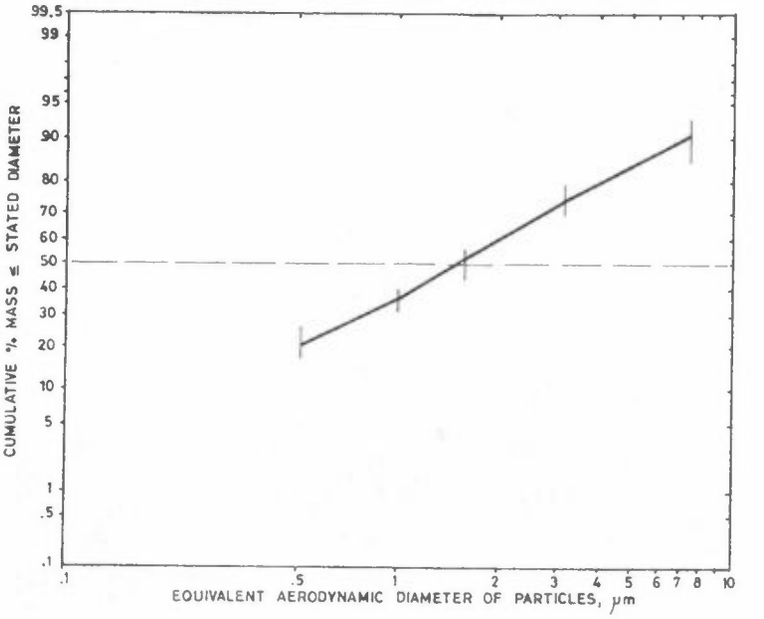

b)

Figure 14: Average and range of cumulative size-mass distributions of Cu-containing particles at Yssen, as measured by the high-volume Sierra cascade impactor during:

a) 17 January - 5 February 1976, and
b) 9 February- 25 February 1976

sampling periods.

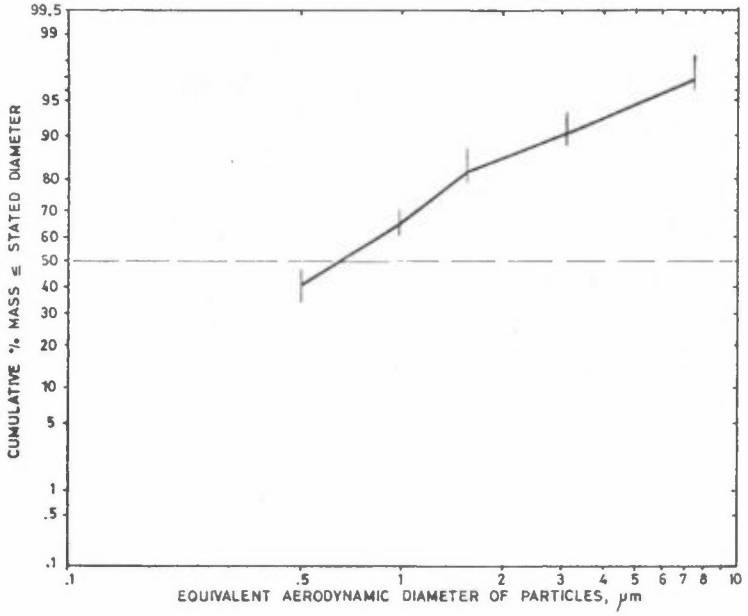

a)

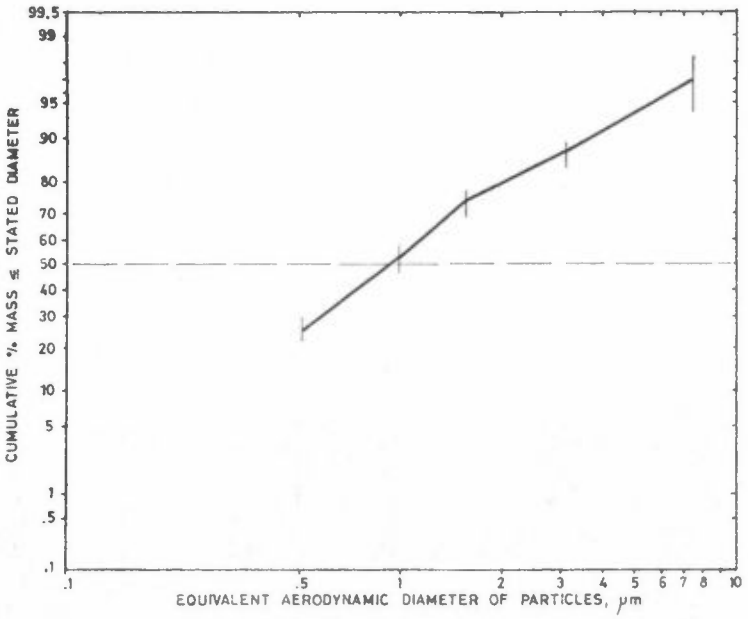

b)

Figure 15: Average and range of cumulative size-mass distributions of Zn-containing particles at Yssen, as measured by the high-volume Sierra cascade impactor during:

a) 17 January - 5 February 1976, and
b) 9 February- 25 February 1976

sampling periods.

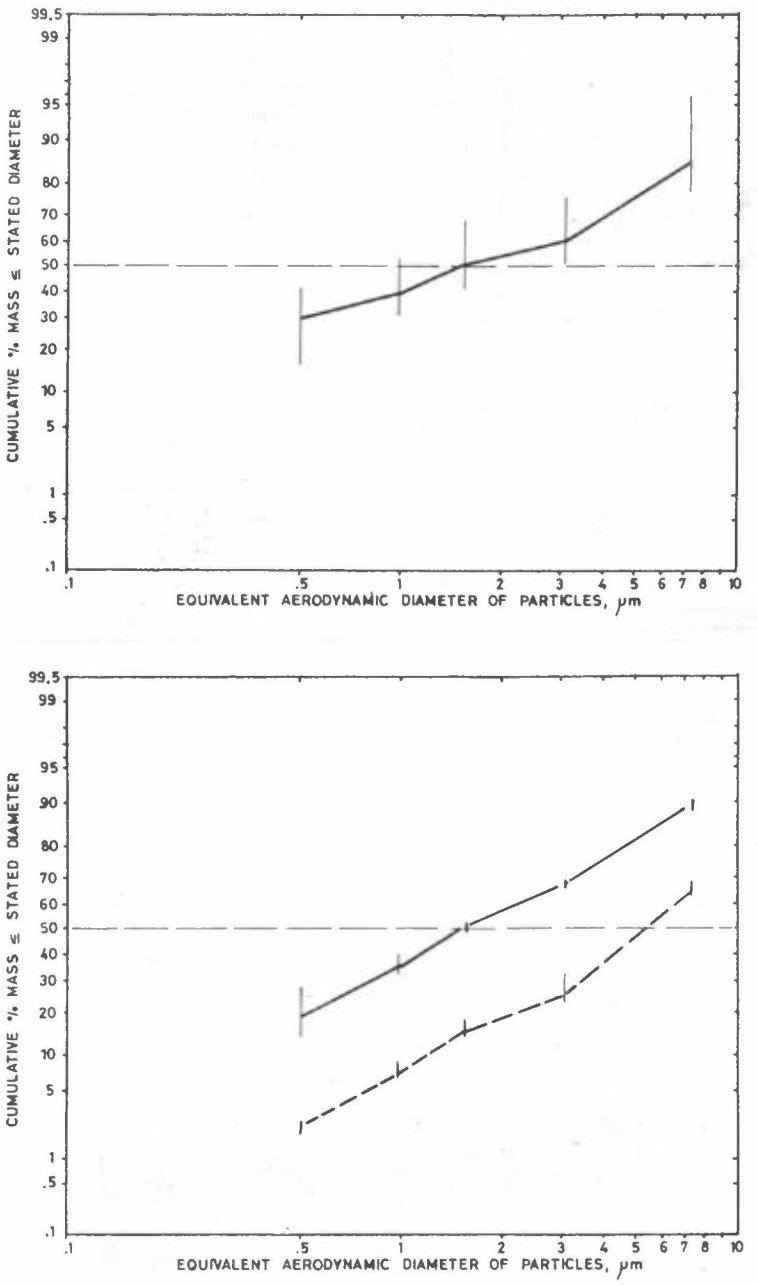

Figure 16: Average and range of cumulative size-mass distributions of water-leached Ca-containing particles at Yssen, as measured by the high-volume Sierra cascade impactor during:

a) 17 January - 5 February 1976, and
b) 9-13 February/17-21 February 1976 (– – –), and 13-17 February/21-25 February 1976 (———)

sampling periods.

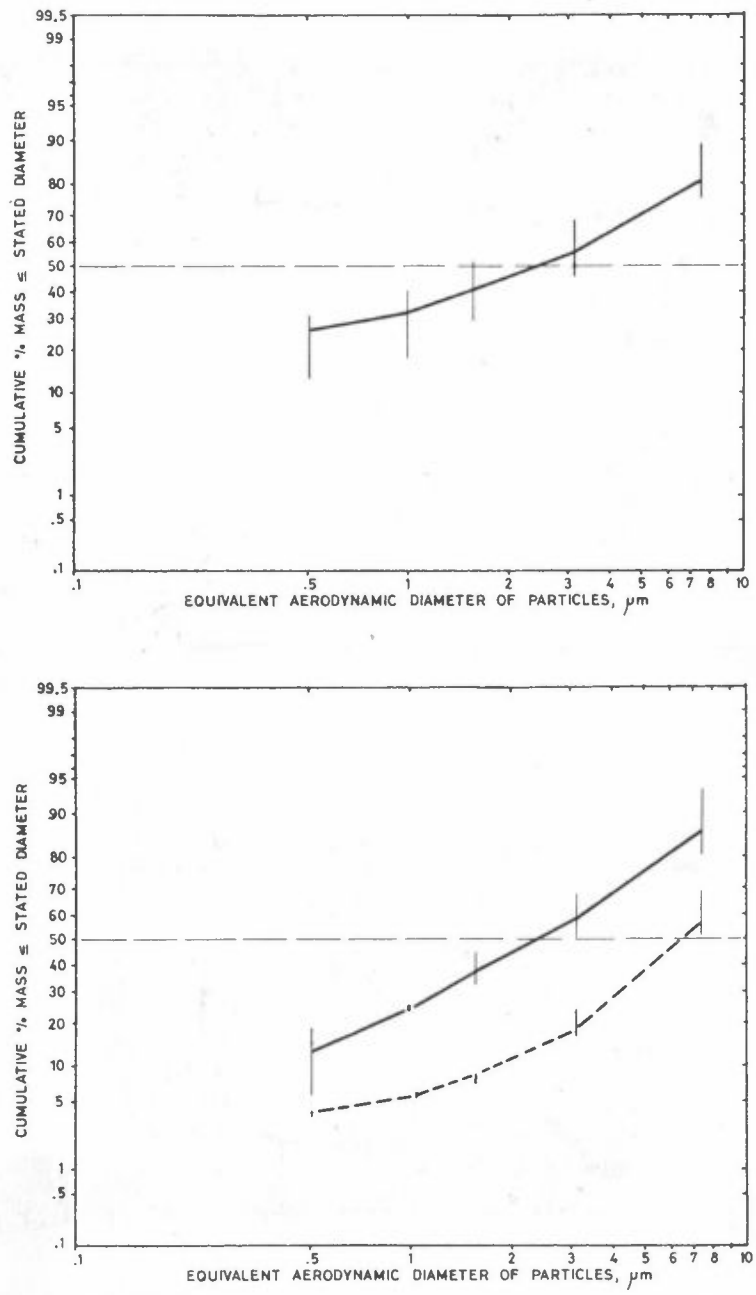

Figure 17: Average and range of cumulative size-mass distributions of acid-leached Ca-containing particles at Yssen, as measured by the high-volume Sierra cascade impactor during:

a) 17 January - 5 February 1976, and
b) 9-13 February/17-21 February 1976 (– – –), and 13-17 February/21-25 February 1976 (———)

sampling periods.

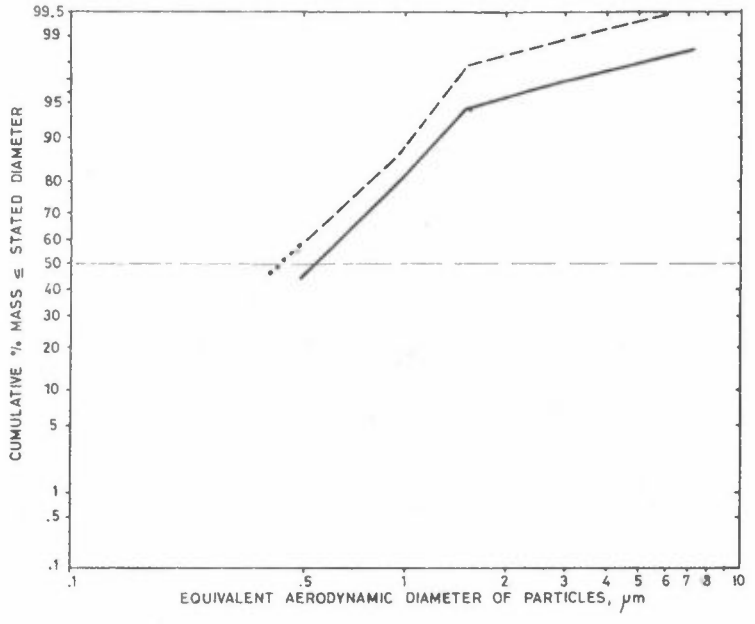

Figure 18: Cumulative size-mass distributions of benzo(a)pyrene (– – –) and total polycyclic aromatic hydrocarbons(——) in particles from the high-volume Sierra cascade impactor sampling at Yssen during the 5 February - 8 February 1976 period.*

**Analysis by the Central Institute for Industrial Research (SI).*

The MMD's in Table 2 were obtained from the 50% cumulative mass points on the plots for each separate sampling run (not shown; cf. Tables A4 through A10 in the Appendix for detailed data), and from Figures 11 through 17. In most cases the plots do not approximate log-normal distributions well, and the MMD's in Table 2 should, therefore, be regarded as estimated only. For the same reason, no attempt was made to evaluate geometric standard deviations for the various chemical components from their respective graphs.

Figures 19 through 26 show size-mass distribution data for the various chemical components in particles as "$\Delta M_i/M_T\Delta$ log D_i* versus particle diameter" histograms. These plots are normalized (to total concentration) so that the area under any portion of a histogram is proportional to the mass fraction in its corresponding particle diameter interval (cf. Table A13 in the Appendix for details).

Because of the large disparities in the durations of the sampling runs, the concentration averages for the 17 January - 5 February period are time-weighted. However, the sampling runs during the 5 February - 25 February period were of approximately equal lengths and arithmetic means of the measured concentrations are used for the averages.

The vertical bars in Figures 3 through 9 and Figures 10 through 17 show the extremes in measured values and indicate the variability in the distributions of the individual sampling runs.

Due to the doubtful validity of Cl, Na, and Mg measurements (cf. Sec. 5.2.3), size-mass distributions for these components are not included.

---

* ΔM_i = *mass concentration of component collected by the* i^{th} *stage of the impactor;*
M_T = *total mass concentration of component on Stages 1 through 5 of the impactor and after-filter;*
$\Delta logD_i$ = $log((ECD_{i-1}/(ECD_i))$.

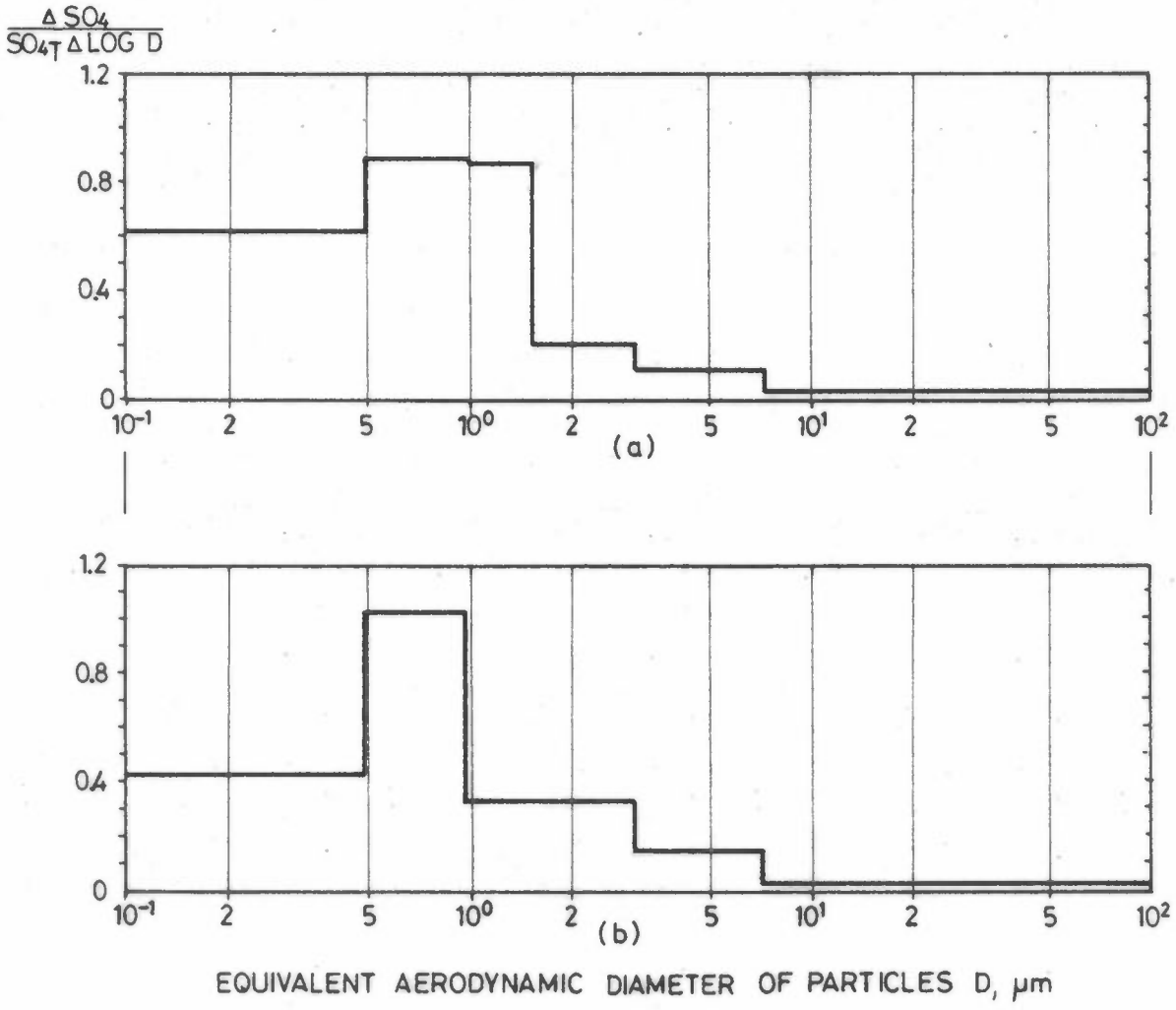

Figure 19: Size-mass histograms for SO_4-containing particles at Yssen, as measured by the high-volume Sierra cascade impactor during:

a) 17 January - 5 February 1976, and
b) 9 February- 25 February 1976

sampling periods.

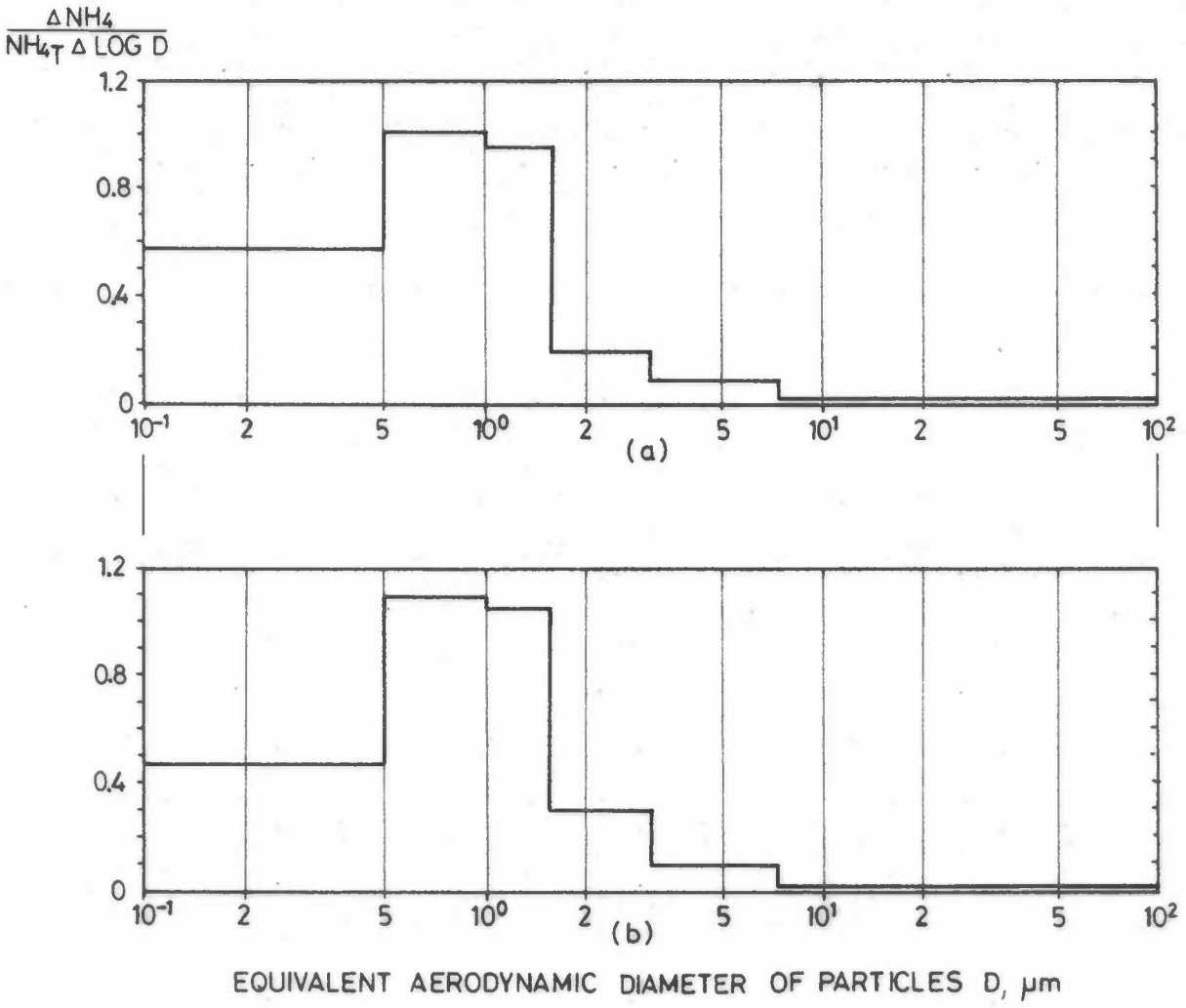

Figure 20: Size-mass histograms for NH_4-containing particles at Yssen, as measured by the high-volume Sierra cascade impactor during:

a) 17 January - 5 February 1976, and
b) 9 February- 25 February 1976

sampling periods.

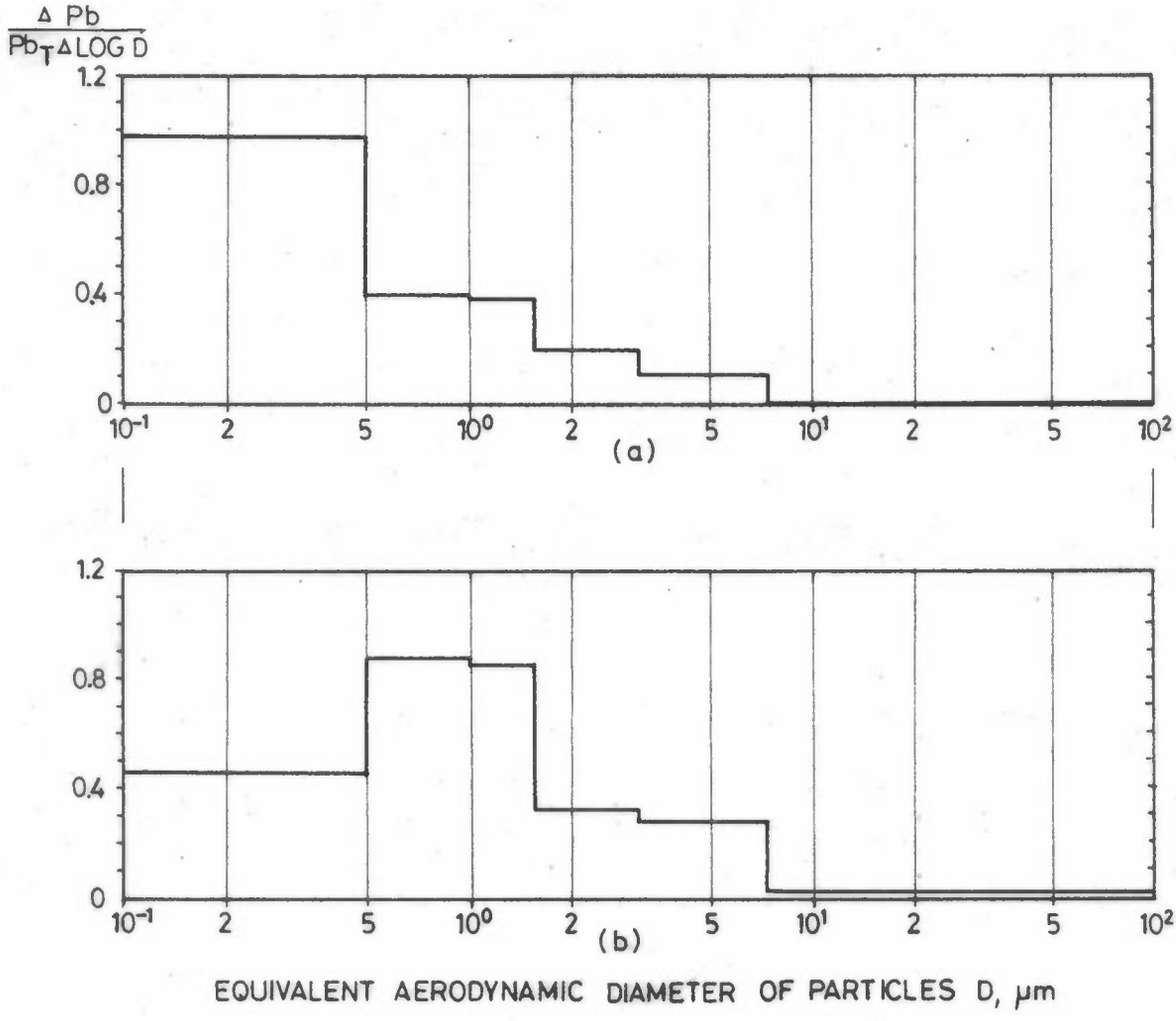

Figure 21: Size-mass histograms for Pb-containing particles at Yssen, as measured by the high-volume Sierra cascade impactor during:

a) 17 January - 5 February 1976, and
b) 9 February- 25 February 1976

sampling periods.

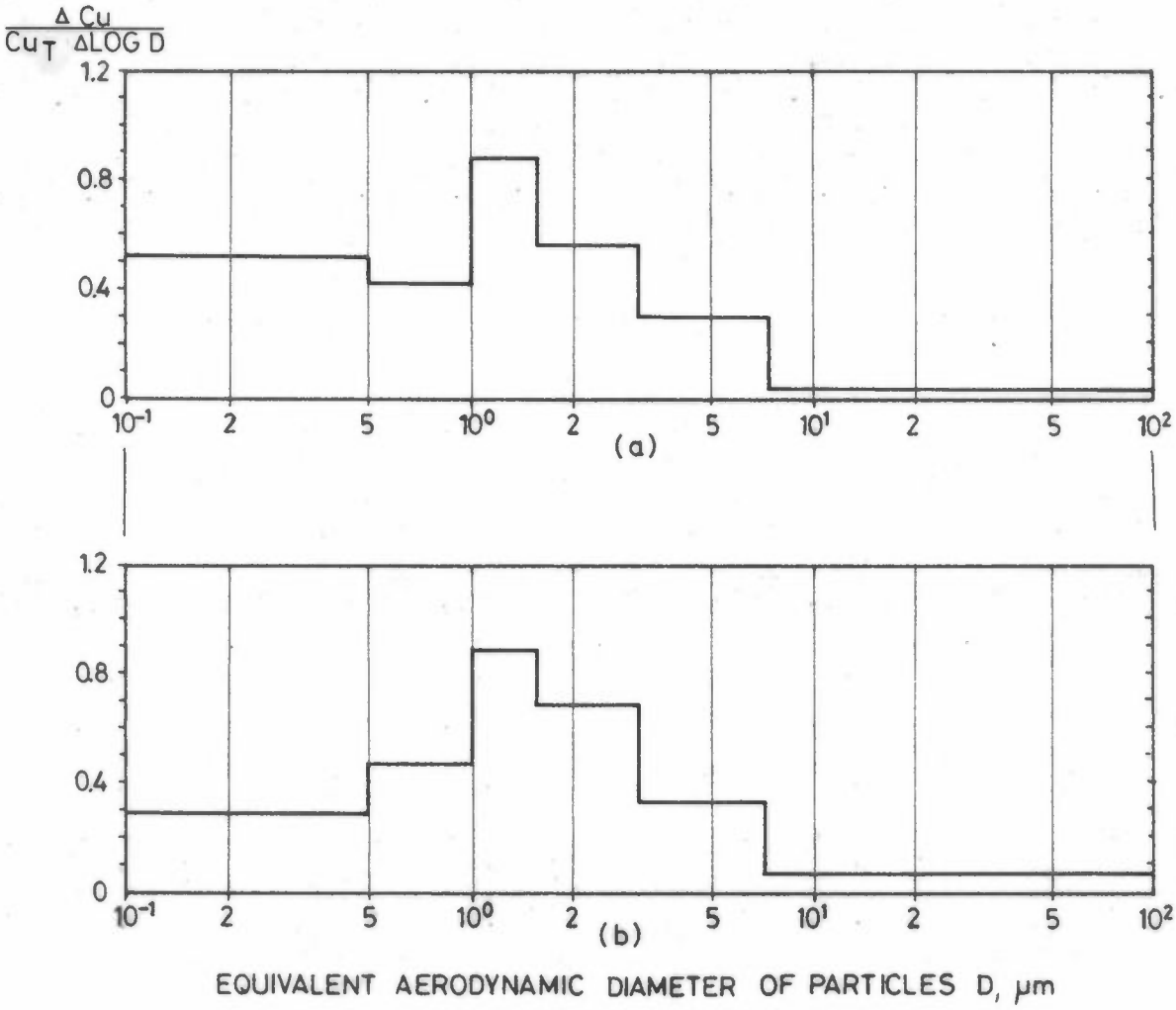

Figure 22: Size-mass histograms for Cu-containing particles at Yssen, as measured by the high-volume Sierra cascade impactor during:

a) 17 January - 5 February 1976, and
b) 9 February- 25 February 1976

sampling periods.

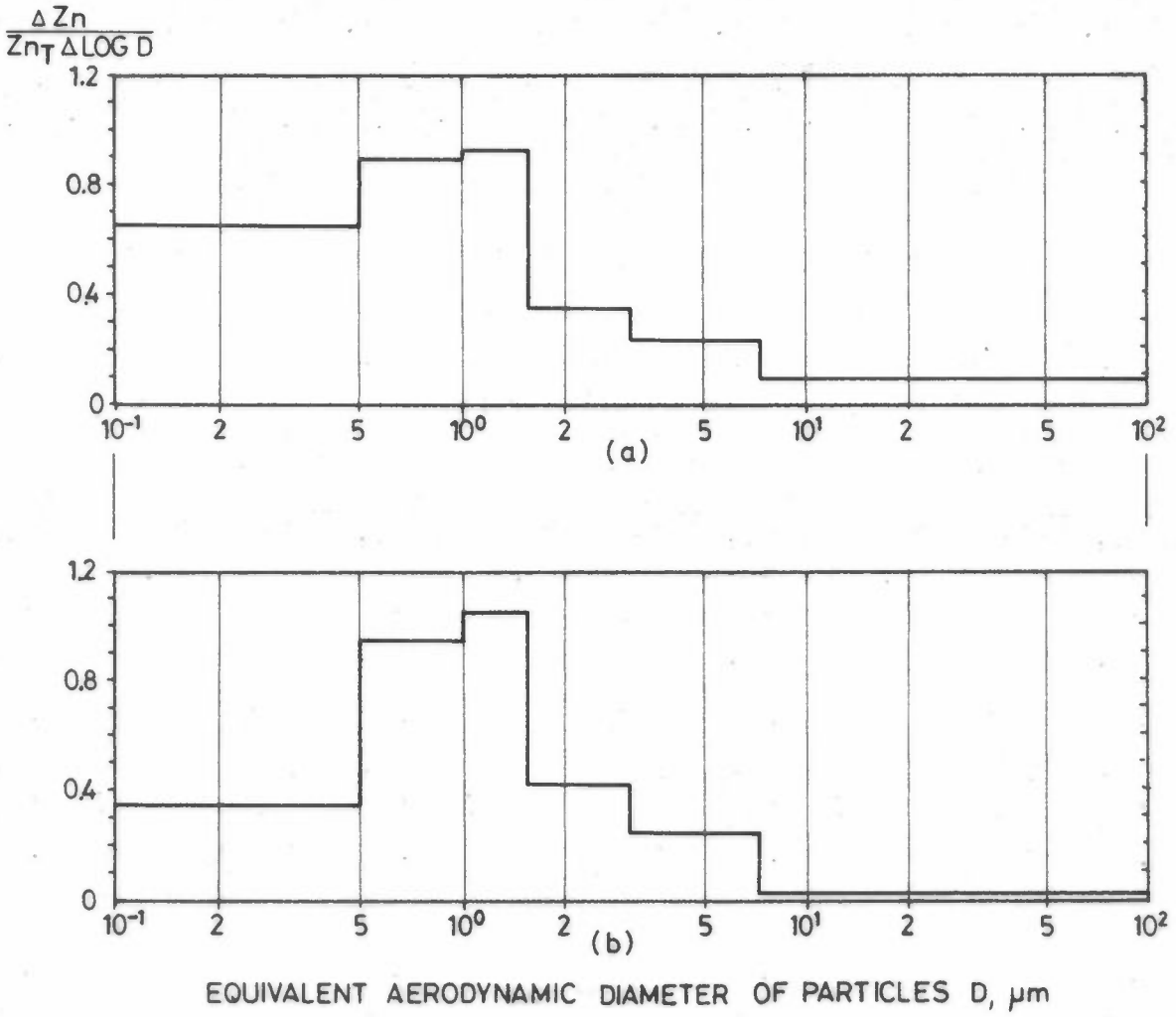

Figure 23: Size-mass histograms for Zn-containing particles at Yssen, as measured by the high-volume Sierra cascade impactor during:

a) 17 January - 5 February 1976, and
b) 9 February- 25 February 1976

sampling periods.

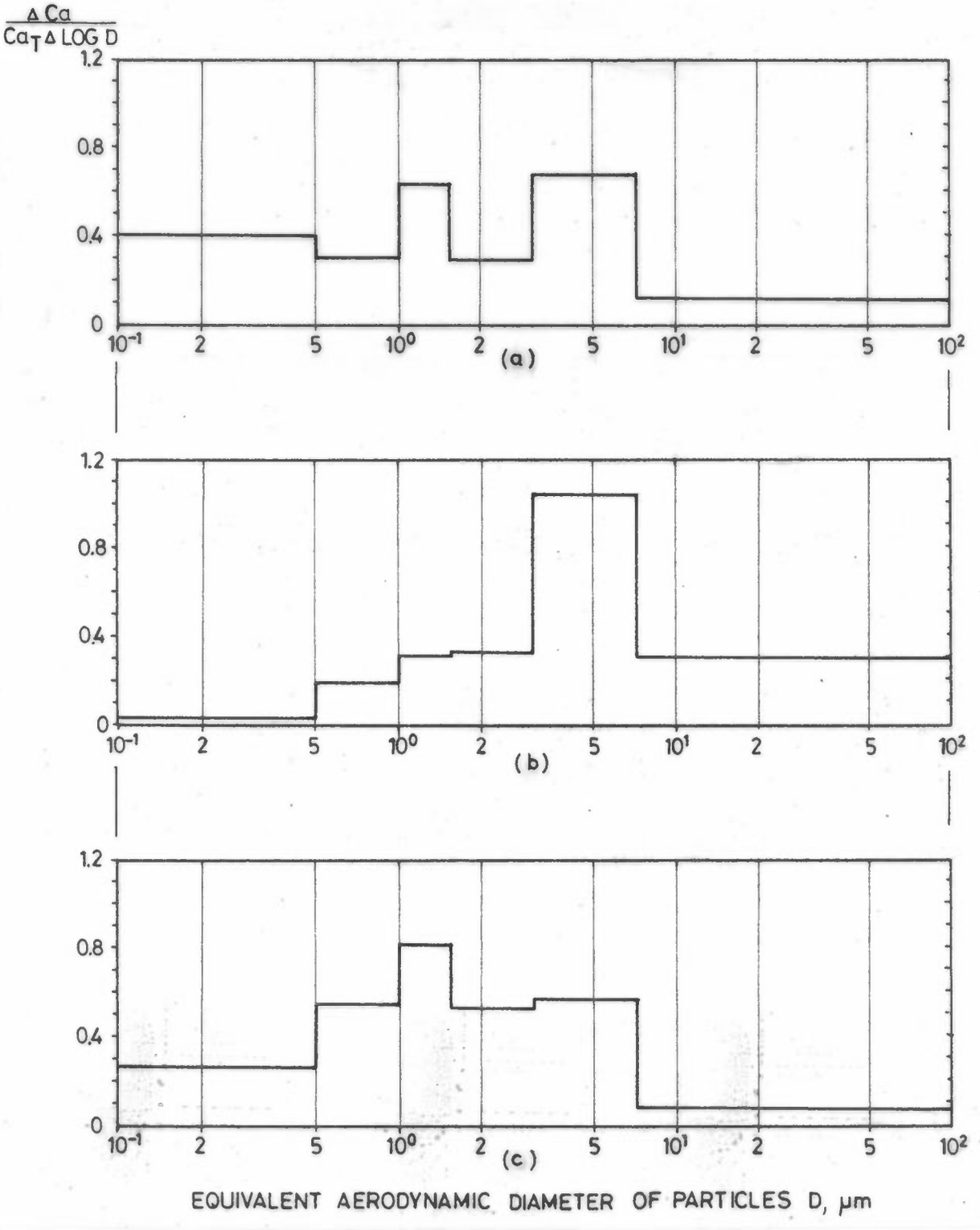

Figure 24: Size-mass histograms for water-leached Ca-containing particles at Yssen, as measured by the high-volume Sierra cascade impactor during:

a) 17 January - 5 February 1976, and
b) 9-13 February/17-21 February 1976, and
c) 13-17 February/21-25 February 1976

sampling periods.

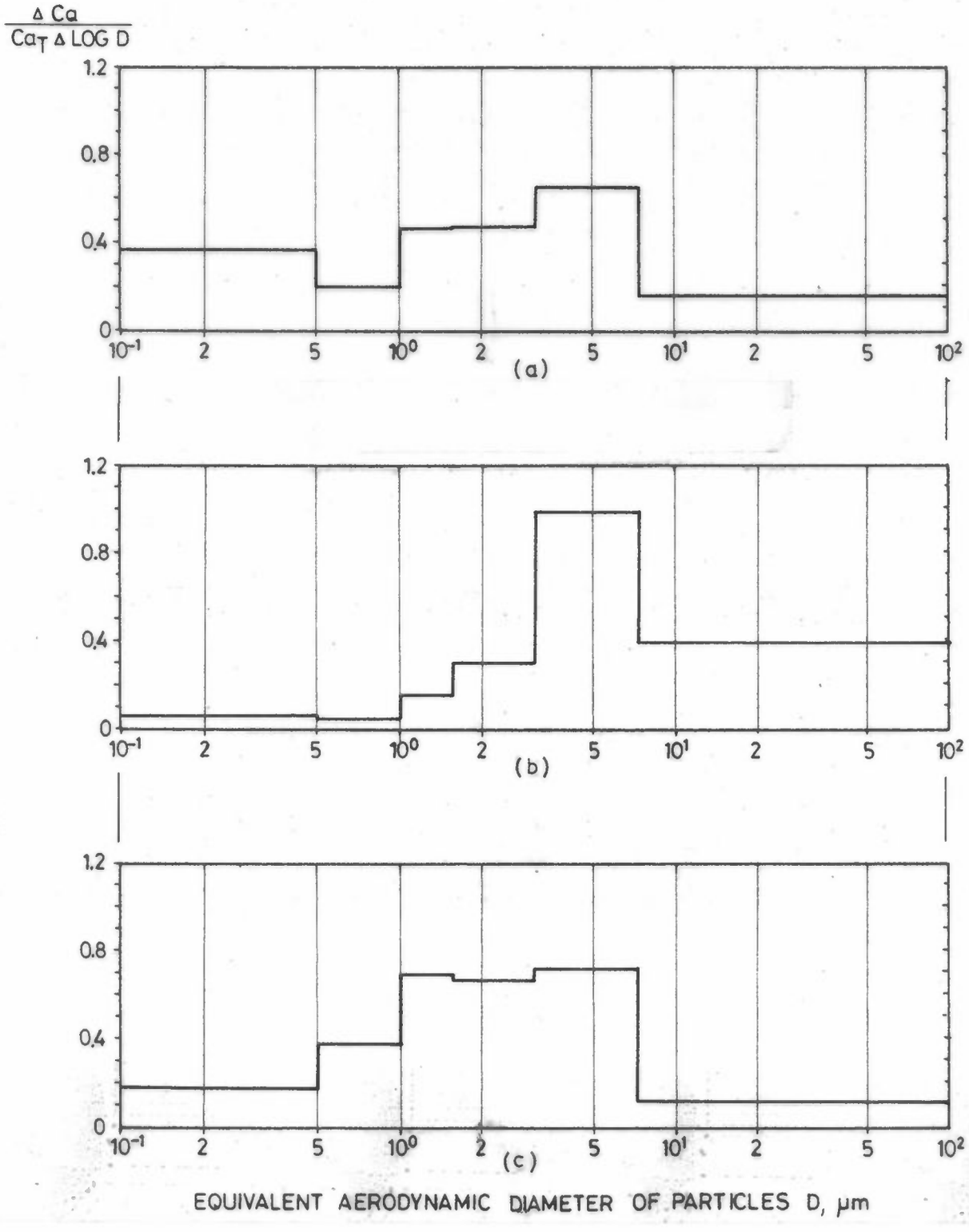

Figure 25: Size-mass histograms for acid-leached Ca-containing particles at Yssen, as measured by the high-volume Sierra cascade impactor during:

a) 17 January - 5 February 1976, and
b) 9-13 February/17-21 February 1976, and
c) 13-17 February/21-25 February 1976

sampling periods.

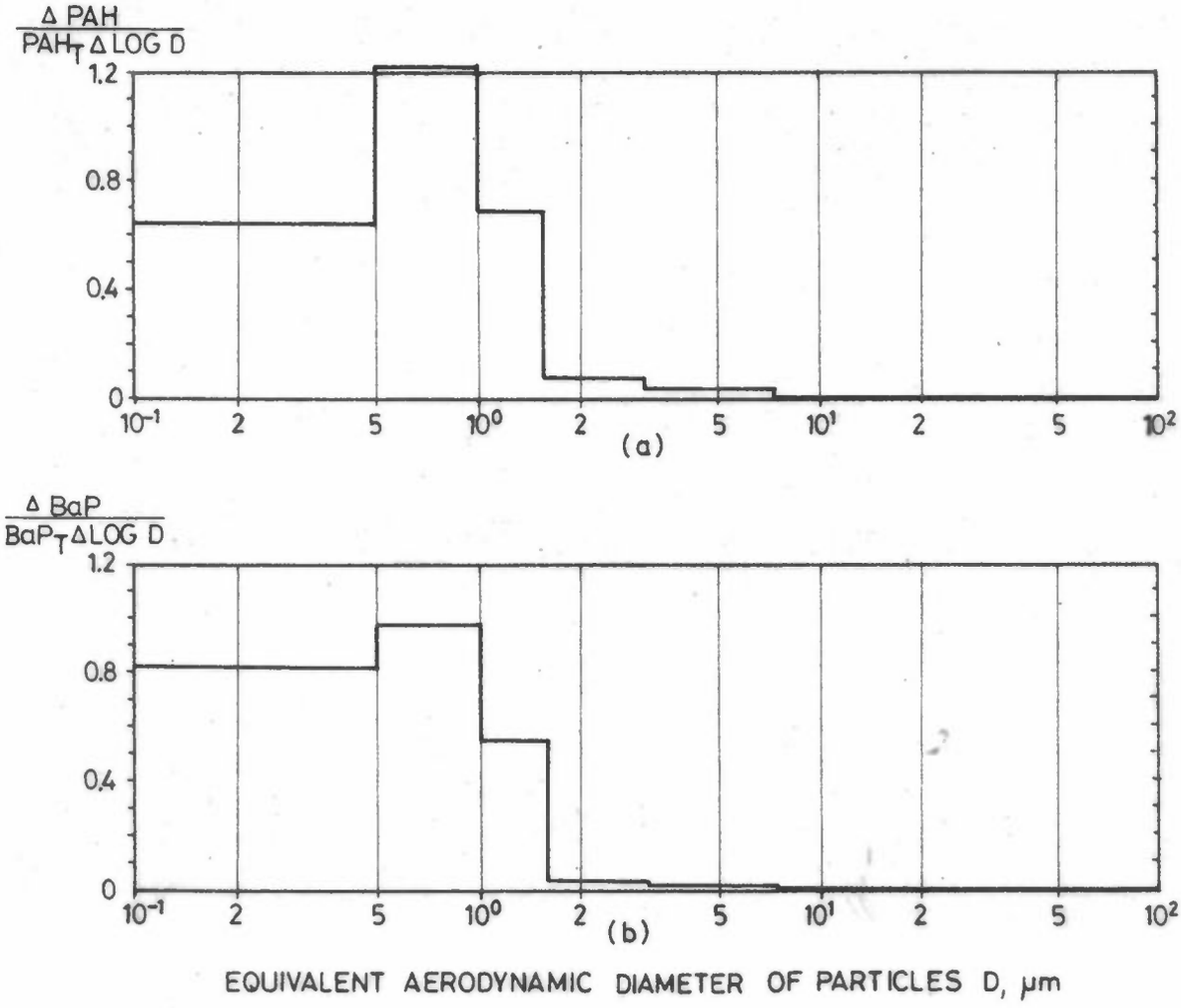

Figure 26: Size-mass histograms for benzo(a)pyrene (BaP) and total polycyclic aromatic hydrocarbons (PAH) in particles from the high-volume Sierra cascade impactor sampling at Yssen during the 5 February - 9 February 1976 period:*

a) PAH
b) BaP

**Analysis by the Central Institute for Industrial Research (SI).*

The separation of the measurement results in two time intervals was done, because of the use of two types of impactor stage substrates (cellulose Whatman 40 and glass-fibre Gelman Spectrograde). The distributions of water- and acid-leached calcium for the 9-25 February periods are presented (in Figs. 8(b) and 9(b)) in two further groupings (cf. Sec. 5.2.2).

5 DISCUSSION OF MEASUREMENT RESULTS

Except for the improved atmospheric ventilation during three short periods of thaw, the weather conditions throughout the 5-week measurement programme were characterized by weak winds and thermal stability that ranged from very stable to neutral (cf. Table 3). With stagnation prevailing, long range transport of airborne particles to the sampling site was probably not significant, and, with the ground remaining largely snow-covered, regional anthropogenic sources were the likely contributors. Industrial and commercial activities, emissions from motor vehicles, and particularly increased home heating with fuel oil during days of freezing temperatures were the major probable sources in the area.

5.1 Mass concentrations

With the exception of SO_4, and probably Ca, the measurement results show no major variations in airborne particle concentrations during the sampling periods, suggesting that most of the chemical constituents were associated with relatively week and widespread sources. Similarly there were no pronounced trends in the concentrations with time. Apparently the brief interludes of thaw with stronger winds prevented any significant buildups of atmospheric concentrations during the general stagnation.

Table 3: Average conditions of wind, air temperature, and stability at the Yssen site during the 17 Jan. - 25 Feb. 1976 sampling periods.

	Air temp.[+] °C		Wind speed[++] m/s		Estimated[+++] atmospheric stability	Approximate wind direction	Remarks
	Mean	Range	Mean	Range			
17 Jan. - 23 Jan	- 4.2	+4.1/-12.0	1.6	0.0/6.7	Very stable	W, N and NW	During a thaw on 20 Jan. winds from SE with speed up to 6.7 m/s
23 Jan. - 30 Jan.	-12.0	-0.1/-16.7	0.7	0.0/2.1	Stable	W and NW	
30 Jan. - 3 Feb.	-14.9	-0.1/-18.7	0.5	0.0/0.8	Stable to neutral	Mainly W	
3 Feb. - 5 Feb.	-12.1	-5.9/-19.0	1.0	0.0/2.6	Neutral	W, NW and SE	
5 Feb. - 9 Feb.	-10.7	-4.1/-17.9	0.6	0.0/1.5	Stable	N, NW and E	
9 Feb. - 13 Feb.	- 1.4	+2.1/-4.5	2.2	0.0/5.7	Neutral	S and SE	Thaw on 10 Feb.; rain, sleet and snow on 10-12 Feb. with winds up to 5.7 m/s after the thaw winds from the N.
13 Feb. - 17 Feb.	- 4.8	-0.9/-11.1	1.7	0.1/4.7	Neutral	W, N and SE	Fog and heavy hoar frost on 16 Feb.
17 Feb. - 21 Feb.	- 3.8	-1.6/-7.4	0.7	0.0/2.0	Neutral to stable	Mainly N	Small amounts of snow on 18-19 Feb.
21 Feb. - 25 Feb.	- 0.4	+8.3/-3.2	1.7	0.0/6.7	Neutral	W, SW and S	Thaw and some rain on 24-25 Feb.

[+] at 1.2 m above ground

[++] at 4.2 m above ground

[+++] estimated from air temperature differences between 1.2 m and 4.2 m levels

5.1.1 Water-soluble sulphate and ammonium

The adjusted concentrations (cf. Sec. 4.1) of sulphate (SO_4) ranged from about 2.6 $\mu g/m^3$ to 12.8 $\mu g/m^3$ for the eight sampling runs. The overall average concentration for the entire measurement period, corresponding to about a monthly average, was 7.8 $\mu g/m^3$. The concentrations for the individual runs were somewhat higher during the later part of the measurements (9-25 February). Since southerly winds were more frequent during this period, these concentrations may reflect the influence of the domestic and commercial heating sources immediately south of the site.

A comparison of Hi-Vol/Sierra adjusted concentrations with those available from NILU's automatic air sampler for three corresponding periods (cf. Table 1) shows an agreement within 10%. This can be considered quite good, because the two samplers and the analytical methods (X-ray fluorescence for the NILU samples)were distinctly different. This would also indicate, that while having a lower intake efficiency for aerodynamically large particles in high winds than the Hi-Vol sampler (VITOLS, 1977), NILU's air sampler is performing satisfactorily when sampling sulphate-containing particles under weak wind conditions. Both the total and adjusted concentrations of SO_4 include any possible contributions from airborne sea salt. In sea salt the ratio of, for example, $Cl/SO_4 = 7.16$, so that the mass of SO_4 in sea salt particles can be expected to be about 14% that of Cl. Thus, if Cl (or any other typical sea salt components, e.g., Na or Mg) mass concentration is measured concurrently with SO_4, "excess SO_4" can be obtained by subtracting sea salt SO_4 from the measured SO_4 concentrations. Due to the uncertain validity of Cl, Na, and Mg measurements (cf. Sec. 5.1.3), excess SO_4 concentrations are not given, but, excluding the two sampling runs for which sample contamination for Cl and Na is suspected, sea salt SO_4 corrections would amount to less than 2%.

Adjusted concentrations of ammonium (NH_4) are not available, but total concentrations during the eight sampling runs ranged from 1.2 $\mu g/m^3$ to 3.5 $\mu g/m^3$, with the monthly average of about 2.1 $\mu g/m^3$. There was only a slight increase in concentrations during the 9-25 February periods.

It is now generally accepted (e.g., MCKAY, 1969; CHARLSON et al., 1973; BROSSET, 1976) that water-soluble SO_4 in aged airborne particles is mostly in the form of ammonium salts, e.g. NH_4HSO_4, $(NH_4)_3H(SO_4)_2$, but principally $(NH_4)_2SO_4$. In Figure 27, total mass concentration pairs of SO_4 and NH_4 of the various sampling runs at Yssen, as well as the paired averages for the 17 January - 5 February and 9 February - 25 February periods are plotted. The two straight lines in the figure represent the ratios of SO_4/NH_4 in pure NH_4HSO_4 (5.33) and pure $(NH_4)_2SO_4$ (2.67). It can be seen that, with one exception (23-30 January run), the measured concentration pairs indicate sulphate particles somewhat deficient in SO_4 during the 17 January - 5 February period, perhaps due to the presence of other water-soluble ions, such as NO_3. All the 9-25 February period pairs (as well as that of 23-30 January) are bracketed by the pure NH_4HSO_4 and $(NH_4)_2SO_4$ lines (cf. also Sec. 5.2.1). It would be expected, that with snow covered ground and farm animals confined to shelter, less ammonia (NH_3) is available from biological activity in wintertime for the more acid particle neutralization. One minor nearby source of NH_3 was a small sheep barn only some 65 m to the southeast of the sampler. However, since southerly wind directions were more frequent during the 9-25 February sampling periods, this local source had obviously no effect on the composition of the airborne particles. The samples collected at Yssen were not analyzed for H^+ concentrations; thus it cannot be further speculated, along the lines suggested by BROSSET et al. (1975), whether the sulphate particles during the 9-25 February period might have been largely composed of NH_4HSO_4 or $(NH_4)_3H(SO_4)_2$.

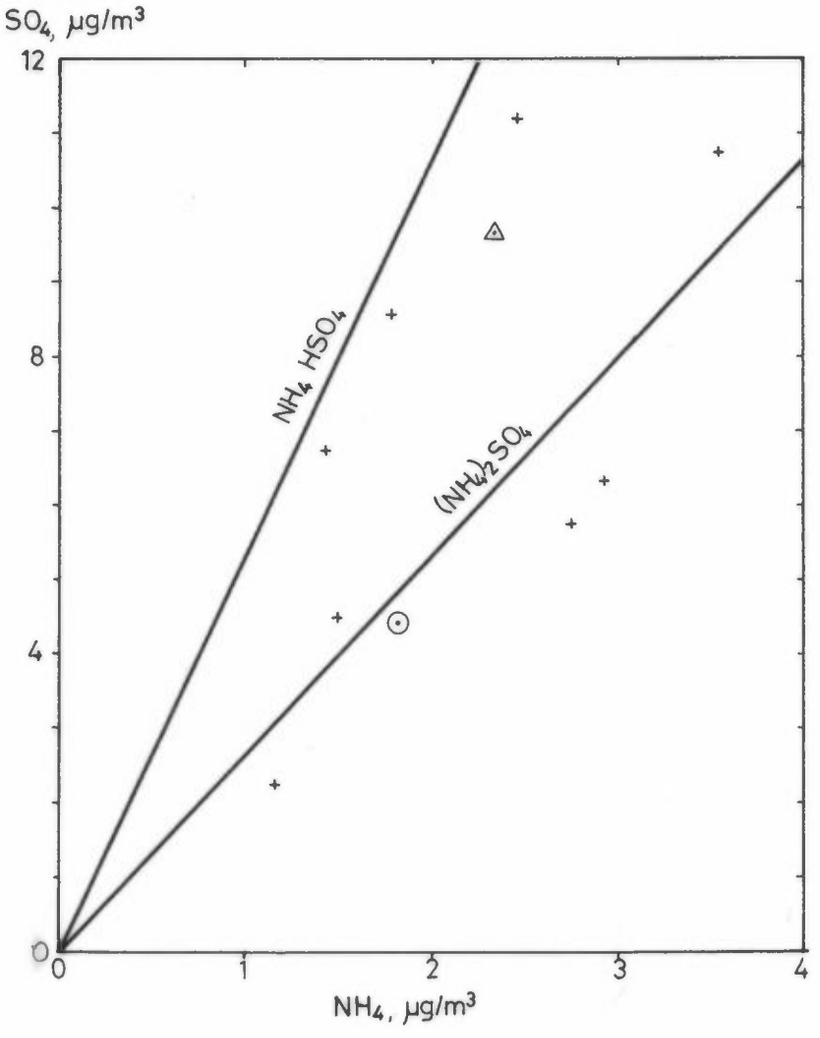

Figure 27: SO_4 and NH_4 total concentration pairs, as measured at Yssen during the eight sampling periods, 17 January - 25 February 1976.

⊙ *17 Jan. - 5 Feb. average*

△ *9 - 25 Feb. average*

5.1.2 Lead, copper, zinc, and calcium

The adjusted concentrations of lead (Pb) for the various sampling runs ranged from 0.12 to 0.20 $\mu g/m^3$, with the monthly average of about 0.14 $\mu g/m^3$.

A comparison with corresponding results from the NILU sampler shows a reasonable agreement for only one of the runs (cf. Table 1). The differences for the other two runs were about 20% and 60%, with the results from the NILU sampler being the lower. No reason for these discrepancies can be given, because Pb- and SO_4-containing particles have approximately the same aerodynamic sizes (cf. Table 2), and the NILU sampler should sample Pb particles with equal or even better efficiency, than sulphate.

The adjusted concentrations of copper (Cu) ranged from about 0.11 to 0.22 $\mu g/m^3$, with a monthly average of 0.14 $\mu g/m^3$. Hi-Vol sampler measurements of Cu are usually suspect, because of the possibility of sample contamination by Cu particles from wear of the sampler pump motor windings. The much-quoted account of this potential source of contamination (HOFFMAN & DUCE, 1971), however, referred to a different type of sampler, while one specific to the Hi-Vol sampler has not received wide dissemination (KING & TOMA, 1975). Although the question of copper generation can be resolved by a simple experiment (say, by connecting two Hi-Vol samplers in series), the extent of sample contamination under a variety of meteorological conditions would be considerably more difficult to quantify.

The adjusted concentrations of zinc (Zn) varied from about 0.08 to 0.16 $\mu g/m^3$, with a monthly average of 0.10 $\mu g/m^3$. Airborne zinc particles can result from the normal wear of automotive tire tread rubber (CARDINA, 1974; PIERSON & BRACHACZAK, 1974; DANNIS, 1974), burning of tires, and the operations of iron and steel industry. The mass concentration ratio of Zn/Pb at Yssen is about twice as high, as the maximum ratio (0.43) between tire and auto exhaust particulates in

traffic tunnels (PIERSON & BRACHAZCEK, 1974), suggesting additional sources of Zn-containing particles at this rural site (cf. also Sec. 5.2.2).

The adjusted water-leached Ca concentrations ranged from 0.06 to 0.82 $\mu g/m^3$, with a monthly average of about 0.25 $\mu g/m^3$. Adjusted concentrations are not available for acid-leached Ca, but the total concentrations varied from 0.10 to 0.60 $\mu g/m^3$, with a monthly average of 0.21 $\mu g/m^3$, as compared to a total concentration range of 0.10 to 0.66 $\mu g/m^3$ and an average of 0.20 $\mu g/m^3$ for water-leached Ca.

Soil dust is a common source of airborne Ca, and there might have been some rapid drying of soil and resuspension of dust by the relatively strong winds from the few bare spots on the ploughed field surrounding the sampler during the periods of thaw. Indeed, the highest Ca concentration was measured during the 9-13 February run, which included a 20-hour period of thaw. On the other hand, the other two thaws, although of longer durations and more intense, apparently had no such pronounced effect on Ca concentrations, so that contamination of the 9-13 February sample cannot be ruled out (cf. also Sec. 5.2.2). If the single high concentration value is excluded, the monthly averages are 0.17 $\mu g/m^3$ for the adjusted water-leached Ca, and 0.14 $\mu g/m^3$ and 0.15 $\mu g/m^3$ for total water- and acid-leached Ca, respectively.

Another oddity in the Ca measurements is the result, that for all runs during the 9-25 February period water-leached Ca concentrations exceeded those for acid-leached Ca. Since acid leaches would extract both water-soluble and insoluble Ca, the reason for the low acid-leached Ca values is not known.

5.1.3 Chloride, sodium, and magnesium

Chloride (Cl), sodium (Na), and magnesium (Mg) are major constituents of sea water, and their presence in airborne particles at inland locations is largely due to transported sea salt. The relative proportions of these elements (i.e., their mass ratios) in sea water are remarkably constant, but are often modified in airborne sea salt (JUNGE, 1972). For example, Cl has been found both enriched (HIDY et al., 1974) and depleted (MARTENS et al., 1973) with respect to Na.

The Hi-Vol/Sierra measurements at Yssen show two sampling periods with conspicuously high concentrations of Cl, Na, and Mg (cf. Table 1). Unfortunately, results from NILU's automatic air sampler* are not available for the same periods. In addition to sea salt, some Cl could come from automotive emissions and the burning of PVC compounds, but land sources for Na and Mg are not readily identified. Winds during the high concentration periods (9-13 February and 13-17 February) were occasionally southerly, but the adjusted concentrations of Cl and Na, particularly for the second period (8.3 and 7.8 $\mu g/m^3$, respectively) are remarkable, because the site is at least 100 km from the nearest body of salt water in that direction, and the winds were light. Airborne sea salt concentrations have been shown to decay rapidly with distance inland (e.g., SEMONIN, 1972), and the concentrations measured at Yssen would imply unrealistic generation rates for the airborne sea salt during the two periods.

In an attempt to ascertain, whether sample contamination was the reason, ratios of Cl/Na, Cl/Mg and Na/Mg (cf. Table A13 in the Appendix) and cumulative size-mass distributions (not shown) for all sampling runs were examined. No consistent proof of contamination is apparent. Ratios of Cl/Na from Hi-Vol/Sierra sampling indicate Cl depletion with respect to Na for most of

---

*available samples were analyzed only after about 1½ year storage period.

the runs, but enrichment for the available samples from the NILU sampler. Results from both samplers show enrichment for Cl and Na with respect to Mg. The cumulative size-mass distribution plots gave MMD's of Cl- and Na-containing particles from about 0.3 to 7 μm, and from 1.5 to 3 μm for Mg. The largest MMD's for Cl and Na were measured during the 9-13 February run, but not for Mg. This would point to possible contamination by NaCl, but on the other hand the elemental ratios of that particular run were nearest to those of sea salt. Thus, no satisfactory explanation for the anamolous concentrations, as measured by the Hi-Vol/Sierra impactor, can be offered at this time.

5.1.4 Polycyclic aromatic hydrocarbons

A single sample from the 5-9 February run was analyzed by the Central Institute for Industrial Research (SI) for 24 species of polycyclic aromatic hydrocarbons. Thus, no average concentrations or trends are available. During 5-9 February the total concentrations of the various species ranged from a low of 22 pg/m^3 for dibenzofuran to about 3960 pg/m^3 of benzo(b&k)fluoranthene.

5.2 Size distributions

Period-to-period differences in the concentrations of the various chemical constituents in airborne particles sometimes tend to obscure size-mass relationships presented in terms of mass distributions over the aerodynamic diameter intervals (Figs. 3 through 10). Log-normal distribution plots (Figs. 11 through 18) and normalized size-mass histograms (Figs. 19 through 26) illustrate the relationships without being affected by the absolute magnitudes of concentrations. It is realized, however, that particles generated by a single production mechanism only (e.g., gas-to-particle conversion and coagulation, condensation of vapours on existing particles, disruption of bulk materials

and resuspension of settled particles) may result in log-normal distributions. Away from single type of sources of production, a measured distribution of airborne particles is likely a resultant of several individual log-normal distributions (WHITBY & CANTRELL, 1975; KELKAR & JOSHI, 1977), corresponding to an "aged" mixture of particles from the different generation processes present. Such mixtures of airborne particles frequently have bimodal mass or volume distributions (WHITBY & CANTRELL, 1975), with a "saddle point" in the 1 to 3 µm diameter range, separating the "fine" and the "coarse" particle fractions. The presence of multimodal features in mass distributions can best be discerned when measurement data are presented as dM/dlogD *versus* particle diameter (D) plots. The quantity dM/dlogD can be approximated from cascade impactor data, stage by stage, as $\Delta M_i/\Delta \log D_i$, or, normalized to the total concentration, M_T, as $\Delta M_i/M_T \Delta \log D_i$, where "i" indicates the i^{th} stage of the impactor (Figs. 19 through 26). Doubts have been expressed, whether the relatively narrow size fractionation ranges and low resolution of most cascade impactors permit reliable definition of multimodal features from impactor measurements alone (LEE & GORANSON, 1976; MCCAIN *et al.*, 1977). Nevertheless, the procedure has been used for urban and background aerosol assessment (e.g., PATTERSON & WAGMAN, 1977). It requires the selection of the upper and lower ECD's for the sampling system to enable the construction of the "tails" of the distribution. For this study, the ECD's for the impactor after-filter and the Hi-Vol sampler shelter inlet were arbitrarily set at 0.10 µm and 100 µm, respectively. The glass-fibre after-filters have a collection efficiency in excess of 99% for particles as small as 0.3 µm in diameter (DOP test). Recent studies of intake efficiencies of Hi-Vol samplers (LUNDGREN & PAULUS, 1975; WEDDING *et al.*, 1977) have found the shelter ECD around 60 µm diameter for wind speeds up to 5 m/s. In view of the stagnant conditions prevailing throughout most of the sampling runs and the relatively small aerodynamic diameters of particles, the choice of the above cut-off

limits seems justified. Thus, the areas included in the end segments, in Figures 19 through 26, are representative of the fractions of mass of the various chemical components in particles below 0.5 μm and above 7.4 μm diameters.

With the exception of Ca, and perhaps Cu, all the trace elements and water-soluble ions in airborne particles were contained in the fine particle fraction, also referred to as the "accumulation mode" (WHITBY & CANTRELL, 1975). These particles, although produced by gas-to-particle conversion and coagulation, are relatively stable and long-lived.

No clear-cut bimodal mass distributions are apparent, but the very long sampling periods could have resulted in varying reentrainment and/or particle bounce from stage to stage (cf. Sec. 5.2.2 and 6.4). Similarly, uncertainties in substrate and after-filter blanks may have caused size distribution distortions.

5.2.1 Water-soluble sulphate and ammonium

Figure 28 shows the cumulative size-mass distribution averages of both SO_4- and NH_4-containing particles for the 17 January - 5 February and 9 - 25 February periods. The shapes of the SO_4 distributions agree well with those of NH_4, and similar agreement can also be seen in Figures 3 and 4, and Figures 19 and 20. It would thus appear, that both SO_4 and NH_4 were contained in the same particles, most likely in the form of NH_4HSO_4 and $(NH_4)_2SO_4$.

There are some differences in the MMD's of the two substances for the different sampling runs (cf. Table 2), but the averages fall within a narrow range between 0.6 and 0.8 μm, which also approximately coincides with the broad mass modes (Figs. 19 and 20).

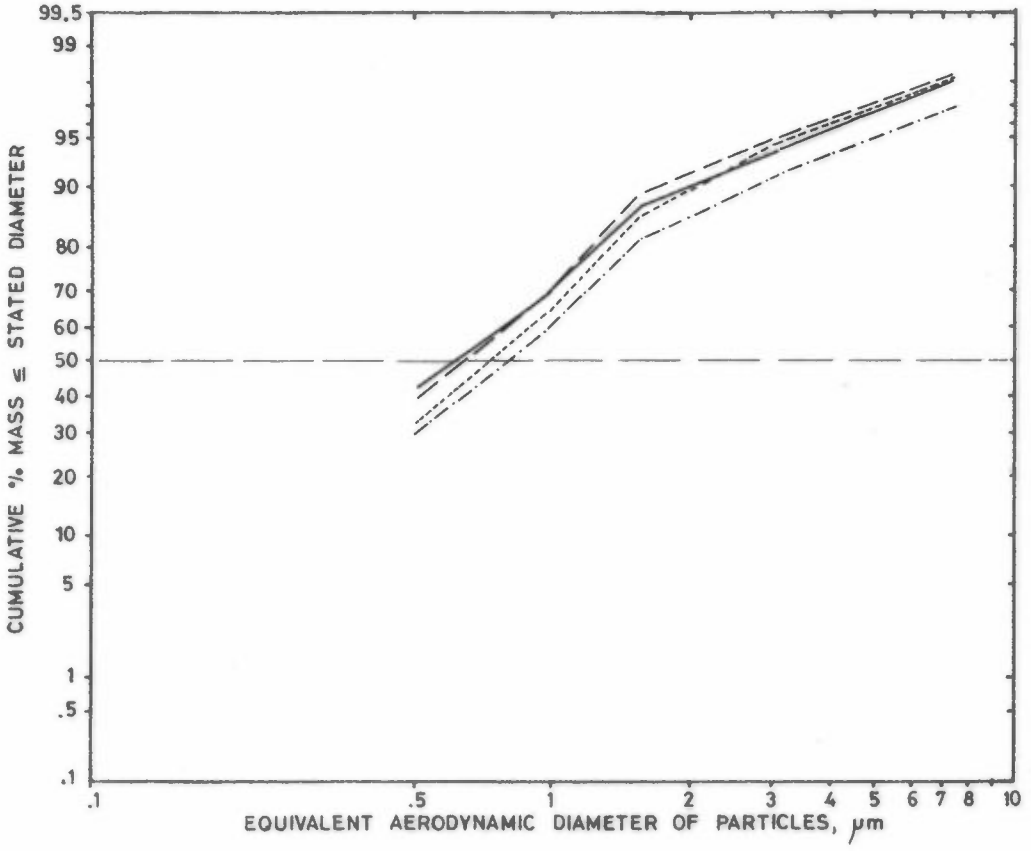

Figure 28: Average cumulative size-mass distributions of SO_4- and NH_4-containing particles, as measured by the high-volume Sierra cascade impactor at Yssen during the 17 January - 5 February 1976 and 9 February - 25 February 1976 sampling periods.

(——) SO_4
(– – –) NH_4 — *17 January - 5 February 1976 period*

(–·–·–) SO_4
(·····) NH_4 — *9 February- 25 February 1976 period*

Since NH_4HSO_4 is a hygroscopic substance and $(NH_4)_2SO_4$ a deliquescent salt, the SO_4- and NH_4-containing particles were probably collected as liquid droplets in the impactor under the prevailing conditions of humidity (cf. also Sec. 6.2). The retention characteristics of most impactor stage substrates are good for liquid particles (WINKLER, 1974; DZUBEY et al., 1976). This seems to be born out by the shapes of the distribution curves, which indicate only slight bias toward smaller particle sizes during the use of the Whatman 40 substrates (cf. Sec. 6.4).

5.2.2 Lead, copper, zinc, and calcium

The burning of gasoline in automotive spark-ignition engines is estimated to account for over 90% of world-wide emissions of lead compounds (JANSSENS & DAMS, 1975). In the absence of known industrial sources of Pb (e.g., non-ferrous metal industries) in the Yssen area, the largely sub-micrometre sized particles from automotive combustion are expected to predominate.

Figure 29 shows cumulative size-mass distribution averages of Pb-containing particles for the 17 January - 5 February and 9-25 February sampling periods, when Whatman 40 and Gelman Spectrograde glass-fibre substrates, respectively, were used for the impactor stages. The average MMD's of about 0.25 µm and 0.8 µm, as well as those of the individual sampling runs (cf. Table 2) are quite different. Figures 5 and 21 indicate, that the difference is mainly due to the very substantial proportion of the particles collected on the impactor after-filters during the 17 January - 5 February periods.

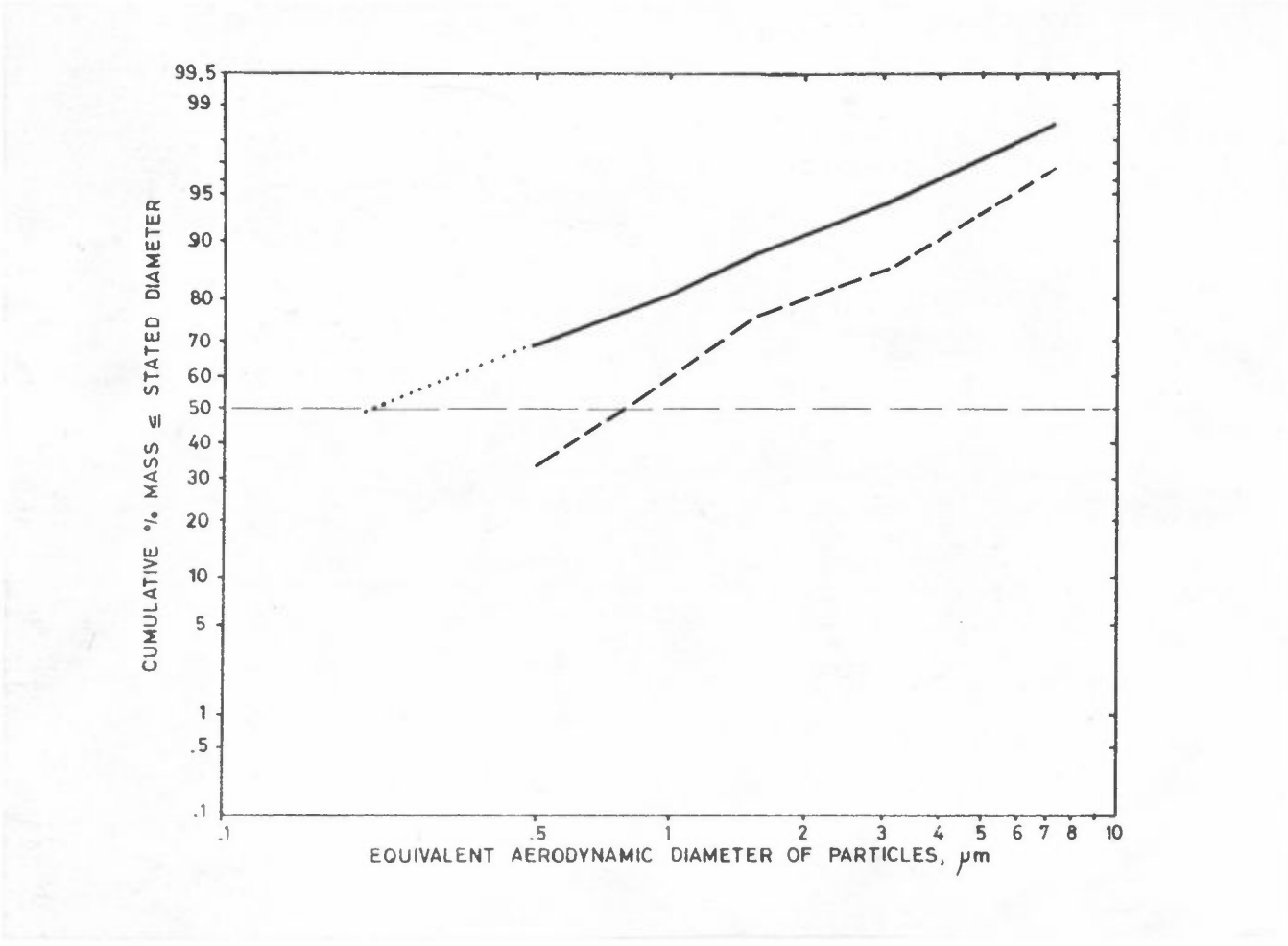

Figure 29: Average cumulative size-mass distributions of Pb-containing particles at Yssen, as measured by the high-volume Sierra cascade impactor with Whatman 40 (——) and Gelman Spectrograde glass-fibre (– – –) impaction stage substrates.

There is, of course, no direct proof, that the populations of Pb particles during the two periods were alike, but the similarity of atmospheric conditions (cf. Table 3) likely rules out any pronounced shifts in Pb source and particle size characteristics. The apparent differences in particle size distributions are, therefore, thought not to be real, but caused by the dissimilar retention ability of the two substrate materials for the dry and non-sticky Pb particles (cf. Sec. 6.4).

The Pb particles are in the accumulation mode, and no bimodality is seen in either of the distributions in Figure 21, confirming a single type generation source (auto exhaust). Consequently, the size distributions during the 9-25 February sampling periods are regarded more representative of the actual Pb particle populations in the air.

High-temperature metallurgical processes produce copper (Cu) and zinc (Zn) particles in the accumulation mode size range, while coarser particles result from the afore-mentioned Hi-Vol motor winding and rubber tire wear, respectively. Figures 6, 14, and 22 for Cu, and Figures 7, 15, and 23 for Zn again show some particle carry-over effects during use of the Whatman 40 substrates, but not nearly as pronounced, as for Pb particles.

The size distributions of both elements have only single, broad mass modes at about the "saddle point" size, between the fine and the coarse fractions. The very slight hint of bimodality during the 17 January - 5 February period for Cu is probably the result of the substrate effect. The average MMD's for the 17 January - 5 February and the 9-25 February periods are 1.0 µm and 1.4 µm for Cu and 0.6 µm and 0.9 µm for Zn, respectively (cf. Table 2). These size distribution features suggest, that mechanically produced coarser particles from motor winding wear were at least a partial source of the measured Cu particles. On the other hand, Zn from tire debris does not seem to contribute substantially to the measured concentrations at Yssen, since rubber tire wear studies (CARDINA, 1974; DANNIS, 1974; PIERSON & BRACHACZEK, 1974) have found Zn particles

exclusively in the coarse particle mode.

Soil and certain industrial operations (e.g., quarrying, aggregate and cement manufacturing) are major sources of airborne calcium (Ca). Thus, mechanical disruption and resuspension processes predominate, and Ca is expected to occur mainly in the coarse particle fraction. The average MMD's of at least 1.5 μm for both the water- and acid-leached Ca (cf. Table 2), as well as Figures 16, 17, 24 and 25 bear this out.

The measured size distributions of the supposedly dry-type Ca particles could also be affected by the stage substrates used. Although the bimodalities seen in Figures 24(a) and 25(a) during the 17 January - 5 February period may reflect this, any clear-cut differences for the two periods are obscured by certain peculiarities in the size-mass distributions during the 9-25 February periods. The cumulative size-mass distributions of the individual runs during this time indicated, that the distributions fell into two distinct groups. That is, the Ca particles had very similar distributions during the 9-13 February/17-21 February runs and the 13-17 February/21-25 February runs, as shown in Figures 16(b) and 17(b). Furthermore, the MMD's of the water- and acid-leached Ca particles for the 13-17 February/21-25 February runs were essentially the same as the averages for the 17 January - 5 February periods (cf. Table 2). As previously noted (cf. Sec. 5.1.2), water- and acid-leached Ca had an elevated mass concentration during the 9-13 February run, with thaw-enhanced resuspension of soil dust the suspected cause. It would be reasonable, that during this time much coarser particles would become airborne and be sampled. Indeed, the MMD's for this run were 6.5 μm for water-leached and 7 μm for acid leached Ca. However, similar MMD's (5 μm for both leaches) were also measured during the 17-21 February run, for which the measured mass concentration is relatively low (cf. Table 1), thus showing no evidence of locally generated Ca particles. No reason can be given for the apparent similiarity in size-mass distributions of Ca-containing particles during the two periods of supposedly dissimilar Ca sources.

5.2.3 Polycyclic aromatic hydrocarbons

Figures 10 and 26 show that the mass of total PAH and the "indicator" BaP particles was entirely confined to the accumulation mode. This is in accordance with the preliminary assessment, that the main source of these particles is home heating with fuel oil, which generates particles in sub-micrometre sizes.

Cumulative size-mass distribution plots for the 5-9 February run in Figure 18 give MMD's of about 0.55 µm for PAH and 0.45 µm for BaP. About 80% of all the mass of PAH and almost 90% of BaP is contained in particles smaller than 1 µm aerodynamic diameter. Although this was the only sample analyzed for PAH, the deposits on stages 4 and 5 of the impactor and the after-filter had an almost carbon-black appearance for every sampling run. This would suggest a more or less continuous presence of these small carbonaceous particles in rural community air during the winter heating season.

6 DISCUSSION OF SAMPLER PERFORMANCE

The high-volume Sierra cascade impactor is well-suited for sampling airborne particulate matter at rural sites. The impactor in the sampler is in front of all other components in the sampling train and the only element preceeding it is the shelter inlet. Thus, any probable loss of particles before they reach the impactor is governed only by the intake characteristics of the shelter inlet.

The relatively high sampling rate (ca. 1.1 m^3/min) allows the collection of sufficient amount of sample on all stages of the impactor during 24- to 48-hour sampling periods for chemical characterization by routine laboratory techniques. Furthermore, the large samples enhance the accuracy of chemical analyses, and minimize the effect of inadvertent sample contamination. In regard to adequacy of collected sample, one exception might be some of the minor constituents of airborne sea salt at inland locations (e.g., Mg), but uncertain blank values could have caused the apparent insufficiency of sample in this study.

All cascade impactors, however, do have non-ideal performance characteristics under real field conditions, and these must be recognized in the interpretation of measurement results. The following discussion will deal mainly with some of the conditions, circumstances and observations which could have had some bearing on the performance of the impactor and consequently the representativity of the results.

The possibility of chemical modification of the sample always exists, when the sampling device, such as the Hi-Vol/Sierra impactor, utilizes sample concentration over a period of time. This is perhaps the most serious limitation of all samplers using filters and substrates, which allow possible reactions among the collected particles themselves and/or gaseous constituents during the sampling process itself, or during subsequent sample handling and analysis. Particularly in the case of

sulphates, questions about the representativeness of the sample of the actual molecular state of the compounds in the atmosphere arise (CHARLSON et al., 1974). Certainly prolonged sampling periods should be avoided whenever possible.

6.1 Sample flowrate

To have known particle size separation characteristics (ECD's), all cascade impactors must be operated at constant flowrates. Constant flow controllers (such as the Sierra Model 310A) provide the currently best available means of achieving reasonable sample flowrate constancy. Deviations of only ±1% from adjusted flowrate have been reported for the Model 310A (KURZ & OLIN, 1975), but under the wintertime conditions prevailing during the January/February 1976 sampling periods, changes as high as about -5% occurred over a period of about two weeks. It seems, that before it can be assumed that the sampler has attained a constant flowrate, sufficient time must be allowed for the controller to "settle down" after the potentiometer adjustment for the appropriate flowrate has been made.

Periodic recalibration in the field during sampling (perhaps every week) or at least at the close of the sampling programme, as well as after every time the sampler is moved, appears necessary to ascertain the actual operating flowrate of the sampler.

6.2 Moisture effects

The impactor stage substrates and after-filters were always moist, when removed from the impactor at NILU after each sampling run. This occurred under all types of weather conditions, including air temperatures well under $0^{\circ}C$. At first it was thought, that the well-known affinity of Whatman cellulose substrates was the cause of this condition. After the switch to the non-hygroscopic Gelman glass-fibre substrates,

the moisture situation remained largely unchanged. At first glance, it could be reasoned, that the progressive drop in pressure as the air passes through the impactor, and the expected slight rise in temperature due to heat conduction from the sampler motor, would likely cause some evaporation of moisture. The obvious condensation of moisture within the impactor then must have resulted from a sufficient lowering of air temperature inside the impactor from radiational heat losses to the surroundings from the aluminum shelter and the aluminum impactor block, particularly during the night. The impactor was never disassembled in the field after a sampling run, so that the actual state of the condensed water collected on the stages is not known. It would seem unlikely, that under freezing conditions the condensate could remain liquid, but would rather accumulate as ice or rime, and melted only after having been returned to room temperature. The deposits on the substrates, however, always had a washed-out appearance, and it is not known, whether this was due to after-sampling melting alone, or whether the spreading of the deposits was caused by actual movement of liquid from stage to stage, caused by radiational heating during sunny days.

The water-logging also had different effect on the two different types of stage substrates. The Whatman 40 material tended to swell, and, being rigidly clamped between the stage plates, bulged up toward the slotted plate above it and would sometimes stick to it. This condition obviously caused uneven stage-to-collection plate distances or even blockage, affecting the collection characteristics to an unknown extent, as well as resulting in enhanced internal losses (cf. Sec. 6.3).

Water-logging of the Gelman glass-fibre substrates gave them a tendency to stick between the clamped stage plates, which usually resulted in some loss of the substrate material upon removal from the impactor. While this does not affect chemical analysis of the samples, it would constitute a serious problem in gravimetric evaluation, since it is doubtful that the stuck material could be entirely and quantitatively recovered.

6.3 Interstage losses

In general, total mass concentration measurements from cascade impactors have been found somewhat lower than those from filtration samplers of similar intake characteristics because of so-called wall or interstage losses. Interstage losses result from the deposition of particles on interior surfaces other than the collection stages, and normally cannot be recovered (LUNDGREN, 1967; SEHMEL, 1973; RAO, 1975; CUSHING et al., 1976; WEDDING et al., 1977; ELDER et al., 1977). Interstage losses can distort the analysis of impactor data by the effective cut-off (ECD) method, which assumes no wall loss or rebound of particles from collection surfaces (ELDER et al., 1977).

WILLEKE (1975) made limited number of wall loss determinations for the high-volume Sierra cascade impactor with laboratory generated, monodispersed aerosols, and found the losses a function of the equivalent aerodynamic diameter of the particles and of the stage.

Interstage losses could be visually observed during the Yssen sampling on the impactor stage plates as dark stains or accumulations of larger deposits along the edges and inside the plate slots. The staining was most pronounced at the ends of the slots where fan-shaped deposits flared out in the direction of flow, and also on the undersides of the slotted plates, when the moist Whatman 40 substrates would swell and stick to them. Occasionally, relatively large, dark-coloured and sticky particles were observed on the slotted plate of the first stage of the impactor. Because of their large aerodynamic sizes, these particles were apparently unable to follow the airflow into the impactor and reach their proper collection surface.

To assess the magnitude of interstage losses, all the slotted plates of the impactor (with the exception of the over-sized support plate for Stage 5 substrate) after the 9-13 February run were ultrasonically cleaned in distilled water and the wash waters analyzed. The results are shown in Table 4 (more detailed

data are given in Table A14 in the Appendix). Most of the larger accumulations in and around the slots could not be removed by ultrasonic cleaning in water. Scrapings of these were subjected to electron microprobe analysis (EMA) at Institutt for Atomenergi (IFA) and were identified as consisting mainly of sulphur and silicon*.

Table 4: Interstage losses of various chemical components in airborne particulate matter for the high-volume Sierra cascade impactor (9 Feb. - 13 Feb. 1976 sampling period at the Yssen site).

Jet-plate number	% interstage loss*									
	SO_4		Pb		Cu		Zn		Ca**	
	per stage+	per total++	per stage+	per total++	per stage+	per total+	per stage+	per total++	per stage+	per total++
1	18.6	2.7	6.6	0.7	34.2	9.2	21.7	7.6	25.6	6.2
2	9.3	1.4	8.8	0.9	18.5	5.0	14.4	5.1	22.4	5.4
3	19.5	2.9	30.8	3.1	13.1	3.5	21.3	7.5	23.6	5.8
4	18.5	2.7	20.9	2.1	11.0	3.0	17.9	6.3	13.0	3.2
5	34.1	5.0	32.9	3.3	23.2	6.2	24.7	8.6	15.5	3.8
Total	100.0	14.7	100.0	10.1	100.0	26.9	100.0	35.1	100.0	24.4

* details on measured interstage losses and total concentrations in Table A12 of the Appendix.

** water-leached only.

\+ loss of mass on each jet-plate as percent of total interstage loss.

++ loss of mass on each jet-plate as percent of total measured concentration.

*Anda, O., NILU, personal communication, March 1976.

Due to the incomplete recovery of the interstage deposits by ultrasonic cleaning and the fact, that such evaluation was done for only one sample, the results can be considered only tentative. The constituents with the smaller MMD's, i.e., SO_4, Pb and Zn, appear to have the highest losses mainly on the walls of the small particle stages (i.e., Stages 4 and 5), while the coarse particles (Cu and Ca) deposit more in the early stages of the impactor. This general dependence of wall losses on the size of the particles is consistent with WILLEKE's (1975) findings, but the relationship is by no means clear-cut, since several of the constituents appear to have more than one loss mode.

The seemingly moderate interstage losses for SO_4 do not include any possible additions from the sulphur-containing substances identified, but not quantified by EMA.

No attempt was made to use the wall loss information from the single run to adjust the measured concentrations in each size fraction for the other sampling runs. The total mass concentrations of the various chemical constituents were, however, corrected for total interstage losses, and are shown as "adjusted concentrations" in Table 1.

6.4 Substrate effects

Cascade impactors, first introduced by MAY (1945), have been widely used for over 30 years in atmospheric particulate size distribution studies. Their true operating characteristics, under the usually nonideal field conditions, however, have only recently been explored and better understood (WINKLER, 1974; RAO, 1975; WILLEKE, 1975; WILLEKE & MCFETERS, 1975; DZUBAY et al., 1976; NATUSCH & WALLACE, 1976; RAO & WHITBY, 1977; MCCAIN et al., 1977).

Although the terms "collection efficiency" and "impaction efficiency", as applied to impactors, are usually regarded synonymous, the collection efficiency is strictly speaking the product of the impaction efficiency of particles on the collection stages and the retention or adhesion efficiency of the impacted particles by the collection surfaces (RAO & WHITBY, 1977). It has been the latter parameter for which definitive information has been lacking, although in the presence of nonideal retention of impacted particles due to particle rebound or reentrainment, and differences in roughness and other characteristics of the collection surface, impaction efficiency and collection efficiency are not equal. At least some of the size classification ability is lost or distorted when particle bounce, or reentrainment and deagglomeration occur within the impactor, resulting in erroneous and misleading size-mass distribution data (RAO & WHITBY, 1977; ELDER et al., 1977; MCCAIN et al., 1977).

In recent years the use of various types of collection stage substrates, particularly fibrous filters, has become commonplace, because they facilitate sample handling and recovery, and appear to reduce particle rebound and reentrainment (HU, 1971; RAO, 1975; WILLEKE, 1975). Recent studies of the retention characteristics of fibrous filter stage substrates (RAO, 1975; RAO & WHITBY, 1977) have shown, that although rebound is significantly reduced, the impaction characteristics of the impactor stages are also changed in such a way, as to reduce the resolution and sharpness of size cuts of the impactor. It is, therefore, essential that cascade impactors be calibrated as units with the intended stage substrates in place.

The stage ECD's of the high-volume Sierra impactor are known for the glass-fibre substrates (WILLEKE, 1975). NILU has used occasionally Whatman 40 filters as stage substrates (e.g., during the first part of this measurement programme; VITOLS, 1977) on the assumption, that they have equivalent retention characteristics to those of glass-fibre substrates. However, RAO (1975), in his studies of the Andersen sampler, found the

Whatman type filters inferior to glass-fibre substrates in retention ability.

On the assumption, that the characteristics of sources, and thus the size distributions, of airborne particles did not change substantially during the two periods when Whatman 40 and Gelman glass-fibre substrates were used for the high-volume Sierra impactor (cf. Sec. 5.2.2), some assessment can be made of their relative retention efficiencies from the measurement results. As has been pointed out (cf. Sec. 5.2.1), the retention of liquid droplets or wetted particles by almost any surface is better than of dry, solid and nonsticky particles (WINKLER, 1974; DZUBAY et al., 1976; MARPLE & WILLEKE, 1976). Thus, differences in retention should best be apparent from the examination of the size distributions of such supposedly dry type particles, as Pb, Cu, Zn and Ca. As earlier mentioned (cf. Sec. 5.2.2), the clearest evidence of differences in retention efficiency of the two substrate materials is provided by the Pb particle size distributions. Figures 5 and 21 show, that the change in substrates also coincides with a shift in the proportion of Pb particles collected on the after-filter of the impactor during the respective periods, causing the large differences in MMD's in Figure 29. The extensive lengths of the sampling runs were also probably quite conducive to reentrainment of particles from the overloaded substrate surfaces and/or rebound from the already impacted layers of particles. In either case, the particles would be deposited on improper collection stages, or they may continue rebounding from successive stages until collected on the after-filter.

MCCAIN et al. (1977) have suggested, that, in what they term "extreme bounce" cases of dry and non-sticky particles, larger than 2.5 µm MMD, more truthful cumulative size distribution plots are obtained, if after-filter collections are omitted from the data. Although Pb particles away from industrial sources cannot be expected to occur in such large sizes, the

suggested procedure was tested for the 17 January - 5 February period Pb particle average distribution. The resulting distribution curve (not shown) moved to the right of the 9-25 February period average curve, with the particle MMD of about 1.2 µm. This is not considered a representative size of typical Pb particles in rural areas, and "extreme bounce" of Pb particles apparently did not occur at Yssen.

6.5 Intake efficiency

True size distributions of airborne particles may be truncated during the sampling process by the size fractionating characteristics of the sampler inlet. The intake efficiency* of sampler inlets is generally a function of the air velocity into the inlet, the aerodynamic sizes of the airborne particles, and the horizontal wind speed at the sampler inlet.

LUNDGREN & PAULUS (1975) were the first to make a quantitative assessment of the intake efficiency of the Hi-Vol sampler shelt They found its 50% cut-off at about 60 µm diameter. More recent WEDDING et al. (1977) measured in a wind tunnel with monodispersed aerosols intake efficiencies of the Hi-Vol sampler at various wind speeds and for different aerodynamic diameters of particles. The Hi-Vol shelter, due to its rectangular shape was found to be extremely sensitive to orientation with respec to airflow direction. With the most favourable orientation (roof ridge of the shelter at 45° to airflow), the intake efficiencies at 15 m/s windspeed were 100%, 55%, 41% and 34% for particles of 5 µm, 15 µm, 30 µm and 50 µm aerodynamic diameters, respectively.

Intake efficiency (or sampling effectiveness) is the ratio of the particle concentration, measured by the sampler, to the true particle concentration in the original air sample, prior to entrance into the sampler.

It is speculated that, with small-sized particles predominanting in Yssen air and with wind speeds seldom exceeding 5 m/s, the intake efficiency of the high-volume/Sierra sampler was essentially 100% for all airborne particles.

6.6 Blank effects

Repeated analyses of Whatman 40 and Gelman Spectrograde Type A stage substrates, and Gelman Spectrograde Type A after-filters, selected from the same batches as used for the high-volume Sierra impactor, yielded a wide range of blank values of the various chemical constituents (Table A15 in the Appendix). Average values of blank concentrations were used to adjust the sample concentrations, but uncertainties about actual blank values can introduce additional distortions in measured particle size distributions. For some of the more scarce trace constituents (e.g., Mg) a proper choice of the blank value is critical, since a too high blank can reduce or entirely eliminate the sample collection. Thus, it is desirable to procure and use stage substrates and after-filters with lower, or at least less variable levels of impurities, to avoid uncertainties in measured concentrations.

7 CONCLUSIONS

Aerosol measurements at a rural site about 30 km north-east of Oslo during January and February 1976 showed that:

1) During a period of relatively stagnant air, regional anthropogenic activities were the most likely sources of water-soluble ions and trace elements in airborne particles.

2) Concentrations of water-soluble ions and trace elements in airborne particles showed little variability with wind direction and time of measurement.

3) Measured SO_4, NH_4, and Pb particles were in the "accumulation" mode, with MMD's less than 1 μm.

4) SO_4 and NH_4 were contained in the same particles and probably were in the form of ammonium sulphate salts.

5) All measured Ca was in the "coarse" particle mode, while Cu and Zn mass was mainly distributed between the "coarse" and "accumulation" modes.

6) About 80% of the mass of PAH compounds was in particles smaller than 1 μm in diameter.

7) The high-volume Sierra cascade impactor was well suited for mass concentration and size distribution measurements, but sampling periods should not exceed about two days.

8) The representativity of measured particle size distributions was probably affected by moisture conditions, nonideal collection characteristics of the impactor, and uncertain blank values.

9) Impactor wall losses amounted to about one-third of the measured concentrations, but varied according to the chemical nature and size of the particles.

10) Differences in impactor stage substrate retention characteristics had a bearing on the representativity of measured particle size distributions.

11) Stage substrates and after-filters with lower or at least less variable levels of impurities are needed.

8 ACKNOWLEDGEMENT

NTNF postdoctoral fellowship support for the author during part of this study is gratefully acknowledged. Fund for the analytical phases of the measurement programme were provided by NILU and the SNSF-project.

8 REFERENCES

BJØRSETH, A.
LUNDE, G.
1975 Teknisk rapport nr. 1, 740312-B. Oslo, Norges Teknisk- Naturvitenskaplige Forskningsråd.

BJØRSETH, A.
LUNDE, G.
1977 Analysis of the polycyclic aromatic hydrocarbon content of airborne particulate pollutants in a Søderberg paste plant. Amer. Ind. Hyg. Assoc. J. 38, 224-228.

BROSSET, C.
1976 Airborne particles: black and white episodes. AMBIO 5, 157-163.

BROSSET, C.,
ANDREASSON, K.
FERM, M.
1975 The nature and possible origin of acid particles observed at the Swedish west coast. Atmos. Envir. 9, 631-642.

CARDINA, J.A.
1974 Particle size determination of the tire-tread rubber in atmospheric dusts. Rubber Chem. Technol. 47, 1005-1010.

CHARLSON, R.J.,
VANDERPOL, A.H.,
COVERT, D.S.,
WAGGONER, A.P.
ALQUIST, N.C.
1973 $H_2SO_4/(NH_4)_2SO_4$ background aerosol: optical detection in St. Louis region. Atmos. Envir. 8, 1257-1267.

CUSHING, K.M.,
MCCAIN, J.D.
SMITH, W.B.
1976 Experimental determination of sizing parameters and wall losses of five commercially available cascade impactors. APCA paper 76-37.4, presented at the 69th Annual Meeting of the Air Poll. Control Assoc., June 27 - July 1, 1976, Portland, Ore.

DANNIS, M.L. 1974 Rubber dust from the normal wear of tires. Rubber Chem. Technol. 47, 1011-1037.

DOVLAND, H. 1975 Målinger av størrelsesfordelingen av partikler i atmosfæren. Ås. (SNSF-prosjektet, TN 14/75.)

DZUBAY, T.G., HINES, L.E. STEVENS, R.K. 1976 Particle bounce errors in cascade impactors. Atmos. Envir. 10, 229-234.

ELDER, J.C., TILLERY, M.I. ETTINGER, H.J. 1977 Calibration of Andersen nonviable impactor under special conditions of high flow and membrane filter surface coating. APCA paper 77-35.4, presented at the 70th Annual Meeting of the Air Poll. Control Assoc., June 20-24, 1977, Toronto, Ont. Canada.

HIDY, G.M. et al. 1974 Observations of aerosols over Southern California coastal waters. J. Appl. Meteorol. 13, 96-107.

HOFFMAN, G.L. DUCE, R.A. 1971 Copper contamination of atmospheric particulate samples collected with Gelman Hurricane air samplers. Envir. Sci. Technol. 5, 1134-1136.

HU, J.N.H. 1971 An improved impactor for aerosol studies: modified Andersen sampler. Envir. Sci. Technol. 5, 251-253.

JANSSENS, M. DAMS, R. 1975 Man's impact on atmospheric lead concentrations - pollution sources and baseline levels in Western Europe. Water, Air and Soil Poll. 5, 97-107.

JUNGE, C.E. 1972 Our knowledge of the physico-chemistry of aerosols in the undisturbed marine environment. J. Geophys. Res. 77, 5183-5200.

KELKAR, D.N.
JOSHI, P.V. 1977 A note on the size distribution of aerosols in urban atmospheres. Atmos. Envir. 11, 531-534.

KING, R.B.
TOMA, J. 1975 Copper emissions from a high volume air sampler. NASA TM X-71693.

KURTZ, J.L.,
OLIN, J.G. 1975 A new flow controller for high-volume air samplers. APCA paper 75-65.6, presented at the 68th Annual Meeting of the Air Poll. Control Assoc., June 15-20, 1975, Boston, Mass.

LAWRENCE BERKELEY LABORATORY 1975 Instrumentation for environmental monitoring. Air, Part 2, LBL-1, Vol.1, Envir. Instr. Group, Lawrence Berkeley Laboratory, Univ. of California, Berkeley, Calif.

LEE, R.E.
CALDWELL, J.S.
MORGAN, G.B. 1972 The evaluation of methods for measuring suspended particulates in air. Atmos. Envir. 6, 593-622.

LEE, R.E.
GORANSON, S. 1972 National Air Surveillance cascade impactor network. I. Size distribution measurements of suspended particulate matter in air. Envir. Sci. Technol. 6, 1019-1024.

LEE, R.E.
GORANSON, S. 1976 National Air Surveillance cascade impactor network. III. Variations in size of airborne particulate matter over three-year period. Envir. Sci. Technol. 10, 1022-1027.

LUNDGREN, D.A. 1967 An aerosol sampler for determination of particle concentration as function of size and time. J. Air Poll. Control Assoc. 17, 225-228.

LUNDGREN, D.A.
PAULUS, H.J. 1975 The mass distribution of large atmospheric particles. J. Air Poll. Control Assoc. 25, 1227-1231.

MARPLE, V.A.
WILLEKE, K. 1976 Inertial impactors: theory, design and use. In Fine Particles. Aerosol Generation, Measurement, Sampling and Analysis, Liu, B.Y.H., editor, Academic Press, New York, N.Y.

MARTENS, C.S.,
WESELOWSKI, J.J.,
HARRISS, R.C.
KAIFER, R. 1973 Chlorine loss from Puerto Rican and San Francisco Bay Area aerosols. J. Geophys. Res. 78, 8778-8792.

MAY, K.R. 1945 The cascade impactor: and instrument for sampling coarse aerosols. J. Sci. Instr. 22, 187-195.

MCCAIN, J.D.,
MCCORMACK, J.E.
HARRIS, D.B. 1977 Non-ideal behaviour in cascade impactors. APCA paper 77-35.3, presented at the 70th Annual Meeting of the Air Poll. Control Assoc., June 20-24, 1977, Toronto, Ont., Canada.

MCKAY, H.A.C. 1969 Ammonia and air pollution. Chem. Ind., 1162-1165.

NATUSCH, D.F.
WALLACE, J.R. 1976 Determination of airborne particle size distributions: calculation of cross-sensitivity and discreteness effects in cascade impactors. Atmos. Envir. 10, 315-324.

PATTERSON, R.K.
WAGMAN, J.
1977 Mass and composition of an urban aerosol as a function of particle size for several visibility levels. J. Aerosol Sci. 8, 269-279.

PIERSON, W.R.
BRACHACZEK, W.W.
1974 Airborne particulate debris from rubber tires. Rubber Chem. Technol. 47, 1275-1299.

RAO, A.K.
1975 An experimental study of inertial impactors. PhD thesis, University of Minnesota. Particle Technology Laboratory publication No. 269, Minneapolis, Minn.

RAO, A.K.
WHITBY, K.T.
1977 Nonideal collection characteristics of single stage and cascade impactors. Amer. Ind. Hyg. Assoc. J. 38, 174-179.

SEMONIN, R.G.
1972 Comparative chloride concentrations between Mauna Loa Observatory and Hilo, Hawaii. J. Appl. Meteorol. 11, 688-690.

SEHMEL, G.A.
1973 An evaluation of a high-volume cascade particle impactor system. ISI ISP 6671, presented at the Second Joint Conference on Sensing of Environmental Pollutants, Dec. 10-12, 1973, Washington, D.C., Instrument Soc. of America, Pittsburgh, Penn.

VITOLS, V.
1977 Airborne sea salt mass concentration and size distribution measurements on Karmøy. (NILU TN 5/76), Lillestrøm.

WEDDING, J.B.,
MCFARLAND, A.R.
CERMAK, J.E.
1977 Large particle collection characteristics of ambient aerosol samplers. Envir. Sci. Technol. 11, 387-390.

WHITBY, K.T.
CANTRELL, B. 1975 Atmospheric aerosols - characteristics and measurement. Paper 29-1, in Proceedings Internat. Conference on Environmental Sensing and Assessment, Vol. 2, Sept. 1975, Las Vegas, Nev.

WILLEKE, K. 1975 Performance of the slotted impactor. Amer. Ind. Hyg. Assoc. J. 36, 683-691.

WILLEKE, K.
MCFETERS, 1975 The influence of flow entry and collection surface on the impaction efficiency of inertial impactors. J. Coll. Interface Sci. 53, 121-127.

WINKLER, P. 1974 Relative humidity and the adhesion of atmospheric particles to plates of impactors. J. Aerosol Sci. 5, 235-240.

APPENDIX
Tables A1-A15

Table A1: Effective stage cut-off diameters[+] (ECD's) of the high-volume Sierra cascade impactor at calibration flowrate (ECD_C) and at operating flowrates (ECD_S) during the various sampling periods at Yssen.

Impactor Stage No.	ECD_C[++], µm at 1.13 m^3/min	ECD_S[+++], µm at 1.09 m^3/min	ECD_S[+++], µm at 1.07 m^3/min
1	7.20	7.35	7.40
2	3.00	3.06	3.09
3	1.50	1.53	1.54
4	0.95	0.97	0.98
5	0.50	0.50	0.50

[+] equivalent aerodynamic diameter

[++] according to Willeke (1975)

[+++] calculated according to Eqn. (1) in text

Table A2: Sampling periods, sampling run durations, sampling rates, and air sample volumes of the high-volume Sierra cascade impactor at Yssen.

Time and date of sampling period	1410/17 Jan. - 1230/23 Jan. 1976	1400/23 Jan. - 1345/30 Jan. 1976	1350/30 Jan. - 1400/3 Feb. 1976	1405/3 Feb. - 1355/5 Feb. 1976	1400/5 Feb. - 1445/9 Feb. 1976	1450/9 Feb. - 1105/13 Feb. 1976	1110/13 Feb. - 0910/17 Feb. 1976	0915/17 Feb. - 1113/21 Feb. 1976	1115/21 Feb. - 1220/25 Feb. 1976
Sampling run duration, min.	8540	10050[+]	5770	2870	5805	5535	5640	5878	5825
Sampling rate[++], m^3/min	1.09	1.07	1.07	1.07	1.07	1.07	1.07	1.07	1.07
Calculated air sample volume[++], m^3	9130	10745[+]	6169	3068	6206	5918	6030	6284	6228

[+] electric power off for ca. 15 min. during run.

[++] at 25°C and 760 mm Hg.

Table A3: Concentrations of water-soluble ions and trace elements in various aerodynamic diameter intervals from the high-volume Sierra cascade impactor measurements of suspended particulate matter during the 17 Jan. - 25 Feb. 1976 sampling periods at Yssen.

	Stage number and diameter interval \ Sampling period	17-23 Jan.	23-30 Jan.	30 Jan.-3 Feb.	3-5 Feb.	9-13 Feb.	13-17 Feb.	17-21 Feb.	21-25 Feb.	AVERAGE* 17 Jan. - 5 Feb.	AVERAGE 9 Feb. - 25 Feb.
Sulphate (SO_4), ng/m^3	1: >7.40 µm	71	117	126	44	487	201	315	96	97	275
	2: 3.09 - 7.40 µm	118	251	190	186	842	378	592	238	189	512
	3: 1.54 - 3.09 µm	123	256	451	381	933	627	1528	626	269	929
	4: 0.98 - 1.54 µm	368	714	1154	1027	1703	2264	2960	1084	732	2003
	5: 0.50 - 0.98 µm	526	1026	1751	1858	2433	3781	3199	1830	1110	2810
	6: Filter <0.50 µm	1032	1985	2633	2288	2149	3930	2139	2864	1856	2771
	Total	2238	4349	6305	5764	8547	11181	10733	6738	4253	9300
Ammonium (NH_4), ng/m^3	1: >7.40 µm	39	21	55	30	29	67	53	9	34.8	39.5
	2: 3.09 - 7.40 µm	49	58	86	71	72	102	129	27	62.5	82.5
	3: 1.54 - 3.09 µm	57	81	193	146	212	125	403	105	104.0	211.3
	4: 0.98 - 1.54 µm	266	267	491	551	360	447	855	253	344.1	478.7
	5: 0.50 - 0.98 µm	284	408	971	935	536	924	1078	432	544.0	742.5
	6: Filter <0.50 µm	478	667	1131	1039	591	799	1015	613	745.2	754.5
	Total	1173	1502	2927	2772	1800	2464	3533	1439	1835	2309
Lead (Pb), ng/m^3	1: >7.40 µm	1.3	2.9	3.2	2.3	5.4	2.3	3.0	1.4	2.4	3.0
	2: 3.09 - 7.40 µm	6.5	7.4	8.9	8.3	11.7	12.6	11.1	5.0	7.5	10.1
	3: 1.54 - 3.09 µm	8.8	10.2	13.0	11.7	6.8	11.6	12.7	6.4	10.5	9.4
	4: 0.98 - 1.54 µm	8.8	11.2	17.8	24.1	13.5	19.9	19.0	11.2	13.3	15.9
	5: 0.50 - 0.98 µm	12.0	18.6	25.9	39.1	28.7	28.1	22.2	18.0	20.2	24.2
	6: Filter <0.50 µm	70.0	118.9	113.3	97.5	23.5	39.6	36.4	22.3	118.7	30.4
	Total	107.4	169.2	182.1	183.0	89.6	114.1	104.4	64.0	172.6	93.0

* Time-weighted averages

NOTE: For the 17-23 Jan. 1976 sampling period only, the diameter intervals were as follows:

Stage 1: >7.35 µm
2: 3.06 - 7.35 µm
3: 1.53 - 3.06 µm
4: 0.97 - 1.53 µm
5: 0.50 - 0.97 µm
6: Filter <0.50 µm

Table A3: continued.

	Stage number and diameter interval \ Sampling period	17-23 Jan.	23-30 Jan.	30 Jan-3 Feb.	3-5 Feb.	9-13 Feb.	13-17 Feb.	17-21 Feb.	21-25 Feb.	AVERAGE* 17 Jan. - 5 Feb.	AVERAGE 9 Feb. - 25 Feb.
Copper (Cu), ng/m^3	1: >7.40 µm	2	7	6	5	13	7	15	6	5	10
	2: 3.09 - 7.40 µm	8	15	12	15	14	19	31	11	12	19
	3: 1.54 - 3.09 µm	15	19	19	21	11	21	43	22	18	24
	4: 0.98 - 1.54 µm	16	19	16	22	20	16	30	12	18	20
	5: 0.50 - 0.98 µm	12	15	10	16	15	16	25	10	13	16
	6: Filter <0.50 µm	30	47	38	28	15	26	30	22	38	24
	Total	83	122	101	107	88	105	174	83	104	113
Zinc, (Zn) ng/m^3	1: >7.40 µm	1	3	2	2	4	2	2	2	2.1	2.5
	2: 3.09 - 7.40 µm	4	6	2	5	7	10	10	5	4.4	8.0
	3: 1.54 - 3.09 µm	7	6	4	7	7	14	15	8	6.0	11.0
	4: 0.98 - 1.54 µm	11	11	11	20	14	26	19	12	11.9	17.8
	5: 0.50 - 0.98 µm	15	16	16	29	19	36	21	18	17.1	23.5
	6: Filter <0.50 µm	21	34	30	32	16	29	19	19	28.8	20.7
	Total	59	76	65	95	67	117	86	64	70.3	83.5
Calcium (Ca), ng/m^3 (distilled water - leached)	1: >7.40 µm	6	37	2	3	240	22	50	12	16	81
	2: 3.09 - 7.40 µm	21	48	10	23	270	45	58	28	29	100
	3: 1.54 - 3.09 µm	10	15	4	3	60	33	22	21	10	34
	4: 0.98 - 1.54 µm	17	15	7	11	39	42	14	12	14	27
	5: 0.50 - 0.98 µm	14	9	6	13	35	39	11	15	10	25
	6: Filter 0.50 µm	36	43	20	10	15	28	3	33	32	20
	Total	104	167	49	63	659	209	158	121	111	287

* Time-weighted averages

NOTE: For the 17-23 Jan. 1976 sampling period only, the diameter intervals were as follows:

Stage 1: >7.35 µm
2: 3.06 - 7.35 µm
3: 1.53 - 3.06 µm
4: 0.97 - 1.53 µm
5: 0.50 - 0.97 µm
6: Filter <0.50 µm

Table A3: continued.

	Stage number and diameter interval \ Sampling period	17-23 Jan.	23-30 Jan.	30 Jan-3 Feb.	3-5 Feb.	9-13 Feb.	13-17 Feb.	17-21 Feb.	21-25 Feb.	AVERAGE* 17 Jan. - 5 Feb.	AVERAGE 9 Feb. - 25 Feb.
Calcium (Ca) ng/m³ (1.0 N HNO - leached)	1: >7.40 µm	21	57	20	46	291	6	43	21	37	90
	2: 3.09 - 7.40 µm	41	62	26	66	223	22	62	32	48	85
	3: 1.54 - 3.09 µm	32	29	17	35	46	20	23	20	28	27
	4: 0.98 - 1.54 µm	22	17	10	23	20	18	3	9	18	13
	5: 0.50 - 0.98 µm	18	10	5	11	8	16	2	6	11	8
	6: Filter <0.50 µm	60	60	24	26	24	5	5	20	49	14
	Total	194	235	102	207	612	87	138	108	191	237
Chloride (Cl), ng/m³	1: >7.40 µm	73	57	29	(-)	1639	1277	395	53	66	841
	2: 3.09 - 7.40 µm	192	103	35	9	1639	1526	162	63	118	848
	3: 1.54 - 3.09 µm	129	65	17	9	68	1692	255	69	92	521
	4: 0.98 - 1.54 µm	157	95	55	32	88	1775	285	18	107	542
	5: 0.50 - 0.98 µm	135	115	110	84	85	1609	120	97	121	478
	6: Filter <0.50 µm	118	169	414	(-)	135	43	127	177	209	121
	Total	790	604	660	-	3654	7922	1290	477	713	3351
Sodium (Na), ng/m³	1: >7.40 µm	28	26	9	14	1186	971	242	65	22	616
	2: 3.09 - 7.40 µm	99	63	14	24	1125	1230	267	86	39	677
	3: 1.54 - 3.09 µm	63	36	11	17	101	1330	248	143	37	456
	4: 0.98 - 1.54 µm	75	41	11	24	206	1960	194	70	44	608
	5: 0.50 - 0.98 µm	41	29	12	24	204	1562	210	115	29	523
	6: Filter <0.50 µm	85	283	426	104	25	318	176	294	232	203
	Total	391	478	483	207	2847	7371	1337	773	403	3083

* Time-weighted averages

(-) Concentration equal to or less than blank concentrations

NOTE: For the 17-23 Jan. 1976 sampling period only, the diameter intervals were as follows:

Stage 1: >7.35 µm
2: 3.06 - 7.35 µm
3: 1.53 - 3.06 µm
4: 0.97 - 1.53 µm
5: 0.50 - 0.97 µm
6: Filter <0.50 µm

Table A3: continued.

	Stage number and diameter interval \ Sampling period	17-23 Jan.	23-30 Jan.	30 Jan-3 Feb.	3-5 Feb.	9-13 Feb.	13-17 Feb.	17-21 Feb.	21-25 Feb.	AVERAGE* 17 Jan. - 5 Feb.	AVERAGE 9 Feb. - 25 Feb.
Magnesium (Mg), ng/m^3	1: >7.40 µm	1	6	0.2	(-)	12	16	5	2	2	9
	2: 3.09 - 7.40 µm	9	14	3.1	2	19	46	10	5	10	20
	3: 1.54 - 3.09 µm	4	5	0.8	1	61	34	7	6	4	27
	4: 0.98 - 1.54 µm	8	5	0.8	1	40	42	5	5	5	23
	5: 0.50 - 0.98 µm	4	8	0.8	(-)	36	40	4	4	5	21
	6: Filter <0.5 µm	3	6	1.0	(-)	25	38	(-)	6	4	17
	Total	29	44	6.7	-	193	216	31	28	30	117

* Time-weighted averages

(-) Concentration equal to or less than blank concentrations

NOTE: For the 17-23 Jan. 1976 sampling period only, the diameter intervals were as follows:

Stage 1: >7.35 µm
2: 3.06 - 7.35 µm
3: 1.53 - 3.06 µm
4: 0.97 - 1.53 µm
5: 0.50 - 0.97 µm
6: Filter <0.50 µm

Table A4: Cumulative mass distributions of water-soluble sulphate (SO_4) from the high-volume Sierra cascade impactor sampling at Yssen.

17-23 Jan. period				23-30 Jan. period			
Cumul. ng/m^3	Cumul. %	Cumul. % < stated ECD	ECD µm	Cumul. ng/m^3	Cumul. %	Cumul. % < stated ECD	ECD µm
71	3.2	96.8	7.35	117	2.7	97.3	7.40
189	8.4	91.6	3.06	368	8.5	91.5	3.09
312	13.9	86.1	1.53	624	14.3	85.7	1.54
680	30.4	69.6	0.97	1338	30.8	69.2	0.98
1206	53.9	46.1	0.50	2364	54.4	45.6	0.50
2238	100.0	-	Filter	4349	100.0	-	Filter
30 Jan. - 3 Feb. period				3-5 Feb. period			
126	2.0	98.0	7.40	44	0.8	99.2	7.40
316	5.0	95.0	3.09	230	4.0	96.0	3.09
767	12.2	87.8	1.54	611	10.6	89.4	1.54
1921	30.5	69.5	0.98	1638	28.3	71.7	0.98
3672	58.2	41.8	0.50	3496	60.4	39.6	0.50
6305	100.0	-	Filter	5784	100.0	-	Filter
9-13 Feb. period				13-17 Feb. period			
487	5.7	94.3	7.40	201	1.8	98.2	7.40
1329	15.5	84.5	3.09	579	5.2	94.8	3.09
2262	26.5	73.5	1.54	1206	10.8	89.2	1.54
3965	46.4	53.6	0.98	3470	31.0	69.0	0.98
6398	74.9	25.1	0.50	7251	64.9	35.1	0.50
8547	100.0	-	Filter	11181	100.0	-	Filter
17-21 Feb. period				21-25 Feb. period			
315	2.9	97.1	7.40	96	1.4	98.6	7.40
907	8.5	91.5	3.09	334	5.0	95.0	3.09
2435	22.7	77.3	1.54	960	14.2	85.8	1.54
5395	50.3	49.7	0.98	2044	30.3	69.7	0.98
8594	80.1	19.9	0.50	3874	57.5	42.5	0.50
10733	100.0	-	Filter	6738	100.0	-	Filter
Average: 17 Jan. - 5 Feb. periods (Wh 40 substr. & glass-fibre filter)				Average: 9-25 Feb. period (glass-fibre substr. & filter)			
Cumul. ng/m^3 *	Cumul. %	Cumul. % < stated ECD	ECD µm	Cumul. ng/m^3	Cumul. %	Cumul. % < stated ECD	ECD µm
97	2.3	97.7	7.40	275	3.0	97.0	7.40
286	6.7	93.3	3.09	787	8.5	91.5	3.09
555	13.1	86.9	1.54	1716	18.5	81.5	1.54
1287	30.3	69.7	0.98	3719	40.0	60.0	0.98
2397	56.4	43.6	0.50	6529	70.2	29.8	0.50
4253	100.0	-	Filter	9300	100.0	-	Filter

* Time-weighted averages.

A 4

Table A5: Cumulative mass distributions of water-soluble ammonium (NH_4) from the high-volume Sierra cascade impactor sampling at Yssen.

17-23 Jan. period				23-30 Jan. period			
Cumul. ng/m³	Cumul. %	Cumul. % < stated ECD	ECD µm	Cumul. ng/m³	Cumul. %	Cumul. % < stated ECD	ECD µm
39	3.3	96.7	7.35	21	1.4	98.6	7.40
88	7.5	92.5	3.06	79	5.3	94.7	3.09
145	12.4	87.6	1.53	160	10.7	89.3	1.54
411	35.0	65.0	0.97	427	28.4	71.6	0.98
695	59.2	40.8	0.50	835	55.6	44.4	0.50
1173	100.0	-	Filter	1502	100.0	-	Filter
30 Jan. - 3 Feb. period				2-5 Feb. period			
55	1.9	98.1	7.40	30	1.1	98.9	7.40
141	4.8	95.2	3.09	101	3.6	96.4	3.09
334	11.4	88.6	1.54	247	8.9	91.1	1.54
825	28.2	71.8	0.98	798	28.8	91.1	0.98
1796	61.4	38.6	0.50	1733	62.5	37.5	0.50
2927	100.0	-	Filter	2772	100.0	-	Filter
9-13 Feb. period				13-17 Feb. period			
29	1.6	98.4	7.40	67	2.7	97.3	7.40
101	5.6	94.4	3.09	169	6.9	93.1	3.09
313	17.4	82.6	1.54	294	11.9	88.1	1.54
673	37.4	62.6	0.98	741	30.1	69.9	0.98
1209	67.2	32.8	0.50	1665	67.6	32.4	0.50
1800	100.0	-	Filter	2464	100.0	-	Filter
17-21 Feb. period				21-25 Feb. period			
53	1.5	98.5	7.40	9	0.6	99.4	7.40
182	5.2	94.8	3.09	36	2.5	97.5	3.09
585	16.6	83.4	1.54	141	9.8	90.2	1.54
1440	40.8	59.2	0.98	394	27.4	72.6	0.98
2518	71.3	28.7	0.50	826	57.4	42.6	0.50
3533	100.0	-	Filter	1439	100.0	-	Filter
Average: 17 Jan. - 15 Feb. period (Wh 40 substr. and glass-fibre filter)				Average: 9-25 Feb. period (glass-fibre substr. and filter)			
Cumul. ng/m³ *	Cumul. %	Cumul. % < stated ECD	ECD µm	Cumul. ng/m³	Cumul. %	Cumul. % < stated ECD	ECD µm
34.8	1.9	98.1	7.40	39.5	1.7	98.3	7.40
97.3	5.3	94.7	3.09	122.0	5.3	94.7	3.09
201.3	11.0	89.0	1.54	333.3	14.4	85.6	1.54
545.4	29.7	70.3	0.98	812.0	35.2	64.8	0.98
1089.4	59.4	40.6	0.50	1554.5	67.3	32.7	0.50
1834.6	100.0	-	Filter	2309.0	100.0	-	Filter

* Time-weighted averages.

Table A6: Cumulative mass distributions of lead (Pb) from the high-volume Sierra cascade impactor sampling at Yssen.

17-23 Jan. period				23-30 Jan. period			
Cumul. ng/m³	Cumul. %	Cumul. % < stated ECD	ECD µm	Cumul. ng/m³	Cumul. %	Cumul. % < stated ECD	ECD µm
1.3	1.2	98.8	7.35	2.9	1.3	98.7	7.40
7.8	7.3	92.7	3.06	10.3	4.7	95.3	3.09
16.6	15.5	84.5	1.53	20.5	9.3	90.7	1.54
25.4	23.6	76.4	0.97	31.7	14.4	85.6	0.98
37.4	34.8	65.2	0.50	50.3	22.9	77.1	0.50
107.4	100.0	-	Filter	219.5	100.0	-	Filter
30 Jan. - 3 Feb. period				3-5 Jan. period			
3.2	1.8	98.2	7.40	2.3	1.3	98.7	7.40
12.1	6.6	93.4	3.09	10.6	5.8	94.2	3.09
25.1	13.8	86.2	1.54	22.3	12.2	87.8	1.54
42.9	23.6	76.4	0.98	46.4	25.4	74.6	0.98
68.8	37.8	62.2	0.50	85.5	46.7	53.3	0.50
182.1	100.0	-	Filter	183.0	100.0	-	Filter
9-13 Feb. period				13-17 Feb. period			
5.4	6.0	94.0	7.40	2.3	2.0	98.0	7.40
17.1	19.1	80.9	3.09	14.9	13.1	86.9	3.09
23.9	26.7	73.3	1.54	26.5	23.2	76.8	1.54
37.4	41.7	58.3	0.98	46.4	40.7	59.3	0.98
66.1	73.8	26.2	0.50	74.5	65.3	34.7	0.50
89.6	100.0	-	Filter	114.1	100.0	-	Filter
17-21 Feb. period				21-25 Feb period			
3.0	2.9	97.1	7.40	1.4	2.2	97.8	7.40
14.1	13.5	86.5	3.09	6.4	10.0	90.0	3.09
26.8	25.7	74.3	1.54	12.8	20.0	80.0	1.54
45.8	43.9	56.1	0.98	24.0	37.5	62.5	0.98
68.0	65.1	34.9	0.50	41.7	65.2	34.8	0.50
104.4	100.0	-	Filter	64.0	100.0	-	Filter
Average: 17 Jan - 5 Feb period (Wh 40 substr. and glass-fibre filter)				Average: 9-25 Feb. periods (glass-fibre substr. and filter)			
Cumul. ng/m³*	Cumul. %	Cumul. % < stated ECD	ECD µm	Cumul. ng/m³	Cumul. %	Cumul. % < stated ECD	ECD µm
2.4	1.4	98.6	7.40	3.0	3.2	96.8	7.40
9.9	5.7	94.3	3.09	13.1	14.1	85.9	3.09
20.4	11.8	88.2	1.54	22.5	24.2	75.8	1.54
33.7	19.5	80.5	0.98	38.4	41.3	58.7	0.98
53.9	31.2	68.8	0.50	62.6	67.3	32.7	0.50
172.6	100.0	-	Filter	93.0	100.0	-	Filter

* Time-weighted averages

Table A7: Cumulative mass distributions of copper (Cu) from the high-volume Sierra cascade impactor sampling at Yssen.

17-23 Jan. period				23-30 Jan. period			
Cumul. ng/m^3	Cumul. %	Cumul. % < stated ECD	ECD µm	Cumul. ng/m^3	Cumul. %	Cumul. % < stated ECD	ECD µm
2	2.4	97.6	7.35	7	5.7	94.3	7.40
10	12.0	88.0	3.06	22	18.0	82.0	3.09
25	30.1	69.9	1.53	41	33.6	66.4	1.54
41	49.4	50.6	0.97	60	49.2	50.8	0.98
53	63.9	36.1	0.50	75	61.5	38.5	0.50
83	100.0	-	Filter	122	100.0	-	Filter
30 Jan. - 3 Feb. period				3-5 Feb. period			
6	5.9	94.1	7.40	5	4.7	95.3	7.40
18	17.8	82.2	3.09	20	18.7	81.3	3.09
37	36.6	63.4	1.54	41	38.3	61.7	1.54
53	52.5	47.5	0.98	63	58.9	41.1	0.98
63	62.4	37.6	0.50	79	73.8	26.2	0.50
101	100.0	-	Filter	107	100.0	-	Filter
9-13 Feb. period				13-17 Feb. period			
13	14.8	85.2	7.40	7	6.7	93.3	7.40
27	30.7	69.3	3.09	26	24.8	75.2	3.09
38	43.2	56.8	1.54	47	44.8	55.2	1.54
58	65.9	34.1	0.98	63	60.0	40.0	0.98
73	83.0	17.0	0.50	79	75.2	24.8	0.50
88	100.0	-	Filter	105	100.0	-	Filter
17-21 Feb. period				21-25 Feb. period			
15	8.6	91.4	7.40	6	7.2	92.8	7.40
46	26.4	73.6	3.09	17	20.5	79.5	3.09
89	51.1	48.9	1.54	39	47.0	53.0	1.54
119	68.4	31.6	0.98	51	61.4	38.6	0.98
144	82.8	17.2	0.50	61	73.5	26.5	0.50
174	100.0	-	Filter	83	100.0	-	Filter
Average: 17 Jan. - 5 Feb. period (Wh 40 substr. and glass-fibre filter)				Average: 9-25 Feb. period (glass-fibre substr. and filter)			
Cumul. ng/m^3*	Cumul. %	Cumul. % < stated ECD	ECD µm	Cumul. ng/m^3	Cumul. %	Cumul. % < stated ECD	ECD µm
5	4.8	95.2	7.40	10	9.0	91.0	7.40
17	16.3	83.7	3.09	29	25.7	74.3	3.09
35	33.6	66.4	1.54	53	47.0	53.0	1.54
53	51.0	49.0	0.98	73	64.6	35.4	0.98
66	63.5	36.5	0.50	89	79.0	21.0	0.50
104	100.0	-	Filter	113	100.0	-	Filter

* Time-weighted averages.

Table A8: Cumulative mass distributions of zinc (Zn) from the high-volume Sierra cascade impactor sampling at Yssen.

17-23 Jan. period				23-30 Jan. period			
Cumul. ng/m³	Cumul. %	Cumul. % < stated ECD	ECD µm	Cumul. ng/m³	Cumul. %	Cumul. < stated ECD	ECD µm
1	1.7	98.3	7.35	3	3.9	96.1	7.40
5	8.5	91.5	3.06	9	11.8	88.2	3.09
12	20.3	79.7	1.53	15	19.7	80.3	1.54
23	39.0	61.0	0.97	26	34.2	65.8	0.98
38	64.4	35.6	0.50	42	55.3	44.7	0.50
59	100.0	-	Filter	76	100.0	-	Filter
30 Jan - 3 Feb. period				3-5 Feb. period			
2	3.1	96.9	7.40	2	2.1	97.9	7.40
4	6.2	93.8	3.09	7	7.4	92.6	3.09
8	12.3	87.7	1.54	14	14.7	85.3	1.54
19	29.2	70.8	0.98	34	35.8	64.2	0.98
35	53.8	46.2	0.50	63	66.3	33.7	0.50
65	100.0	-	Filter	95	100.0	-	Filter
9-13 Feb. period				13-17 Feb. period			
4	6.0	94.0	7.40	2	1.7	98.3	7.40
11	16.4	83.6	3.09	12	10.3	89.7	3.09
18	26.9	73.1	1.54	26	22.2	77.8	1.54
32	47.8	52.2	0.98	52	44.4	55.6	0.98
51	76.1	23.9	0.50	88	75.2	24.8	0.50
67	100.0	-	Filter	117	100.0	-	Filter
17-21 Feb. period				21-25 Feb. period			
2	2.3	97.7	7.40	2	3.1	96.9	7.40
12	14.0	86.0	3.09	7	10.9	89.1	3.09
27	31.4	68.6	1.54	15	23.4	76.6	1.54
46	53.5	46.5	0.98	27	42.2	57.8	0.98
67	77.9	22.1	0.50	45	70.3	29.7	0.50
86	100.0	-	Filter	64	100.0	-	Filter
Average: 17 Jan - 5 Feb. periods (Wh 40 substr. and glass-fibre filter)				Average: 9-25 Feb. periods (glass-fibre substr. and filter)			
Cumul. ng/m³*	Cumul. %	Cumul. % < stated ECD	ECD µm	Cumul. ng/m³	Cumul. %	Cumul. < stated ECD	ECD µm
2.1	3.0	97.0	7.40	2.5	3.0	97.0	7.40
6.5	9.2	90.8	3.09	10.5	12.6	87.4	3.09
12.5	17.8	82.2	1.54	21.5	25.7	74.3	1.54
24.4	34.7	65.3	0.98	39.3	47.1	52.9	0.98
41.5	59.0	41.0	0.50	62.8	75.2	24.8	0.50
70.3	100.0	-	Filter	83.5	100.0	-	Filter

* Time-weighted averages.

Table A9: Cumulative mass distributions of water-leached calcium (Ca) from the high-volume Sierra cascade impactor sampling at Yssen.

17-23 Jan. period				23-30 Jan. period			
Cumul. ng/m³	Cumul. %	Cumul. % < stated ECD	ECD µm	Cumul. ng/m³	Cumul. %	Cumul. % < stated ECD	ECD µm
6	5.8	94.2	7.35	37	22.2	77.8	7.40
27	26.0	74.0	3.06	85	50.9	49.1	3.09
37	35.6	64.4	1.53	100	59.9	40.1	1.54
54	51.9	48.1	0.97	115	68.9	31.1	0.98
68	65.4	34.6	0.50	124	74.3	25.7	0.50
104	100.0	-	Filter	167	100.0	-	Filter
30 Jan. - 3 Feb. period				3-5 Feb. period			
2	4.1	95.9	7.40	3	4.8	95.2	7.40
12	24.5	75.5	3.09	26	41.3	58.7	3.09
16	32.7	67.3	1.54	29	46.0	54.0	1.54
23	46.9	53.1	0.98	40	63.5	36.5	0.98
29	59.2	40.8	0.50	53	84.1	15.9	0.50
49	100.0	-	Filter	63	100.0	-	Filter
9-13 Feb. period				13-17 Feb. period			
240	36.4	63.6	7.40	22	10.5	89.5	7.40
510	77.4	22.6	3.09	67	32.1	67.9	3.09
570	86.5	13.5	1.54	100	47.8	52.2	1.54
609	92.4	7.6	0.98	142	67.9	32.1	0.98
644	97.7	2.3	0.50	181	86.6	13.4	0.50
659	100.0	-	Filter	209	100.0	-	Filter
17-21 Feb. period				21-25 Feb. period			
50	31.6	68.4	7.40	12	9.9	90.1	7.40
108	68.4	31.6	3.09	40	33.1	66.9	3.09
130	82.3	17.7	1.54	61	50.4	49.6	1.54
144	91.1	8.9	0.98	73	60.3	39.7	0.98
155	98.1	1.9	0.50	88	72.7	27.3	0.50
158	100.0	-	Filter	121	100.0	-	Filter

Average: 17 Jan. - 5 Feb. periods (Wh 40 substr. and glass-fibre filter)				Average: 9-13 Feb. and 17-21 Feb. periods (glass-fibre substr. and filter)			
Cumul. ng/m³*	Cumul. %	Cumul. % < stated ECD	ECD µm	Cumul. ng/m³	Cumul. %	Cumul. % < stated ECD	ECD µm
16	14.4	85.6	7.40	145.0	35.5	64.5	7.40
45	40.5	59.5	3.09	309.0	75.6	24.4	3.09
55	49.5	50.5	1.54	350.0	85.7	14.3	1.54
69	62.0	38.0	0.98	376.5	92.2	7.8	0.98
79	71.1	28.9	0.50	399.5	97.8	2.2	0.50
111	100.0	-	Filter	408.5	100.0	-	Filter

Average: 13-17 Feb. and 21-25 Feb. periods (glass-fibre substr. and filter)			
Cumul. ng/m³	Cumul. %	Cumul. < stated ECD	ECD µm
17.0	10.3	89.7	7.40
53.5	32.4	67.6	3.09
80.5	48.8	51.2	1.54
107.5	65.2	34.8	0.98
134.5	81.5	18.5	0.50
165.0	100.0	-	Filter

* Time-weighted averages.

Table A10: Cumulative mass distributions of acid-leached calcium (Ca) from the high-volume Sierra cascade impactor sampling at Yssen.

17-23 Jan. period				23-30 Jan. period			
Cumul. ng/m^3	Cumul. %	Cumul. % < stated ECD	ECD µm	Cumul. ng/m^3	Cumul. %	Cumul. % < stated ECD	ECD µm
21	10.8	89.2	7.35	57	24.3	75.7	7.40
62	32.0	68.0	3.06	119	50.6	49.4	3.09
94	48.5	51.5	1.53	148	63.0	37.0	1.54
116	59.8	40.2	0.97	165	70.2	29.8	0.98
134	69.1	30.9	0.50	175	74.5	25.5	0.50
194	100.0	-	Filter	235	100.0	-	Filter
30 Jan. - 3 Feb. period				3-5 Feb. period			
20	19.6	80.4	7.40	46	22.2	77.8	7.40
46	45.1	54.9	3.09	112	54.1	45.9	3.09
63	61.8	38.2	1.54	147	71.0	29.0	1.54
73	71.6	28.4	0.98	170	82.1	17.9	0.98
78	76.5	23.5	0.50	181	87.4	12.6	0.50
102	100.0	-	Filter	207	100.0	-	Filter
9-13 Feb. period				13-17 Feb. period			
291	47.5	52.5	7.40	6	6.9	93.1	7.40
514	84.0	16.0	3.09	28	32.2	67.8	3.09
560	91.5	8.5	1.54	48	55.2	44.8	1.54
580	94.8	5.2	0.98	66	75.9	24.1	0.98
588	86.1	3.9	0.50	82	94.3	5.7	0.50
612	100.0	-	Filter	87	100.0	-	Filter
17-21 Feb. period				21-25 Feb. period			
43	31.2	68.8	7.40	21	19.4	80.6	7.40
105	76.1	23.9	3.09	53	49.1	50.9	3.09
128	92.8	7.2	1.54	73	67.6	32.4	1.54
131	94.9	5.1	0.98	82	75.9	24.1	0.98
133	96.4	3.6	0.50	88	81.5	18.5	0.50
138	100.0	-	Filter	108	100.0	-	Filter
Average: 17 Jan. - 5 Feb. periods (Wh 40 substr. and glass-fibre filter)				Average: 9-13 Feb. and 17-21 Feb. periods (glass-fibre substr. and filter)			
Cumul. ng/m^3*	Cumul. %	Cumul. % < stated ECD	ECD µm	Cumul. ng/m^3	Cumul. %	Cumul. % < stated ECD	ECD µm
37	19.4	80.6	7.40	167.0	44.5	55.5	7.40
85	44.5	55.5	3.09	309.5	82.5	17.5	3.09
113	59.2	40.8	1.54	344.0	91.7	8.3	1.54
131	68.6	31.4	0.98	355.5	94.7	5.3	0.98
142	74.3	25.7	0.50	360.5	96.1	3.9	0.50
191	100.0	-	Filter	375.0	100.0	-	Filter
Average: 13-17 Feb. and 21-25 Feb. periods (glass-fibre substr. and filter							
13.5	13.8	86.2	7.40				
40.5	41.5	58.5	3.09				
60.5	62.1	37.9	1.54				
74.0	75.9	24.1	0.98				
85.0	87.2	12.8	0.50				
97.5	100.0	-	Filter				

* Time-weighted averages.

Table A11: Cumulative mass distributions of benzo(a)pyrene (BaP) and total polycyclic aromatic hydrocarbons (PAH) in particles from high-volume Sierra cascade impactor sampling at Yssen during the 5-9 Feb.1976 period.

Total PAH*				BaP*			
Cumul. pg/m^3	Cumul. %	Cumul.% < stated ECD	ECD µm	Cumul. pg/m^3	Cumul. %	Cumul. % < stated ECD	ECD µm
233	1.2	98.8	7.40	6	0.4	99.6	7.40
551	2.7	97.3	3.09	17	1.0	99.0	3.09
1048	5.2	94.8	1.54	34	2.0	98.0	1.54
3830	19.0	81.0	0.98	214	12.9	87.1	0.98
11015	54.8	45.2	0.50	693	41.8	58.2	0.50
20092	100.0	-	Filter	1657	100.0	-	Filter

* Chemical analyses results provided by the Central Institute for Industrial Research (SI).

Table A12: Data for size-mass distribution histograms of the various trace elements, water-soluble ions, and PAH in particles at Yssen, as measured by the high-volume Sierra Cascade impactor during the 17 Jan. - 25 Feb. sampling periods.

Particle (a) diameter	(c) ΔM_i	$\frac{\Delta M_i}{M_T \Delta \log D_i}$	ΔM_i	$\frac{\Delta M_i}{M_T \Delta \log D_i}$	ΔM_i	$\frac{\Delta M_i}{M_T \Delta \log D_i}$	ΔM_i	$\frac{\Delta M_i}{M_T \Delta \log D_i}$	ΔM_i	$\frac{\Delta M_i}{M_T \Delta \log D_i}$	ΔM_i	$\frac{\Delta M_i}{M_T \Delta \log D_i}$
(b) interval	SO_4				NH_4				Pb			
	Ave.: 17Jan.-5Feb.		Ave.9-25Feb.		Ave.: 17Jan.-5Feb.		Ave. 9-25Feb.		Ave.: 17Jan.-5Feb.		Ave.: 9-25Feb.	
1	97	0.020	275	0.026	34.8	0.017	38.5	0.015	2.4	0.012	3.0	0.029
2	189	0.117	512	0.145	62.5	0.090	82.5	0.094	7.5	0.114	10.1	0.287
3	266	0.207	929	0.331	104.0	0.188	211.3	0.303	10.5	0.201	9.4	0.335
4	742	0.878	2003	1.099	344.1	0.957	478.7	1.058	13.3	0.392	15.9	0.872
5	1110	0.894	2810	1.035	544.0	1.015	742.5	1.101	20.2	0.400	24.2	0.891
6	1856	0.624	2771	0.426	745.2	0.581	754.5	0.468	118.7	0.982	30.4	0.468
	(d) M_T= 4253 ng/m^3		M_T= 9300 gn/m^3		M_T= 1835 ng/m^3		M_T= 2309 ng/m^3		M_T= 173 ng/m^3		M_T= 93 ng/m^3	

Particle diameter interval	Cu				Zn				(e) PAH		(e) BaP	
	Ave.: 17Jan.-5Feb.		Ave.: 9-25Feb.		Ave.: 17Jan.-5Feb.		Ave.: 9-25Feb.		5-9Feb.		5-9Feb.	
1	5	0.043	10	0.078	2.1	0.026	2.5	0.027	233	0.010	6	0.003
2	12	0.304	19	0.444	4.4	0.165	8.0	0.253	318	0.042	11	0.018
3	18	0.573	24	0.703	6.0	0.283	11.0	0.436	497	0.082	17	0.034
4	18	0.883	20	0.903	11.9	0.864	17.8	1.069	2782	0.706	180	0.554
5	13	0.428	16	0.485	17.1	0.833	23.5	0.964	7185	1.225	479	0.990
6	38	0.523	24	0.304	28.8	0.586	20.7	0.355	9077	0.646	964	0.832
	M_T= 104 ng/m^3		M_T= 113 ng/m^3		M_T= 70.3 ng/m^3		M_T= 83.5 ng/m^3		M_T= 20092 pg/m^3		M_T= 1657 pg/m^3	

Particle diameter interval	Ca (water-leached)						Ca (acid-leached)					
	Ave.: 17Jan.-5Feb.		Ave.: 9-13Feb. & 17-21Feb.		Ave.: 13-17Feb. & 21-25Feb.		Ave.: 17Jan-5Feb.		Ave.: 9-13Feb. & 17-21Feb.		Ave.: 13-17Feb. & 21-25Feb.	
1	16	0.128	145	0.314	17	0.091	37	0.171	167	0.394	14	0.126
2	29	0.689	164	1.058	37	0.592	48	0.663	143	1.006	27	0.727
3	10	0.298	41	0.332	27	0.542	28	0.485	35	0.309	20	0.676
4	14	0.644	26	0.324	27	0.835	18	0.481	12	0.163	14	0.729
5	10	0.309	23	0.193	27	0.560	11	0.197	5	0.046	11	0.384
6	32	0.412	9	0.032	31	0.269	49	0.307	15	0.057	13	0.189
	M_T= 111 ng/m^3		M_T= 409 ng/m^3		M_T= 165 ng/m^3		M_T= 191 ng/m^3		M_T=375 ng/m^3		M_T= 98 ng/m^3	

(a) equivalent aerodynamic diameters

(b) intervals:

1: 7.40 - 100 µm
2: 3.09 - 7.40 µm
3: 1.54 - 3.09 µm
4: 0.98 - 1.54 µm
5: 0.50 - 0.98 µm
6: 0.10 - 0.50 µm

$\Delta \log D_i = \log \frac{ECD_{i-1}}{ECD_i}$

where: ECD_i is the 50% cut-off diameter of the i^{th} stage of impactor

The ECD's for the Hi-Vol sampler inlet (100 µm) and for the Sierra impactor after-filter (0.10 µm) as assumed (cf. 5.2)

	$\Delta \log D_i$
1:	1.13
2:	0.379
3:	0.302
4:	0.196
5:	0.292
6:	0.699

(c) mass concentration of chemical component on i^{th} stage of impactor

(d) total concentration of chemical component

(e) analysis by the Central Institute for Industrial Research (SI)

Table A13: Ratios of chloride to sodium (Cl/Na), chloride to magnesium (Cl/Mg), and sodium to magnesium (Na/Mg) in airborne particles at Yssen, as measured by the high-volume Sierra cascade impactor (Hi-Vol/Sierra) and the "Kommunekasse" automatic sampler (KK).

Period of sampling	Concentration, ng/m³								
	Hi-Vol/Sierra						KK		
	Cl		Na		Mg		Cl	Na	Mg
	Tot.++	Adj.+++	Tot.	Adj.	Tot.	Adj.			
17 Jan. - 23 Jan.	790	830	390	410	29	36	460	150	8
23 Jan. - 30 Jan.	600	630	480	510	44	51			
30 Jan. - 3 Feb.	660	690	480	510	7	9			
3 Feb. - 5 Feb.	130	140	210	220	(-)	(-)			
9 Feb. - 13 Feb.	3650	3830	2850	3020	193	237			
13 Feb. - 17 Feb.	7920	8300	7370	7810	216	365	690	220	18
17 Feb. - 21 Feb.	1290	1350	1340	1420	31*	38*			
21 Feb. - 25 Feb.	480	500	770	820	28	34			

Period of sampling	Ratio+								
	Hi-Vol/Sierra						KK		
	Cl/Na		Cl/Mg		Na/Mg		Cl/Na	Cl/Mg	Na/Mg
	Tot.	Adj.	Tot.	Adj.	Tot.	Adj.			
17 Jan. - 23 Jan.	2.03	2.02	27.2	23.1	13.4	11.4	3.07	57.5	18.8
23 Jan. - 30 Jan.	1.25	1.24	13.6	12.4	10.9	10.0			
30 Jan. - 3 Feb.	1.38	1.35	94.3	76.7	68.6	56.7			
3 Feb. - 5 Feb.	0.62	0.64							
9 Feb. - 13 Feb.	1.28	1.27	18.9	16.2	14.8	12.7			
13 Feb. - 17 Feb.	1.07	1.06	36.7	22.7	34.1	21.4	3.14	38.3	12.2
17 Feb. - 21 Feb.	0.96	0.95	41.6	35.5	43.2	37.4			
21 Feb. - 25 Feb.	0.62	0.61	17.1	14.7	27.5	24.1			

+ sea water ratios are: Cl/Na ~ 1.8, Cl/Mg ~ 14.9, and Na/Mg ~ 8.3

++ sum of concentrations on Stages 1 through 5 of cascade impactor and after-filter

+++ total concentration adjusted for interstage losses (cf. 4.1)

(-) concentration equal or less than blank concentration on Stages 1 and 5, and after-filter

* concentration equal or less than blank concentration on after-filter

Table A14: Interstage losses and total concentrations of various chemical components in airborne particulate matter for the high-volume Sierra cascade impactor, as measured during the 9 Feb. - 13 Feb. 1976 sampling period at Yssen.*

Jet-plate number	Interstage loss concentration, ng/m³					Stage number	Measured concentration, ng/m³				
	SO_4	Pb	Cu	Zn	Ca***		SO_4	Pb	Cu	Zn	Ca***
1	235	0.6	8.1	5.1	41	1	487	5.4	13	4	240
2	117	0.8	4.4	3.4	36	2	842	11.7	14	7	270
3	246	2.8	3.1	5.0	38	3	933	6.8	11	7	60
4	233	1.9	2.6	4.2	21	4	1703	13.5	20	14	39
5	431	3.0	5.5	5.8	25	5	2433	28.7	15	19	35
6	**	**	**	**	**	Filter	2149	23.5	15	16	15
Total	1262	9.1	23.7	23.5	161	Total	8547	89.6	88	67	659

* determined from ultra-sonic cleaning (in distilled water) of jet-plates of the impactor.

** losses to the slotted support plate of substrate for Stage 5 not determined because of its oversize for ultra-sonic cleaning.

Table A 15: Blank analyses of the stage substrates and after-filters used for the high-volume Sierra cascade impactor.

Date of analysis	Type of filter or substrate	Amount of constituent, µg, per filter or substrate									
		leached in distilled water						leached in 1N HNO_3			
		SO_4	NH_4	Ca	Cl	Na	Mg	Pb	Cu	Zn	Ca
Feb. 1976	Whatman 40 slotted substrate	~0	22	14	50	<10	<2				
" "					50	<10	2				
" "					210	40	14	<0.4	4.2	2.0	
Mar. "											20
Apr. "		~0	7	1	110	<1	1				
" "		~0	8	2	130	<1	1				
" "		~0	7	11	130	<1	12				
Feb. 1976	Gelman Spectro-grade Type A glass-fibre slotted substrate							0.4		2.0	
" "									4.2		
Mar. 1976											58
" "		~0	24	54	5100*	2400*	14				
" "					280						
" "					275						
" "					340						
Apr. "		15	<5	9	280	194					
" "		7	<5	18	275	184					
" "		~0	30	12	340	168					
Feb. 1976	Gelman Spectro-grade Type A after-filter			44	1040	600	4				
" "				44	900	480	4				
" "								0.8		8.0	
" "								<0.8		4.0	
" "									32.8		
Mar "									8.2		
" "											156
" "											120
" "					1480						
" "					1400						
Apr. "		~0	<20		1480	1056					
" "		~0	<20		1400	1128					
May "				88			36				
" "				124			52				

* Values not included in determining average blank concentrations for Cl and Na.